UNIVERSITY OF CAPE TOWN
IYUNIVESITHI YASEKAPA • UNIVERSITEIT VAN KAAPSTAD

THESIS REPORT

The influence of various factors on the results of carbonation, cover depth, half-cell potential and resistivity tests that are used in the assessment of reinforcement corrosion

16/10/2020

MOHAMMED FARAAZ AKHALWAYA (AKHMOH003)

Plagiarism declaration

I know the meaning of plagiarism and declare that all the work in the document, save for that which is properly acknowledged, is my own. This thesis has been submitted to the Turnitin module (or equivalent similarity and originality checking software) and I confirm that my supervisor has seen my report and any concerns revealed by such have been resolved with my supervisor

Signed by candidate

Signature _____

Date: 16/10/2020

Abstract

Reinforcement corrosion is the main cause of deterioration in concrete structures. Condition assessment tests help to predict whether reinforcement corrosion is occurring and aid in the prevention of its consequences. The results of these condition assessment tests can, however, be affected by certain factors. A set of experiments that included carrying out four of these tests, namely the half-cell potential (HCP), cover depth, carbonation and resistivity tests was performed on several concrete structures on upper campus at UCT. The half-cell potential and resistivity tests were carried out across a four-month period between August and November 2018 during both dry and wet periods and on days with different temperatures. This was done to assess how changing weather conditions can affect the test results. The results from these tests were also used to do a comparison between HCP and cover depth results and HCP and resistivity results. A second set of experiments involved taking cover depth measurements and cores for carbonation testing from different locations across a building and assessing how variations in measurement location and sample size can affect the results.

The HCP and resistivity results showed changes due to the effects of rain and temperature. Rainy weather caused the values to become more negative, while dry weather led to more positive values. An increase in temperature showed a slight decrease in the values of both the half-cell potential and resistivity measurements. The changes suggest that using prescribed value ranges to interpret the risk of corrosion may prove to be too simplistic. Contour plots of the HCP results proved to be a more stable method for assessing reinforcement corrosion than using prescribed value ranges. The overall trend for the comparison between HCP and cover depth results showed that HCP values decrease as cover depths decrease. The comparison between HCP and resistivity results was expected to show an overall decrease in HCP values as resistivity values decrease, but this did not hold true for some of the test locations. The results of the cover depth analysis showed significant changes in calculated statistics due to both changes in location and sample size. A cover depth analysis should thus be widespread and include a large number of measurements in order to provide useful results. The variation in results for the carbonation testing was contradictory for the two buildings that were tested, with one building showing significant variations with measurement location and the other building showing very little variation.

Acknowledgements

Supervisor: Professor Hans Beushausen for assistance, guidance and provision of resources.

The University of Cape Town Postgraduate Funding Office & the Civil Engineering CoMSIRU unit for the provision of funding.

CoMSIRU also provided access to equipment and other forms of assistance.

DR. Philemon Arito for his assistance in the statistical analysis.

The Civil Engineering lab staff for their assistance in providing the equipment for the tests.

Lab technician Christopher Ceasar for his help in drilling the cores for carbonation testing.

The South African Weather Service for the provision of the weather data used in the analysis of the half-cell potential and resistivity measurements.

Contents

List of Figures

`

List of Tables

Report outline

This report is broken down into 5 key sections:

1. Introduction to the topic: this section introduces the motivation behind the study and the objectives of the thesis.

2. Literature review: this is a 2-part literature review. Part 1 is a smaller section, which provides a look into the processes of corrosion in reinforced concrete structures. Part 2 forms the majority of the literature review, providing an understanding of the main condition assessment tests which are used to predict whether reinforcement corrosion is occurring or not.

3. Methodology & Approach: in this section, the process for selecting test locations and carrying out the different tests are discussed. The processes that are used to analyse the data are also explained in this section.

4. Results & Interpretation of results: Section 4 presents the results that were collected across the 4-month period for the 4 different test methods. The interpretation of the results takes the form of graphs, contour plots, tables, analysis procedures and calculations that are used to discuss findings with regards to the objectives that were set out.

5. Summary: a summary of the main aspects of this work based on both the experimental analysis and literature review.

6. Conclusion: this section draws conclusion on the work.

7. Recommendations: recommendations for carrying out a condition assessment to assess the state of reinforcement corrosion of a structure as well as recommended areas for further research are proposed.

1. Introduction

1.1. Background of study

Reinforced concrete structures, throughout the world, are faced with the problem of reinforcement corrosion. This corrosion is caused by the ingress of harmful substances such as carbon dioxide and chloride ions, through the concrete cover layer. Corrosion leads to a loss in the cross-section of the steel reinforcement, as well as expansive stresses in the concrete due to the formation of corrosion products and subsequent damage to the concrete surrounding the steel. The consequences of reinforcement corrosion can be severe as they can lead to substantial damage and may even cause structural failure (Otieno, 2014). Condition assessments help to fight the problem by serving as a guide in deducing what the current state of a structure may be. This understanding of the state of the structure allows for the planning of maintenance, repair and rehabilitation in a way that can protect the safety of a structure and its users whilst providing economic benefits (Arndt & Jalinoos, 2009).

Visual assessment is most often the first tool used in carrying out a condition assessment. While quality visual assessments are deemed valuable, it is often the case that visual evidence of reinforcement corrosion may only become obvious years after the process of corrosion has begun. This makes the use of other tests such as cover depth, carbonation, half-cell potential and resistivity important to predict whether corrosion is likely to occur or not (Phares, 2001). The use of these tests has been suggested in several standards and recommendations which provide guidance on how to carry out the tests and some guidance on how to interpret the results.

Value ranges are available for the interpretation of the probability of reinforcement corrosion and reinforcement corrosion rates based on the results of the half-cell potential and resistivity tests. A widely used example of these ranges can be found in the ASTM C876 standard which addresses half-cell potential mapping and provides a guide for interpreting results (Gu & Beaudoin, 1998). Through empirical testing similar types of ranges have been deduced for resistivity measurements, some of which are suggested for use in the instruction manuals of commonly used resistivity meters (e.g. (Proceq, 2017)).

Structures are designed to meet a minimum reinforcement cover depth requirement based on guidelines and standardised values (BS-1881, 1988). It is often the case that during construction these requirements are not met, and this may result in durability problems (Sivasubramanian, et al., 2013). Assessing the achieved cover depth is important for the purpose of a condition assessment. Locations with low cover depths contribute to increased reinforcement corrosion as corrosion-inducing substances can reach the level of the reinforcement quickly (Arito, 2017; Otieno, et al., 2010). In general, the information pertaining to concrete cover depth measurements which are found in standards and guidelines speak about what concrete cover depth is, what the required depths should be, the importance of measuring cover depths and the processes which should be used to take measurements.

1.2. Problem statement

The different condition assessment tests that are used to predict the presence of reinforcement corrosion are fairly well known in terms of the manner in which they function and how they should be carried out. There is however a shortage of information on the tests when it comes to details such as how the results of the different tests relate to each other and how certain factors may influence the information that is collected with only few discussions in some specialist literature and RILEM TC reports.

The onsite measurements of half-cell potentials and resistivity values are subject to change due to environmental conditions such as the occurrence of rain and changes in atmospheric temperature, which are not addressed by the standards or guidelines. These changes may lead to misinterpretation of the actual corrosion state of a structure when conclusions are drawn by comparing measured values to the prescribed value ranges. The effects of changes in moisture content and temperature on half-cell potential and resistivity values have been studied on samples in the laboratory but research into the effects of rain and temperature on actual onsite measurements is lacking. In laboratory tests, it has been found that both half-cell potential and resistivity measurements become more negative with an increase in moisture content, and become more positive with a decrease in temperature (Azarsa & Gupta, 2017; Keßler & Gehlen, 2016). Some empirical relationships have been developed which cater for changes due to temperature, but laboratory and field conditions can be very different due to the exposure environment and fluctuating conditions. Developing a better understanding of how field measurements are affected by environmental conditions is important, as it is these measurements that will be used to make decisions concerning the state of a structure.

When assessing concrete cover and the conformity achieved not much information is available concerning how many measurements should be taken and how these measurements should be used for the purpose of a construction assessment or condition assessment. RILEM TC 230-PSC (Polder, et al., 2000), which is a report that discusses the control of concrete durability, suggests a few methods including the German prescribed methods for assessing the conformity of reinforcement cover depth. The methods are meant to help with durability and control assessments. These methods for assessment of conformity are useful tools, but they also depend on the amount of information that is input into the analysis. It is very rarely possible that cover depth measurements can be taken along a full structure as this will prove to be time-consuming and costly. It is therefore important to assess how different variables impact on the conclusions that are drawn from these measurements.

1.3. Objectives

The objective of this thesis is to develop a better understanding of how certain factors influence the interpretation of condition assessment test results and to provide guidance on how to carry out a condition assessment when assessing the state of reinforcement corrosion in concrete structures. The objective is broken down into the following sub-objectives that this thesis aims to address:

I. Determine how changes in weather in the form of rain and temperature fluctuations impact on the onsite measurements of half-cell potential and resistivity tests. Ascertain whether any changes that occur in the measured results can lead to changes in the interpretation of the state of reinforcement corrosion of a structure based on available recommendations for assessment from standards and literature.

II. Assess whether field measurements show a relationship between half-cell potential and cover depth tests and half-cell potential and resistivity tests.

III. Determine how variations in measurement locations and sample sizes impact on the interpretation of cover depth and carbonation results.

IV. Provide guidance on how to perform a cover depth analysis for the purpose of a condition assessment.

V. Provide recommendations for carrying out a condition assessment to assess the state of reinforcement corrosion of a structure based on the findings of this work.

1.4. Limitations of the study

I. The specific locations chosen for the analysis are limited to 3 buildings on upper campus of the University of Cape Town. Results may thus be specific to these buildings as materials used and construction may vary from one building to the next.

II. The locations that were determined to be adequate for testing were limited to locations that were easily accessible and safe for one person to carry out the testing. Testing was carried out at the University of Cape Town, however, a number of locations have access restrictions and the buildings are multi-story thereby making it difficult to reach adequate locations above the ground level.

III. Environmental conditions are outside human control and therefore difficulty in testing an ideal range of conditions in a limited period arises. The tests were carried out between the period of August-November 2018 and so testing was limited to the weather conditions which occurred during these months.

IV. Another challenge faced was that the influence of rain and temperature infield occurs simultaneously making it difficult to distinguish between the individual effects that the two variables have on half-cell potential and resistivity tests. The temperature tests were carried out after a period of dry weather to prevent rain from influencing the results. This meant that a short period of dry days between rainy weather could not be utilized for the temperature assessment even if they were of an ideal temperature to create a wider range of variation in test conditions.

V. Environmental conditions may change throughout a day leading to slight variances in the exposure conditions when moving from one location to the next over a period of ±10 hours. To complete the tests for all the locations on a particular day, it would take testing from the morning until the evening. During the hours of testing, the environmental conditions such as temperature would fluctuate, and this would mean that conditions at the location tested in the morning were not exactly the same as those at the location tested in the evening.

VI. The number of locations that were tested for the purpose of assessing variations in environmental conditions was limited due to time constraints. In order to have measurements taken at each location under comparable conditions, all the locations would have to be tested on the same day to prevent the influence of overnight changes or changes over a couple of days. It was found that five locations could be fully tested in one day from the morning to the evening.

2. Literature review

2.1. Introduction

Concrete has been used as the foremost construction material for infrastructure for many years, but the early deterioration of the infrastructure due to the occurrence of reinforcement corrosion has placed it under threat (Alexander, et al., 2012). The steel which is used for the reinforcement of concrete is not a naturally occurring material and is produced through smelting and refining of iron ore. Corrosion is thus bound to occur as the refined metals return to more stable forms (Portland Cement Association, 2002).

In spite of the protection that the concrete cover layer provides to the embedded reinforcement, reinforcement corrosion still remains to be one of the main causes of damage and failure in reinforced concrete structures (Arndt & Jalinoos, 2009). There are a number of reasons for the continuing occurrence of reinforcement corrosion which include but are not limited to; low cover depths, inadequate construction practices, exposure to aggressive environments and the use of de-icing salts (Mackechnie & Alexander, 2001).

The effects of reinforcement corrosion can be catastrophic in terms of safety and costs. It is therefore extremely important that these effects be minimised to protect quality of life and to fight a large amount of unnecessary expenditure caused by corrosion-induced damage. The damage that is caused by reinforcement corrosion can occur over a short period of time and in many cases, visible effects of corrosion only become noticeable once the integrity of the structure has already become compromised (Mackechnie & Alexander, 2001).

Condition assessment tests help to provide information on the environment that the structures are exposed to as well as information on the current state of the structure. Monitoring of structures using condition assessment techniques have thus become crucial to ensuring that these structures are well maintained, and that repair and rehabilitation occur on a timeous basis. Some of the more commonly used condition assessment tests, which aid in the assessment of possible reinforcement corrosion includes the carbonation, chloride, cover depth, half-cell potential and resistivity tests (Coimbatore, 2014).

Various standards, guidelines and works of literature that provide information about what the different tests are used for and details on how the tests should be carried out are available. In order to know when to apply the different test methods and how to interpret the results, it is important to understand the process of reinforcement corrosion, how to apply each method and the different factors which may influence the results of these tests.

2.2. Reinforcement corrosion

2.2.1. Fundamentals of corrosion in reinforced concrete

Reinforcement corrosion is known to be the main cause of deterioration in concrete structures throughout the world (Portland Cement Association, 2002; Song & Saraswathy, 2007). The corrosion process is as a result of an electrochemical reaction that takes place when the reinforced concrete is exposed to corrosive environments. During the electrochemical reaction, iron particles are oxidized at the anode, while oxygen is reduced at the cathode (Otieno, 2014). The anode and cathode are found at different points on the reinforcement and can be either on the same reinforcement bar or connected reinforcement bars (Smith & Virmani, 2000).

The anode is the location at which the corrosive products are formed and from which the electrons flow. Corrosion does not occur at the cathode, but this is the location to which the electrons flow. Along with the anode and cathode, the electrochemical process also requires an electrolyte and a metallic path for the process to take place. In reinforced concrete structures the electrolyte, which is responsible for the conduction of the electric current through the flow of ions, is found in the form of the alkaline concrete pore solution. The steel reinforcement forms the metallic path, which completes the circuit as it facilitates current return by providing the pathway for the electrons to flow from the location of the anode to that of the cathode (Otieno, 2014). Figure 1 shows a schematic representation of the process of reinforcement corrosion.

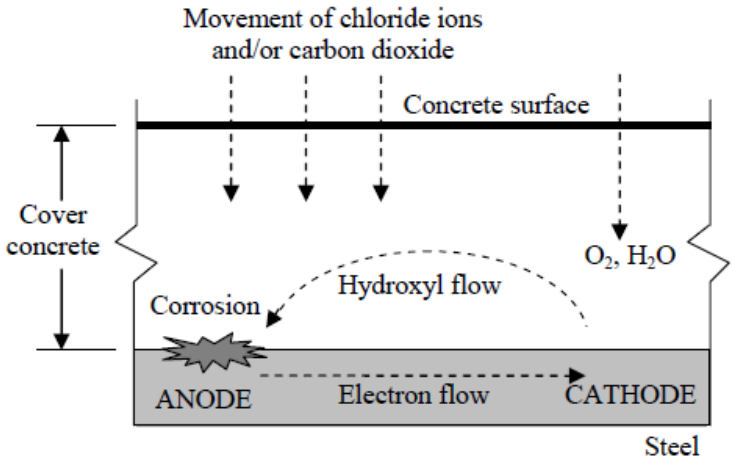

Figure 1: Schematic illustration of the process of corrosion in reinforced concrete (Mackechnie, 2001)

The two main causes of reinforcement corrosion are carbonation or chloride-induced corrosion (Song & Saraswathy, 2007). Irrespective of the cause of the corrosive process, there will be basic anodic and cathodic reactions that take place (Otieno, 2014). During the anodic reaction (also known as the oxidation reaction), iron ions are formed as electrons are lost from the iron atoms. In the cathodic /reduction reaction, oxygen accepts the electrons from the anode in the presence of water, which leads to the

formation of hydroxyl ions. If the anodic and cathodic reactions do not take place concurrently, corrosion will not be possible. The anodic and cathodic half-reactions are shown in Equations 1 and 2 respectively (Smith & Virmani, 2000).

Anodic reaction: $Fe \rightarrow Fe^{2+} + 2e^{-}$ … (1)

Cathodic reaction: $2H_2O + O_2 + 4e^{-} \rightarrow 4OH^{-}$ … (2)

The corrosive product that forms at the anode is commonly known as rust. Rust has a greater volume than the volume of the steel reinforcement from which it was formed. The rust tends to be deposited in the restricted space at the interface between the concrete and the steel. Since the volume of the rust is greater than the steel from which it was formed, and it is located in a restricted space, it results in the build-up of expansive stresses, which induces cracking, delamination and spalling of the concrete cover. Progressive deterioration of the structure occurs with the build-up of rust and rust-induced defects. Together with the loss of strength due to damaged concrete and the promotion of further deterioration, rust also leads to a reduction in steel diameter, which reduces the ability to carry the load. The damage also has a negative visual aspect, as it can be quite unsightly (Otieno, 2014; Song & Saraswathy, 2007; Tuutti, 1982).

2.2.2. The passive layer

Concrete has a naturally alkaline environment with a pH of approximately 12-13 (Broomfield, 2007). These high levels of pH are one of the advantages of concrete use as they lead to the formation of a thin protective layer over the reinforcement. This protective layer, also known as the passive layer, prevents metal atoms from dissolving and thus basically nullifies the corrosion rate by retarding the rate to negligible or imperceptible values (Portland Cement Association, 2002). Loss of metal when the passive layer is still intact is found to be in the region of 0.1-1.0 µm/year. With such low passive corrosion rates, it is generally agreed that no noticeable damage to the steel or induced stresses will occur in the concrete within a 75-year lifespan (Hansson, et al., 2012). Serious effects of corrosion through active corrosion rates will only be seen once the passive layer is destroyed and this predominantly happens under the effects of carbonation and chloride attack. Once the passive layer is destroyed, the rate of corrosion can increase by a magnitude of a thousand (Portland Cement Association, 2002).

2.2.3. Corrosion cells

There are two types of corrosion cells, namely microcells and macrocells. A microcell occurs when the anode and cathode are located directly next to each other on the same piece of metal, such that both the dissolution of the metal and reduction of the oxygen are adjacent to each other on a microscopic level. The corrosion cell is termed a macrocell when there is a finite distance between the anode and cathode. These cells occur due to potential differences between different parts of the reinforcement that are in contact and so can be located on the same bar or different bars as long as they are in both electrical and electrochemical contact. Microcells tend to lead to a more uniform corrosion, while macrocells tend to lead to a localized form of corrosion (Arito, 2017; Broomfield, 2007; Smith & Virmani, 2000). Microcell corrosion tends to always occur in practice and is found to be the dominant corrosion process in most cases, although macrocell corrosion is found to be dominant where multiple layers of reinforcement are present. Corrosion due to a combination of both microcells and macrocells is also possible (Hansson, et al., 2012).

The corrosion can progress uniformly across the reinforcement with more even and regular loss from the corroding surface or in localized spots along the reinforcement where the metal loss occurs at discrete areas (Roberge, 2008). The uniform corrosion covers large areas of the reinforcement within a structure and is characterised by the occurrence of continuous microcells. The usual cause of uniform corrosion is due to the effects of carbonation; however, uniform corrosion also occurs when chloride ions are present in large concentrations. The localized/pitting corrosion occurs in specific anodically active areas, with large passive cathodic regions either next to or some distance away from the anode. This type of corrosion is characterised by the presence of macrocells and is usually caused by chloride attack, where critical chloride concentrations are reached at these specific locations (Arito, 2017). The difference in potential values, which exists between the anodic and cathodic areas, is what allows for the prediction of ongoing reinforcement corrosion by half-cell potential mapping. This is discussed in greater detail in the half-cell potential section 2.3.5.

2.2.4. Service life phases

Research shows that there are two phases during the service life of reinforced concrete structures, namely the reinforcement corrosion initiation and propagation phases. The initiation phase is defined as the time between the end of the construction process and the beginning of the reinforcement corrosion process. During the initiation phase, the passive layer remains intact, chlorides and carbon dioxide enter into the concrete pore solution and cause changes to occur over time. Some reinforcement corrosion may occur during the initiation phase, but this will take place at a very low rate. The propagation phase then follows the initiation phase and at this point, the corrosive effects become more and more problematic, proceeding at a significant rate and causing damage to both the reinforcement and the concrete. There is a time when reinforcement corrosion will be present, but its effects will not be visible, thus creating the

need for non-destructive evaluation techniques (Arito, 2017; Hansson, et al., 2012). Another phase that occurs after the propagation phase is known as the acceleration phase and during this phase reinforcement corrosion rates are rapid and major damage occurs. The acceleration phase, however, falls out of the definition of the service life as this is the stage during which the structure begins to fail to meet the design requirements and falls beyond a critical limit state (Arito, 2017; Andrade, 2007).

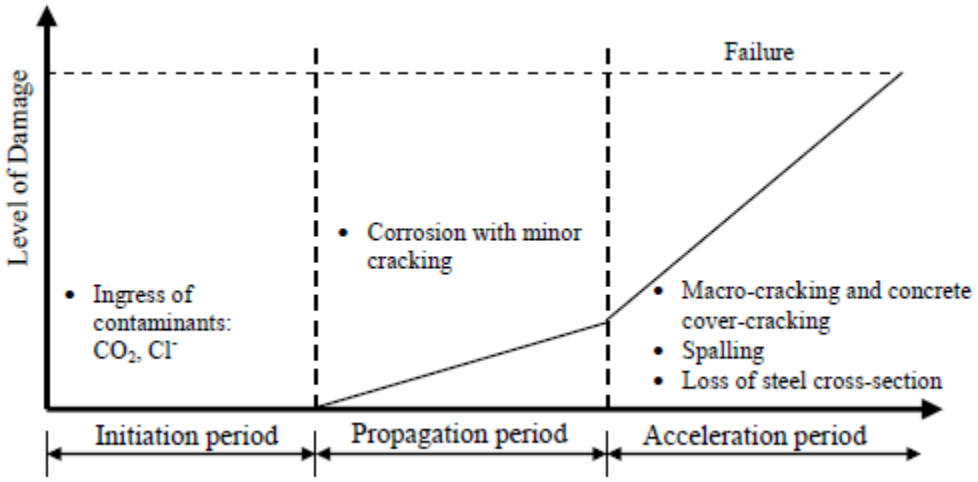

Figure 2: Reinforced concrete service life phases and corresponding damage (Heckroodt (2002), as redrawn by Otieno, et al (2010))

2.2.5. Factors which influence reinforcement corrosion

Reinforcement corrosion can only take place if the following three parameters are available simultaneously (Arito, 2017):

I. Moisture in the concrete.

II. Oxygen.

III. Aggressive species are present (such as carbon dioxide or chloride ions).

There are several factors, which affect both the initiation and propagation of corrosion in reinforced concrete structures, such as the following (Otieno, 2014):

I. Moisture content of the concrete and relative humidity.

II. Thickness and quality of the concrete cover.

III. Water/binder (w/b) ratio.

IV. The chloride threshold.

V. Concrete composition (binder type).

VI. Temperature.

VII. Presence of cracks, delamination or spalling.

2.2.5.1. Moisture content

Moisture content is the main influencing parameter on corrosion from the different environmental conditions (Vavpetic, 2008). It is not possible for corrosion to be in an active state if moisture is not present in the correct amount (Arito, 2017). Daily and seasonal cycles result in a change in corrosion rates due to changes in moisture content (Vavpetic, 2008).

Under very dry conditions, there is little to no water available to support the process of reinforcement corrosion and the level of concrete resistivity is high. When the concrete is highly saturated the resistivity is low, but the rate of oxygen transportation to the level of steel is slowed, as oxygen does not readily dissolve in water. This is why fully submerged reinforced concrete does not corrode easily unless exposed to cyclic dry and wet conditions. Intermediate moisture contents facilitate the most corrosion as these conditions lead to a reduction in resistivity, provide sufficient moisture to act as an electrolyte and allow for higher rates of oxygen transportation into the concrete (Ahlström, 2014; Otieno, et al., 2010).

Moisture affects carbonation and chloride attack in different ways. Both carbon dioxide and oxygen penetration are controlled by the level of moisture. Water saturated concrete delays the process of carbonation as limited amounts of oxygen can penetrate the concrete. Chloride ions, on the other hand, penetrates quicker when the concrete is more highly saturated (Vavpetic, 2008). The most suitable moisture condition for the progress of reinforcement corrosion due to carbonation is when the relative humidity is above 80% (Arito, 2017). When it comes to chloride-induced reinforcement corrosion, the maximum corrosion rate was found to be reached at a relative humidity of 90-95% (Richardson, 2002).

Cover depth and temperature both play a role in how moisture content affects the rate of corrosion. The effects of moisture content vary with depth as a moisture gradient exists from the surface moving into the concrete. The greatest effects on moisture content due to environmental conditions are thus found closer to the surface as these layers of concrete are most exposed to the environment. The depth of cover over the reinforcement thus plays an important role in the occurrence of corrosion as it increases the time taken for moisture to reach the reinforcement. A rise in temperature is known to have the effect of speeding up the reactions necessary for the occurrence of corrosion, but this rise can also have an inhibiting effect on the corrosion process due to the impact that it has on the moisture content. A temperature increase leads to an increased rate of evaporation as well as the removal of oxygen from the pore solution as there is less solubility (Vavpetic, 2008).

Periods of rain can have a significant effect on the degree of concrete saturation (Vavpetic, 2008). Rain has the ability to move through cracks and pores in a structure. The polar nature of water molecules gives water a high surface tension and a greater ability to wet surfaces. The nature of the water molecules allows for water to penetrate very small openings without the need for an external driving force, due to the process of capillarity (BEG, 2002). The movement of water into concrete by capillary action is favoured in concrete with a greater number of smaller pores and cracks than concrete with larger pores and cracks as it is the smaller openings that are filled more easily under this action. The pore size distribution, pore system and crack properties vary from structure to structure and so different structures will have different amounts of capillary condensed water, even when subject to the same exposure conditions (Ahlström, 2014). For the occurrence of capillary action, the wetted surface must be hydrophilic (BEG, 2002).

Sarkar & Bhattacharjee (2014) carried out tests to determine the effects of varying rainfall intensities on the degree of moisture penetration of a concrete surface. Each test was carried out over an hour with the concrete subject to rainfall intensities of 1,25 mm/h, 5 mm/h and 25 mm/h respectively. These rainfall intensities are categorized as light (<2.5 mm/h), medium (2.5-7.5 mm/h) and heavy (>7.5 mm/h) rains respectively by Deodhar (2008). The light intensity rain causes lower ingress of moisture than the medium and high-intensity rainfalls. Although the high-intensity rain has a slightly higher penetration profile than the medium intensity rainfall, their moisture profiles are very similar even though the high-intensity rain is fivefold greater. Each of the three moisture penetration profiles can be seen in Figure 3. From the penetration profiles it can be concluded that the depth of moisture penetration into concrete depends on the intensity for light rains, but for higher intensity rains this is not the case. The penetration of higher intensity rains into concrete is instead governed by the duration of exposure.

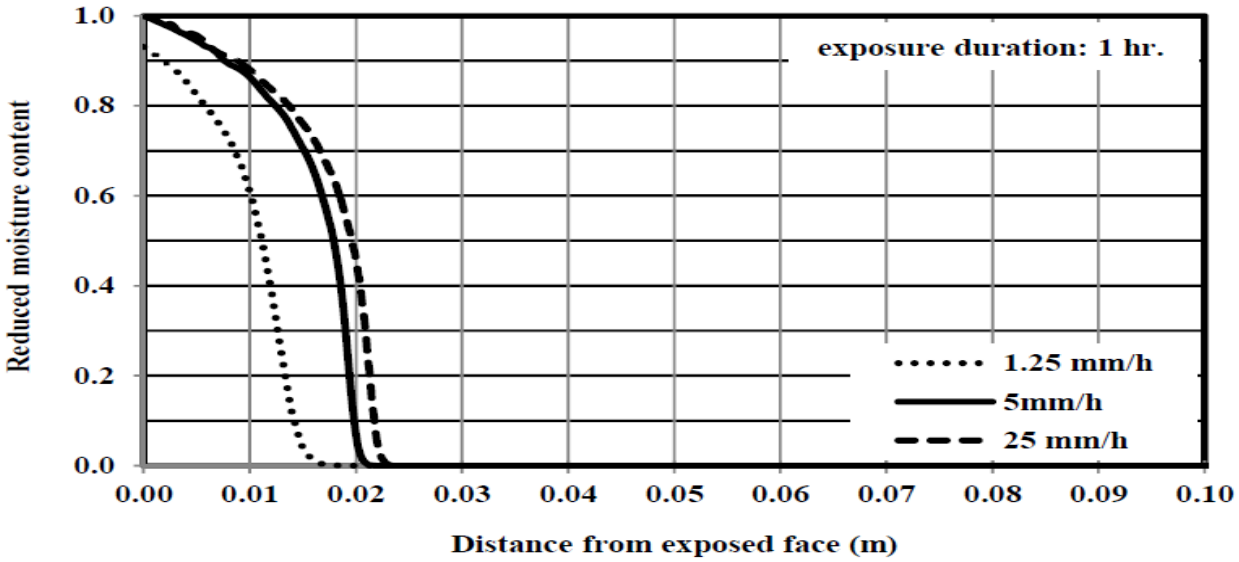

Figure 3: Profiles of moisture penetration for concrete subject to light, medium and high-intensity rainfalls for a period of 1 hour. (Sarkar & Bhattacharjee, 2014)

A second set of experiments by Sarkar & Bhattacharjee (2014) were carried out to determine how the moisture penetration depth is affected by different intensity-duration combinations where an exposed surface is subject to the same quantity of incident water. The combinations that were tested includes an intensity of 1.25 mm/h over 1 hour, 5 mm/h over 0.25 hours and 25mm/h over 0.05 hours. The moisture penetration profiles for these combinations are shown in Figure 4. These results show that for impinging rains of the same quantity, the higher intensity rains that fall over shorter spells result in a smaller degree of penetration. This relates well to real-life conditions where high-intensity rainfalls usually occur over shorter periods and lighter intensity rainfalls occur over longer periods.

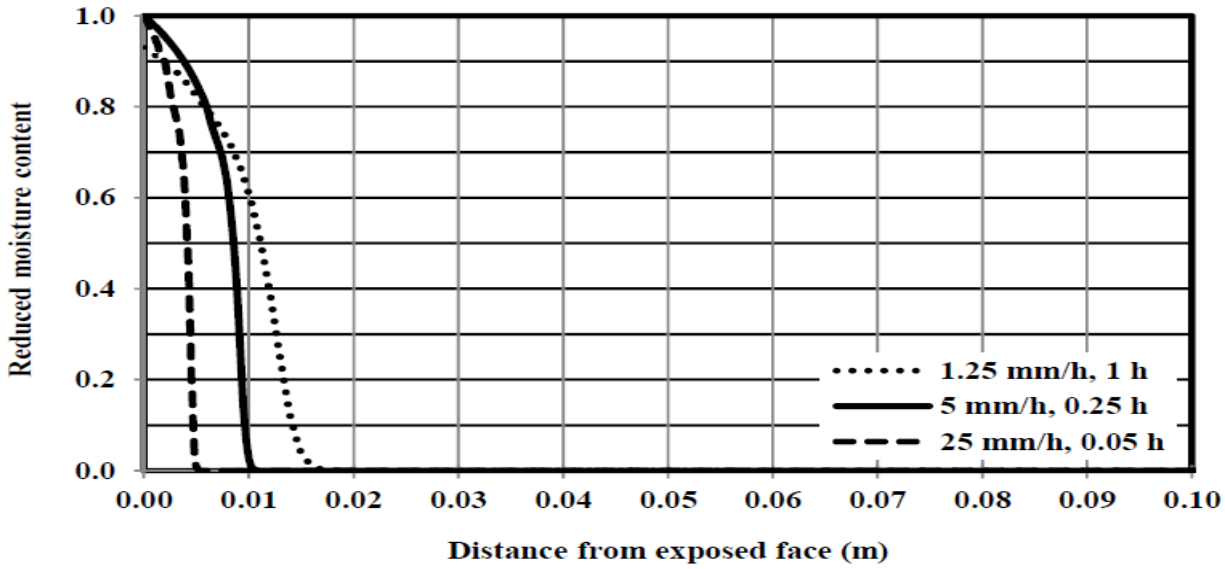

Figure 4: Profiles of moisture penetration for concrete exposed to light, medium and high-intensity rain each with the same quantity of impinging water due to decreasing exposure times with increasing intensity. (Sarkar & Bhattacharjee, 2014)

2.2.5.2. Cover depth and quality

The thickness of the concrete cover has an influence on the rate of reinforcement corrosion as moisture, oxygen and aggressive chemical species such as carbon dioxide and chlorides must pass through the cover first before reaching the reinforcement. The onset of reinforcement corrosion grows closer as the harmful agents progress towards the reinforcement and with a greater depth to penetrate through (thicker cover), it will take longer for active corrosion to begin. Lower cover depths also facilitate for faster rates of corrosion propagation due to the increased availability of moisture and oxygen and the more regular occurrence of wetting/drying cycles. The quality of the cover also plays an important role in allowing harmful species to progress through the concrete as the quality influences the permeability. Thus, with improved quality, the rate of reinforcement corrosion will be slowed (Arito, 2017; Otieno, et al., 2010).

2.2.5.3. W/b ratio

The water/binder ratio has an impact on the penetrability of the concrete due to its influence on the concrete pore structure. As the w/b ratio increases so does the rate of reinforcement corrosion and vice versa (Arito, 2017; Otieno, et al., 2010). Due to the lower penetrability of the concrete at a lower w/b ratio, it becomes more difficult for both oxygen penetration and chloride diffusion to take place thus leading to a reduction in the rate of corrosion initiation. Concrete with a lower w/b ratio has greater resistivity. The increased resistivity reduces the ease with which current by ionic transport can flow through the concrete. A lower w/b ratio thus also leads to a reduction in the rate of corrosion propagation (Otieno, et al., 2010).

2.2.5.4. Binder type

The rate of reinforcement corrosion decreases when cement extenders are used in the concrete mix, instead of using plain Portland cement concrete. The cement extenders increase the chloride binding capacity, thus reducing the number of free chlorides, which are present by binding with the chloride ions. They also result in the concrete microstructure being denser, thus reducing the penetrability of the concrete and increasing the time taken for corrosion inducing substances to reach the level of the reinforcement. These factors thus hinder the initiation of the corrosion process (Arito, 2017). Cement extenders do not only have an influence on corrosion initiation but can play an important role in reducing the rate of corrosion propagation. This occurs largely as a result of the increase in resistivity of the concrete that occurs when extenders such as fly ash, slag and silica fume are used. The increased resistivity reduces corrosion currents thus slowing the rate of corrosion propagation (Otieno, et al., 2010).

2.2.5.5. Temperature

The rate of the chemical reactions in the corrosion process increases as the temperature increases; this is because both oxygen solubility and electrode reaction rates tend to increase due to the temperature increase (Zivica, 2003). A limiting maximum temperature exists, above which the rate of reinforcement corrosion propagation begins to slow again. This temperature is found to be at 40 degrees Celsius and the reason for this effect is due to oxygen solubility decreasing above this temperature and moisture being driven away (Arito, 2017; Otieno, et al., 2010).

2.2.5.6. Cover cracking

The presence of cracks in the concrete cover tends to speed up the reinforcement corrosion process, as these cracks make it easier for aggressive agents to enter the concrete by reducing its penetrability. In uncracked concrete, the permeability of the concrete depends on the concrete pore structure. In cracked concrete transport of moisture, oxygen and aggressive species is a coupled phenomenon between the combination of cracks and the pore structure. The cracks are however more important than the pore structure. To what degree the impact of these cracks influences the corrosion process depends on several

factors such as the crack characteristics, depth of the cover and the quality of the concrete. Higher quality concrete such as concrete made with cement extenders corrodes at a slower rate than Portland cement concrete under the effects of cracking. Cover depth has an even more significant effect than concrete quality, with greater cover depths leading to a significant reduction in the corrosion rate (Arito, 2017 & Otieno, et al., 2010).

The permeability of concrete can be significantly affected by crack properties such as the width, frequency, orientation and dormancy or activity of the cracks. Both wider and more frequent cracks increas the permeability of the concrete thus reducing the time to corrosion initiation and increasing the rate of corrosion. Should the cracks be longitudinal then the risk of corrosion increases as it becomes easier for corrosion inducing substances to penetrate to the depth of the reinforcement and attack larger areas of steel. When it comes to the dormancy or activity of the cracks, cracks that are dormant due to self-healing lead to the concrete being less penetrable, whereas cracks that are frequently open allow for an increased rate of corrosion (Otieno, et al., 2010).

The resistivity in concrete that is saturated or near-saturated remains the same whether the concrete is cracked or not (Otieno, et al., 2010). Concrete cover depth measurements also remain constant regardless of the presence of cracks. The cover depth and resistivity tests are often used in condition assessments to determine the risk of reinforcement corrosion of a structure. Since these tests do not consider the influence that cracking can have on reinforcement corrosion, they can lead to an underestimation of any such risk.

2.2.6. Carbonation

During carbonation, chemical reactions take place where carbon dioxide reacts with the alkalinity of the cement leading to the formation of calcium carbonate and a consequent drop in the pH levels of the concrete (Andrade, 2007). The process starts when carbon dioxide from the environment moves into the concrete through the process of diffusion. Once the carbon dioxide is in the concrete it reacts with the moisture that is present in the concrete pore solution and results in the formation of a weak carbonic acid as shown in Equation 3 (Otieno, 2014). The carbonic acid that is formed then dissociates into CO_3^{2-} and OH^- ions. These ions react with calcium hydroxide and this leads to the formation of the calcium carbonate precipitate as seen in Equation 4 (Arito, 2017; Tuutti, 1982). Calcium is responsible for the high pH of the concrete pore solution. As the calcium levels become depleted through the carbonation process, the pH begins to drop (Otieno, 2014). The drop in the pH levels is from values above 12 to values between 8.5 and 9. The consequence of this drop in pH is the destruction of the protective passive layer, so once this carbonation front reaches the level of the reinforcement, with oxygen and water available, corrosion begins (Broomfield, 2007; Otieno, et al., 2010).

$$CO_2 + H_2O \rightarrow H_2CO_3 \quad \text{... (3)}$$

$$H_2CO_3 + CA(OH)_2 \rightarrow CaCO_3 + 2H_2O \quad \text{... (4)}$$

2.2.7. Chloride attack

Chloride attack differs from carbonation induced reinforcement corrosion in that the corrosion does not progress in a front, but rather leads to localized destruction of the passive layer when a critical chloride concentration is achieved. This critical chloride concentration is known as the chloride threshold. The chloride ions that lead to the destruction can either be present as a part of the concrete mixture or as a result of external sources, which lead to these ions penetrating the pore solution (Andrade, 2007; Tuutti, 1982). The internal source of chlorides in the concrete mixture may be due to the use of admixtures such as $CaCl_2$ or salt contaminated raw materials. The two main external sources of chlorides come from exposure to seawater in coastal areas and the use of de-icing salts in the colder regions of the world. These are however not the only sources of external chlorides and other sources include for example contaminated soils, PVC fires, salt sprays and industrial brine (Arito, 2017; Otieno, 2014).

Chloride ions lead to the formation of hydrochloric acid within the concrete pore solution and this acid contributes to the destruction of the passive layer. The destruction occurs in localized areas that form the anodic region, while the steel, which remains under passive protection, forms the cathodic region. The reinforcement corrosion that occurs, as a result, is a pitting type of corrosion due to the localized nature of the chloride attack. It is said that the chloride ions react with iron ions to form chloride or oxychloride compounds, which in turn reacts with the moisture leading to the formation of the hydrochloric acid as shown in Equations 5 and 6 (Melchers & Li, 2006).

$$Fe^{2+} + 2Cl^{-} \rightarrow FeCl_2 \quad \text{... (5)}$$

$$FeCl_2 + 2H_2O \rightarrow Fe(OH)_2 + 2HCl \quad \text{... (6)}$$

There is no single unique value for the chloride threshold as it is dependent on several factors such as the following (Andrade, 2007; Hansson, et al., 2012; Otieno, 2014):

I. Curing and compaction.
II. Type and surface area of the cement.
III. Concrete mix proportions.
IV. W/b ratio.
V. Use of supplementary cementitious materials.
VI. Availability of oxygen.
VII. Temperature and relative humidity.
VIII. Reinforcement type and finishing.

2.3. Condition assessment procedures

Condition assessment tests for corrosion monitoring of reinforced concrete structures can be semi-destructive or non-destructive. The semi-destructive tests require the removal of samples or a minor breach of the integrity of the structure, whereas non-destructive tests do not breach the integrity of the structure (HOŁA, et al., 2015). The tests aid in the provision of knowledge on the deterioration processes to which the structures are exposed and the current conditions that the structures are in (KURZ, et al., 2012). Each test has its advantages and disadvantages and it is usually the case that several tests are used in combination to formulate the best conclusions on the state of a structure. The condition assessment tests aid in early detection of distress and deterioration, enabling repair rehabilitation and maintenance before replacement becomes necessary (Jedidi & Kaouther, 2014).

2.3.1. Visual assessment

The visual assessment forms the first part of a condition assessment with the aim of identifying areas of potential risk. This assessment creates the basis for further testing or immediate repair and rehabilitation in critical cases. For this visual assessment both the visible parts of the structure as well as the environment with which the structure interacts are assessed. The visual examination details the levels and locations of deterioration observed on the structure and allows inferences to be made as to the cause of the damage based on knowledge of deterioration mechanisms (Phares, 2001). The best inspections come from trained individuals who carry out the assessments using inspection manuals and defined codes as their guideline (Omar & Nehdi, 2016).

Some common defects, which are found on the structure during the visual inspections, include cracks in the concrete, concrete spalling & delaminations (commonly found around the locations of the reinforcement bars), discolouration, leaching, rust stains, etc. To assess these defects properly it is often necessary to use cameras, magnifying glasses and binoculars so that one can get a clearer image of the finer details and view defects that are further away and difficult to access. Sometimes ladders or scaffold towers are used to allow access to areas that would otherwise be out of view or reach. Other important tools, which tend to be used on these inspections, include gauges for crack width measurements, chisels, hammers, pocketknives and screwdrivers (Al-Neshawy & Sistonen, 2015). The camera is not only used to get a clearer image of hard to access areas but is also necessary to take close-up and perspective scale photographs which are used to document and further analyse conditions in key locations. The recording of videos may also be useful when they provide a visual dimension, which the still photographs fail to show (ACI, 2008).

2.3.1.1. Common reinforcement corrosion-induced defects

There are certain defects which occur because of reinforcement corrosion and which serve as a guide in the visual inspection when trying to ascertain the cause and level of damage of a concrete structure and making decisions concerning further investigations. These defects include the following: (ACI, 2008; Beushausen, 2017)

- **Cracking**: cracks in concrete may occur due to a number of reasons but cracking as a result of reinforcement corrosion tends to occur at locations above the reinforcement due to the rust that forms between the concrete cover and the reinforcement.
- **Delamination**: a delamination is a separation of a piece of concrete cover along a plane parallel to the surface. Delaminations as a result of corrosion are also found above the location of the reinforcement.
- **Spalling**: when a delaminated piece of concrete detaches from the concrete mass and falls off. This often leads to the corroding reinforcement that was situated beneath the piece of concrete that had fallen off, becoming exposed.
- **Rust stains**: stains on the surface of the concrete above the location of the reinforcement. These stains have an orange-red or brown colour like that of the rust.

Images of these types of defects are shown in Figures 5-8.

Figure 5: Reinforcement corrosion-induced cracking. (Gromicko & Shepard, 2006)

Figure 6: Delaminated concrete

Figure 7: Concrete, which has spalled

Figure 8: Rust staining

2.3.1.2. Advantages and disadvantages of the visual assessment

The visual inspection is very important and may be considered the primary tool in condition assessments. It also has the advantage of being both inexpensive and quick to carry out (Alsharqawia, et al., 2018). It is very important to conduct rapid investigations in many cases and particularly following the occurrences of natural disasters as quick decisions need to be made to ensure that no lives are put at risk from using any building which may have become compromised. One disadvantage of visual inspections is that the results are not always reliable since they are based largely on the experience and knowledge of the inspectors and hence decisions tend to be qualitative and subjective (Alsharqawia, et al., 2018; Broomfield, 2007; Omar & Nehdi, 2016). A second disadvantage is that these inspections only detect damage once it can be seen and it sometimes happens that the damage which is witnessed on the surface may appear to be minor, but the inner concrete layers have become significantly damaged (Phares, 2001).

2.3.2. Chloride testing

It is important to be able to determine what type of reinforcement corrosion is occurring and what may be the source of potential corrosion so that corrosion can be prevented, or the best method of repair or maintenance can be undertaken should corrosion already be taking place. Chloride-induced reinforcement corrosion is common in coastal areas and in countries where de-icing salts are used to clear snow build up. Reinforcement corrosion due to chlorides can result in serious consequences and it is important that a reliable chloride analysis for concrete structures exists so that evaluations of structures can take place and predictions of remaining service life can be made possible (RILEM, 2002).

Destructive tests, which require the removal of concrete cores from structures, are very commonly used for chloride analysis tests (Otieno, 2014; Price, 1985; RILEM, 2002; TxDOTa, 2005; TxDOTb, 2005). The British standard BS-1881 Part 124 recommends that at least 2 samples be taken when information about the constituents of a volume of concrete up to 10 cubic meters is needed and at least 10 samples are taken when analysing very large volumes of concrete. This can help to find areas that require further investigation (BS-1881, 1988). To determine the probability of reinforcement corrosion, the concentration of chloride ions need to be determined at various depths to see how far the ions have progressed from the surface of the structure towards the reinforcement. For this purpose, the concrete cores that are extracted are usually taken to a lab where they are cut into thin slices of ±10 mm before each slice is ground into a powder (Otieno, 2014).

On occasions dust drillings are taken directly from a structure instead of extracting cores, this is also done in increments of depth. A sufficient amount of concrete dust must be collected for each depth to ensure that the sample is representative, and care must be taken to ensure that all the dust is collected for testing as studies have shown that a large amount of chlorides is found in the finer dust components. Once the powder samples from either the dust collections or ground slices are ready, acids are used to remove the chlorides from the powder; thereafter a chemical analysis is performed on the chloride solution to determine the chloride content (Otieno, 2014).

2.3.2.1. Non-destructive alternatives

Non-destructive techniques for the chloride analysis of reinforced concrete do exist and are mainly centred on electrochemical and electromagnetic techniques. These electrochemical and electromagnetic techniques work either through the use of sensors that are embedded in the concrete or through the use of external measurements. Literature on non-destructive techniques for chloride analysis has been found to be present for over two decades but the challenge remains to find a reliable technique that will allow the concrete to be adequately monitored and maintained (Abbas, et al., 2018).

2.3.3. Carbonation testing

The most common way to test for the carbonation depth of concrete involves using a phenolphthalein solution as an indicator. Phenolphthalein is a crystalline material, which is usually white or pale yellow in colour. The crystalline material is dissolved in a solvent such as isopropyl alcohol for use as an indicator. (Winter, 2012). The indicator forms part of the proposed methods in most standards for determining carbonation depths (Choi, et al., 2017). The normal pH value of concrete is usually higher than 12, but less alkaline concrete with pH values lower than 12 are sometimes used. The pH value of concrete falls when it is subject to carbonation attack and can drop to a value as low as 7. The protective layer surrounding the reinforcing steel starts to depassivate when the pH drops to values below 11 and this leads to the occurrence of reinforcement corrosion (Chandra Paula, et al., 2018).

The phenolphthalein indicator works by changing colour when applied to concrete with high alkali levels (the non-carbonated concrete). The colour changes to a pink/purple colour when it is applied on freshly exposed concrete. On the other hand, the indicator remains colourless when applied to concrete that has undergone carbonation. It is this distinction in colour difference when the indicator is applied to carbonated and non-carbonated concrete that makes it possible to measure the carbonation depth (Chandra Paula, et al., 2018; Broomfield, 2007; Lee, et al., 2012). An illustration of the colour change that occurs is shown in Figure 9.

2.3.3.1. Advantages & disadvantages of carbonation testing

The use of the Phenolphthalein indicator has its shortfalls. The indicator turns to the pink/purple colour when applied to concrete with a pH greater than 8.6 and so will remain colourless when the pH is below this value. Depassivation of the corrosion protective layer begins to occur at pH levels below 11 and so concrete at a pH level where depassivation has already begun to occur may still display a pink/purple colour down to pH levels of 8.6. The change in colour at pH levels closer to 8.6 is usually of a faintly discernible slightly pink colour and so this is easier to identify as likely carbonated than pH levels above 9 or 10 which show a strong colour change when the indicator is applied. The indicator test is thus likely to underestimate the actual depth of carbonation (Lo, 2005; Tuutti, 1982; Winter, 2012). The phenolphthalein indicator remains very popular although it has deficiencies. This is in part because it is quick, simple and the cheapest and easiest method to carry out (Dayaram, 2010). It also creates a continuous line representing the carbonation front thus creating a good visual aspect, especially for initial assessments (Winter, 2012).

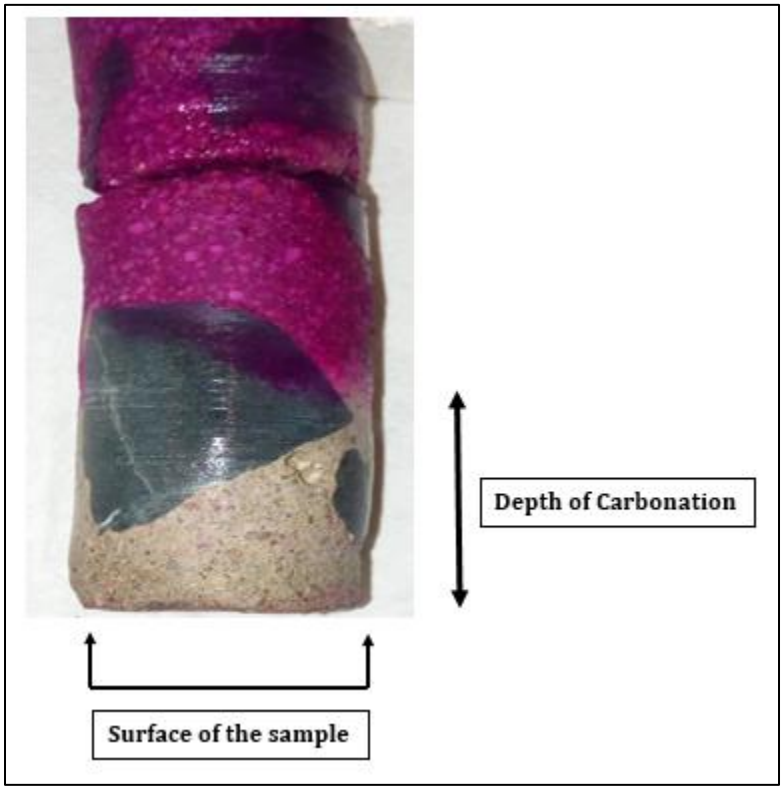

Figure 9: Indicator colour change on a carbonated concrete sample

2.3.3.2. Methodology

When taking specimens for testing it is important to take samples from more than one location so that an average value that is more representative of the state of the structure, location or structural member can be obtained (Chandra Paula, et al., 2018). Fresh cores are usually extracted from the structure to be used as a sample. The longer the sample is left the more skewed the readings become as contamination of the samples makes it more difficult to observe the colour change. It is, therefore, best to apply the phenolphthalein as soon as possible after the removal of the sample; sometimes this is done on-site before transportation to the lab even takes place. When applying the phenolphthalein in a short period after extraction is not possible, it is recommended to cut through the centre of the sample and apply the phenolphthalein on the cut area for measurements (Lee, et al., 2012). It is also possible to do a quick preliminary assessment before removing samples, by chipping off pieces of concrete at different locations and applying the indicator to these chipped spots (Sagues, et al., 1997). For more accurate maximum, minimum and average depth measurements, vernier callipers are often used (Choi, et al., 2017) and in cases where a greater accuracy than this is needed a microscopic examination is performed (Winter, 2012).

2.3.4. Cover depth

Concrete cover at any location in a structure is defined as the thickness of the concrete from the surface of the member to the top of the reinforcing bar that is embedded in the concrete (Barnes & Zheng, 2008). The concrete cover layer is crucial for maintaining the durability of a structure as it is the layer through which harmful gases, liquids and ions from the environment need to pass through before these substances can cause deterioration of the structure (Otieno, 2014).

In practice, it becomes very important to determine both the locations and sizes of the embedded reinforcement bars and whether the cover depths are adequate at the various points in the structure. Knowing the depth of the cover is important to ensure that requirements have been met, so as to provide a good condition assessment and quality maintenance and rehabilitation programmes. Knowing the diameters and locations of the reinforcement bars are key to understanding both bar spacing and placement when existing drawings are not available. These details are also important for other condition assessment tests such as tests that require coring as well as the half-cell potential and resistivity tests. Concerning concrete cores, these details are needed, as they will provide the guide for safe locations to remove cores so that reinforcement bars are not cut and hence the ductility and tensile strength of the structure will not be compromised (Sivasubramanian, et al., 2013). Details pertaining to the importance of knowing the reinforcement information for half-cell potential and resistivity tests will be discussed in subsequent sections.

2.3.4.1. Covermeter

A covermeter is a device that allows for the determination of cover depth as well as the location and orientation of rebars and in some cases the rebar diameters (Elcometer, 2012; Sivasubramanian, et al., 2013). The device is an electromagnetic one composed of a search head and a control box. The outputs from the older and newer devices tend to be different. A number of the older devices have an analogous output where a needle moves across a scale. The newer devices have a digital readout and may create a sound, which gets louder as the search head nears the point on the concrete surface below which the reinforcement lies (ConcreteSociety, 2018).

Covermeters are based on the induction principle, which is applied to the ferromagnetic reinforcement material. The device has a primary coil and a secondary coil. The primary coil delivers a 10-50 Hz alternating current from a power supply, while the secondary coil feeds into an amplifier circuit. When there is no ferromagnetic material nearby the coils, the primary coil only induces a minor voltage in the secondary coil, but when a ferromagnetic material is in close vicinity of the coil a much larger voltage is induced in the secondary coil, which increases until the coils are right over the location of the reinforcement material. How large or how small the induced signal in the secondary coil is, depends on the location, geometry and magnetization characteristics of the rebar (Malhotra & Carino, 2004).

2.3.4.2. Methodology

The test itself is not time-consuming, as it simply requires running the search head slowly across the concrete surface and using the device outputs to obtain the required data for interpretation and mapping (ConcreteSociety, 2018). The first step in the process involves locating the reinforcement bars. The appropriate search head must be connected to the covermeter and then the covermeter must be zeroed. When moving the search head across the concrete, it must be aligned differently and moved in different directions for the location of vertical and horizontal reinforcement respectively. For the location of the vertical reinforcement, the search head must be aligned parallel to the vertical bars and then moved from side to side, whereas for the location of the horizontal reinforcement the search head must be aligned parallel to the horizontal bars and moved up and down. The location of a bar will be found when the signal from the covermeter reaches a peak and the cover depth reaches a minimum as the search head is being moved along the concrete. The signal may be in the form of a sound, light, bar display or a combination of these (Elcometer, 2012).

As the locations of the reinforcement bars are found, they should be marked off using chalk. Once the full area for testing has been marked off, the cover depths at required locations can be recorded. Here the appropriate bar diameter needs to be input into the covermeter, thereafter the covermeter must be zeroed. The search head can then be placed on a location along the mapped-out reinforcement and the cover depth measurement at that location can be recorded. This should be done for as many locations as is deemed adequate to map out the cover depths in a particular area or to meet the purpose for which the cover depths are being measured (Elcometer, 2012).

The exact time of the test will depend on the size of the structure and how much of the structure needs to be analysed. Where it is necessary for a large area to be covered, it can become very time-consuming to use a hand-held device to map the entire area and this has led to the development of a rolling covermeter by the US Federal Highway Administration. This device was found to work at speeds 20 times faster than the hand-held devices and proved rather accurate and reliable (Malhotra & Carino, 2004).

When it comes to assessing the quality of the concrete cover on a structure a choice needs to be made as to how much of the structure needs to be surveyed in order to draw appropriate conclusions. To survey the whole structure would be far too time-consuming, particularly when assessing larger structures. One option for reaching suitable conclusions is to group similar structural elements together and then analyse them as a normal statistical population to determine how many points should be surveyed to draw adequate conclusions on the state of a structure. A second option, which does not require the manual computation of sample sizes, involves using specifications, which provide the minimum expected testing requirements. An example of such a specification can be found in Vic Roads section 610.33, which states that at least 10 readings should be taken in a 3 m^2 area for every 25 m^2 of area along a new construction (PCTE, 2014).

Standards and guidelines provide information on the minimum cover depths which are needed to ensure a low risk of reinforcement corrosion and also provide information on how to carry out cover depth measurements. What is lacking in these standards and guidelines is information on how to assess the measurements that are obtained, and this is important for a condition assessment. Recommendations on

how to assess measured concrete cover depths for a quality assessment are also found to be lacking in most countries. The EN standards do not provide sufficient recommendations on the assessment of concrete cover depth, while the UK guidelines only provide information on how to use covermeters. A few guidelines for the practical assessment of concrete cover depths for quality control purposes have been developed. Methods include the RILEM suggested methods, methods by the German Concrete & Construction Association and those developed by the Building and Construction Authority of Singapore (Corbett, 2015). The RILEM and German suggested methods are discussed in the sections to follow.

2.3.4.3. RILEM methods for assessing conformity (Monteiro, et al., 2015)

Construction of structures or structural members, which do not meet the required cover depth specifications, is a major cause of early failure in reinforced concrete structures. Most available standards and codes for durability design and control require that a safety depth be added to the specified minimum cover depth in order to combat inconsistencies or faults in construction. What the codes seem to lack are tools for guidance on how to assess the actual cover depths, which are achieved in structures. It is impractical to assess the entire structure and so the European Standard EN 13670:2009 suggests using a statistical method to ensure that a sufficient number of measurements are equal to or greater than the minimum required cover depth. The standard, however, fails to provide direction on how to perform such a method.

RILEM TC 230-PSC aims to solve this problem by providing a basis for the evaluation of measured cover depths in reinforced concrete structures. It provides several methods for evaluation of cover depths based on quantitative or qualitative inspections, including a section that describes the procedures used in a German code of practice. The methods of the German code of practice have been found to be some of the best standardized approaches for assessing the minimum cover depth in a reinforced concrete structure when using a statistical approach.

The three RILEM procedures each begin in a similar way, where the cover depth population that is to be inspected is first selected. The sampling method and sample size are then chosen, following which cover depth measurements are taken at these locations using a calibrated covermeter. When defining the cover depth population, it should be selected such that the areas comprising the population will concern a specific reinforcement layer with the same requirements in terms of cover depth. The reinforcement layer should also belong to elements which have similar dimensions, the same construction procedure and construction team and where possible the same bar and spacers detailing.

The sample points should be fairly distributed over the concrete surface of the set-out population. Random sampling is often used for the selection of sample points, however, to try to avoid spatial autocorrelation it is suggested that the measurement points are regularly spaced over the population by using a systematic sampling method. Autocorrelation because of reinforcement continuity and rigidity may mean that neighbouring areas of measurement will show similar deviations from the mean value and thus lead to the assumption of statistical independence being violated. To minimise the spatial

autocorrelation there should be a distance between successive measurement points. The choice of the sample size will depend on the structural importance, population size and inspection costs. Greater sample sizes tend to lead to a more precise analysis. Once the sample points have been defined, the measurements should be taken following the instructions found in the covermeter manual.

Procedure 1: Quantitative inspection:

This procedure assumes that the cover depth population follows a normal or lognormal distribution. The procedure does not work well when assessing areas with geometrical discontinuities, single surfaces with limited size and common columns and beams. This is because it is difficult to approximate these populations using well-known statistical distributions and so procedures 2 and 3 or the German qualitative approach may prove more suitable. The normal distribution is often the distribution of choice as it is well understood and has been proven suitable on a large number of occasions. The lognormal distribution is however found to be the better option when the mean cover depth is low, in the region of approximately 20mm, as this distribution does not allow for the occurrence of negative values. Once the appropriate distribution has been chosen, the actual minimum cover depth will be determined by using the one-sided tolerance limit calculations shown in Equations 7 & 8.

Tolerance limit calculation for a normal distribution:

$$c_{min}, \text{estimated} = \bar{c} - ks \quad \ldots (7)$$

Tolerance limit calculation for a lognormal distribution:

$$c_{min}, \text{estimated} = e^{\bar{c}ln - k \cdot sln} \quad \ldots (8)$$

Where:

c_{min}: actual minimum cover depth

$\bar{c}$: mean of the normal distribution

s : standard deviation of the normal distribution

$\bar{c}ln$: mean of the lognormal distribution

sln : standard deviation of the lognormal distribution

k : tolerance factor

The tolerance factor k depends on three factors, namely the size of the population, the desired confidence level and the percentile on which the required minimum cover depth is based. A section of

the table from which the tolerance factor is obtained is shown in Table 1. Once the actual cover depth has been calculated, the conformity of the population can be determined by checking to see whether the actual cover depth of the population is equal to or greater than the minimum required cover depth.

Table 1: Table used to obtain tolerance factors for RILEM procedure 1 (Monteiro, et al., 2015).

Sample size (N)	k value for the 5th percentile				k value for the 10th percentile			
	Confidence level (1-y)				Confidence level (1-y)			
	50%	75%	90%	95%	50%	75%	90%	95%
10	1.7	2.1	2.57	2.91	1.32	1.67	2.07	2.35
11	1.7	2.07	2.5	2.81	1.32	1.65	2.01	2.28
12	1.69	2.05	2.45	2.74	1.31	1.62	1.97	2.21
13	1.69	2.03	2.4	2.67	1.31	1.61	1.93	2.16
14	1.68	2.01	2.36	2.61	1.31	1.59	1.9	2.11
15	1.68	1.99	2.33	2.57	1.31	1.58	1.87	2.07
20	1.67	1.93	2.21	2.4	1.3	1.53	1.77	1.93
25	1.67	1.89	2.13	2.29	1.3	1.5	1.7	1.84
30	1.66	1.87	2.08	2.22	1.29	1.47	1.66	1.78
40	1.66	1.83	2.01	2.13	1.29	1.44	1.6	1.7
50	1.65	1.81	1.97	2.06	1.29	1.43	1.56	1.65
60	1.65	1.79	1.93	2.02	1.29	1.41	1.53	1.61
80	1.65	1.77	1.89	1.96	1.29	1.39	1.49	1.56
100	1.65	1.76	1.86	1.93	1.29	1.38	1.47	1.53
120	1.65	1.75	1.84	1.9	1.28	1.37	1.45	1.5
150	1.65	1.74	1.82	1.87	1.28	1.36	1.43	1.48
190	1.65	1.73	1.8	1.85	1.28	1.35	1.42	1.46
200	1.65	1.72	1.79	1.84	1.28	1.35	1.41	1.45
300	1.65	1.71	1.76	1.8	1.28	1.34	1.39	1.42
400	1.65	1.7	1.75	1.78	1.28	1.33	1.37	1.4
Infinity	1.64	1.64	1.64	1.64	1.28	1.28	1.28	1.28

Procedure 2: Qualitative inspection:

Unlike the first procedure, this procedure does not use an assumed statistical distribution for the population of cover depth measurements. This procedure follows the same initial steps as previously discussed, up to and including the point where the actual cover depth measurements are taken using the covermeter. The difference between procedure 2 and procedure 1 comes into play when evaluating the conformity of the population. In this case, the conformity is evaluated by checking to see how many actual cover depth measurements fall below the required minimum cover depth and whether this is less than or equal to a given acceptance number.

The acceptance number depends on three factors, namely the size of the sample, the percentile on which the minimum required cover depth is based and the level of risk that the owner accepts to take. The sample size and risk taken by the owner should be agreed upon before the measurements are taken, should they not have previously been addressed. A section of the table that is used to determine the acceptance number can be seen in Table 2.

Table 2: Section of the table used to determine the acceptance number for RILEM procedure 2 (Monteiro, et al., 2015).

Sample size (N)	Acceptance number, Ac							
	5th percentile				10th percentile			
	Maximum owner's risk				Maximum owner's risk			
	50%	25%	10%	5%	50%	25%	10%	5%
10	1.7	2.1	2.57	2.91	1.32	1.67	2.07	2.35
11	1.7	2.07	2.5	2.81	1.32	1.65	2.01	2.28
12	1.69	2.05	2.45	2.74	1.31	1.62	1.97	2.21
13	1.69	2.03	2.4	2.67	1.31	1.61	1.93	2.16
14	1.68	2.01	2.36	2.61	1.31	1.59	1.9	2.11
15	1.68	1.99	2.33	2.57	1.31	1.58	1.87	2.07
20	1.67	1.93	2.21	2.4	1.3	1.53	1.77	1.93

Procedure 3: Qualitative inspection - Large Lots

This procedure like procedure 2 does not make use of an assumed statistical distribution for the population of cover depth measurements. This method is suitable for large lots or lots where the accessibility is hindered. A lot is defined as the number of concrete elements or surface zones, which have cover depths that are assumed to be from the same population. With this method, a small number of elements or subdivisions on long elements are tested in detail, instead of focusing on dispersed individual measurements.

The initial steps for this procedure are similar to that of the first 2 procedures although there is a difference when defining the sampling method and size. When using this method, the spatial autocorrelation is not taken into account as the locations chosen for inspection are tested in detail to get a confident estimate in each location. Prior to choosing the locations for measurements, the lot should be evenly separated into units with the same dimensions as far as is possible. From here, a well-distributed sample of these locations must be chosen at random for inspection.

When it comes to assessing the conformity of the lot, each unit must first be assessed to determine whether it is deemed defective. This is based on how many measurements on a unit are found to be lower than the required minimum depth and whether the number of measurements is greater than a given percentage of 5 or 10%. The next step is then to ascertain whether the number of defective units is less

than or equal to an acceptance number. The acceptance number depends on the size of the lot, the sample size, the risk percentage that the owner accepts to take as well as the allowed percentage of defective units in the lot. To get the acceptance number, the cumulative distribution function of the hypergeometric distribution given in Equation 9 must be solved for the highest value of acceptance number that satisfies the inequality. This approach is also used in the international standard ISO 2859-2. The standard uses the lot size and limiting quality (percentage of defective units found in the lot) to give both the sample sizes and acceptance numbers.

$$\sum_{I=N-A_c}^{N} \frac{\binom{N_{lot}-p.N_{lot}}{i}\binom{p.N_{lot}}{N-i}}{\binom{N_{lot}}{N}} \leq owner's\ risk \quad \ldots(9)$$

Where:

N_{lot} : size of the lot
N : sample size
p : allowed percentage of defective units
A_c : acceptance number

2.3.4.4. German code of practice

The German code describes both a qualitative and quantitative method for checking whether the required minimum cover depth has been achieved. Both methods work by checking whether the percentage of cover depth values in a sample of measurements which fall below the minimum required cover depth is found to be less than or greater than a given percentage. The percentage depends on how much tolerance was added to the minimum required cover depth in order to deal with construction issues. This percentage is 10% (10^{th} percentile) for a tolerance of 10 mm and 5% (5^{th} percentile) for a tolerance of 15 mm. The measurement points should be taken along comparable measurement surfaces and should be widely and randomly distributed along each surface.

Qualitative procedure

There are minimum required sample sizes to start the procedure. The sample sizes depend on whether the percentage mentioned earlier is 10% or 5%. Should the percentage be 10% then the minimum sample size needed for the method is 10 and should it be 5% then the minimum sample size needed is 15. To check the conformity of the population the number of measurements, which fall below the required minimum cover depth, is checked against an acceptance number. This number depends on the sample size and percentile as is obtained from Figure 10.

Quantitative procedure

This method makes use of the Neville distribution in the statistical analysis. Like the lognormal distribution, the Neville distribution does not allow for negative values. In order to use this procedure, the

sample size must contain at least 20 measurements. Once all the measurements have been taken, the sample median and smallest value must be determined in order to calculate the upper limit. Should any measurement fall above this upper limit then it will be considered as an outlier and will be left out of the sample, requiring a new median to be determined.

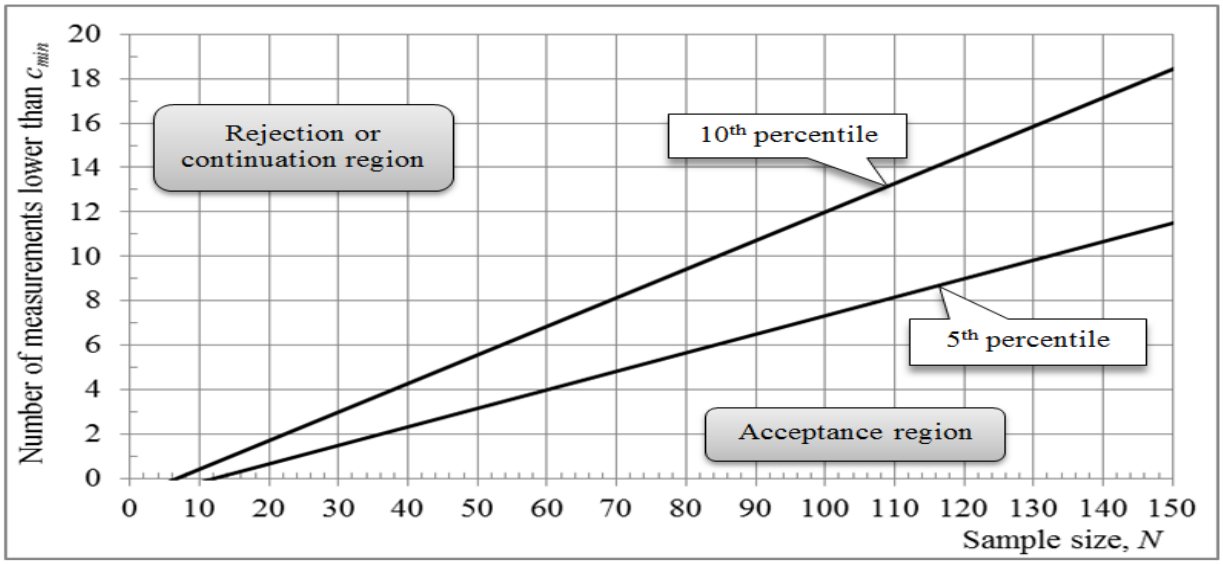

Figure 10: Graph to obtain the acceptance number for German qualitative procedure (Monteiro, et al., 2015).

There are two methods for checking whether the cover depth population conforms to the requirements when using this quantitative procedure. The first method uses a cumulative distribution function of the Neville's distribution to estimate what proportion of cover depth values from the population is likely to fall below the minimum required cover depth. This cumulative distribution function (FX) is shown in Equation 10. The second method uses the inverse of the cumulative distribution of the Neville's distribution to estimate the 5th or 10th percentile of the cover depth population c(x). The Equations for the 5th and 10th percentile is shown in Equations 11 and 12 respectively. For conformity using the first method, FX must be less than or equal to the proportion of the population of cover depth values which are permitted to be less than the minimum required cover depth. Using the second method, conformity is achieved when the value of c(x) is found to be greater than or equal to the minimum required cover depth.

$$\mathrm{FX} = \frac{\left(\frac{x}{r}\right)^m}{1+\left(\frac{x}{r}\right)^m} \quad \ldots (10)$$

$$c(5\%) = \frac{r}{19^{\frac{1}{m}}} \quad \ldots (11)$$

$$c(10\%) = \frac{r}{\frac{1}{9\bar{m}}} \quad \text{... (12)}$$

Where:

$r = \frac{\bar{c}+\bar{c}m}{2}$ ... (13) And $m = 1.8\left(\frac{r}{s}\right)$ ... (14)

s : standard deviation of the cover depth sample
$\bar{c}$: mean of the cover depth sample
$\bar{c}m$: median of the cover depth sample
x : minimum required cover depth

This procedure is similar to RILEM procedure 1. It differs mainly in that it uses a different statistical distribution in the form of the Neville's distribution. The use of a cumulative distribution function instead of tolerance limits means that the statistical uncertainty as a result of the limited size of the sample, is not considered.

2.3.4.5. Limitations of covermeters

In many covermeters, it is necessary to first input the bar diameter. For this purpose, it may be necessary to expose the reinforcement so that the diameter can be measured. This will lead to some destruction of the cover (ConcreteSociety, 2018). For covermeters that can measure rebar diameters, it is necessary to choose a location in the structure with sufficient spacing between the rebars so that the results are not falsely influenced (Sivasubramanian, et al., 2013). Other factors which are found to influence cover depth measurements include the effects of neighbouring bars parallel to the bar under consideration, the input bar diameter, the different types of search heads or setting on the search head and the scan location when there are secondary bars below the bar being measured. Some less influential factors include changes in the properties or cross-sections of the reinforcement, roughness of the concrete surface and magnetic effects from the aggregate mix of the concrete (Barnes & Zheng, 2008). It is important that all the limitations are considered when inspections are carried out.

2.3.5. Half-cell potential measurements

There are times when it becomes clear that reinforcement corrosion is present such as in cases where spalling occurs over the reinforcement or discolourations occur, but these visual keys are only useful in structures where they are visible and many a time reinforcement corrosion has already started progressing without any of these visual indicators being present. When the effects of reinforcement corrosion are not clear, it becomes important for condition assessments, maintenance and rehabilitation that we are able to determine whether the corrosive process has begun or not (Coimbatore, 2014).

The half-cell potential technique is one test method that helps to aid in such determinations in a non-destructive way and can thus be very important in preventing the occurrence of unforeseen failures (Coimbatore, 2014). The difference in voltage between the actively corroding and passive zones causes current to flow from the anode to the cathode when an active state of corrosion is present. The current flow causes potentially differentiated electric fields to exist which surround the reinforcement. It is through measurement of these potentials that we can determine in which parts of the structure's reinforcement corrosion is likely to be occurring (Maierhofer, et al., 2010; Malhotra & Carino, 2004). The measurements that are obtained are of a qualitative nature, as they do not provide information on the actual presence of reinforcement corrosion but rather on the probability of corrosion being present (Maierhofer, et al., 2010).

2.3.5.1. Methodology & setup

In a typical half-cell potential setup, the reinforcement is connected to the positive terminal of the voltmeter, while the half-cell is connected to the negative terminal. As seen in the ASTM C 786 setup shown in Figure 11 electrical contact between the half-cell and the concrete is present through the porous plug and moistened sponge (Malhotra & Carino, 2004). In order to prevent the current that flows through the reference electrode from affecting the stability of the potential of the reference electrode, the current flow through the circuit needs to be kept low. For this purpose, high impedance voltmeters are used and hence the open-circuit potential is what is measured. When the tests are being carried out on normal outdoor concrete, the voltmeter is said to need a minimum input impedance of 10 mV to be deemed suitable for the test (Costa, 2011; Elsener, et al., 2003).

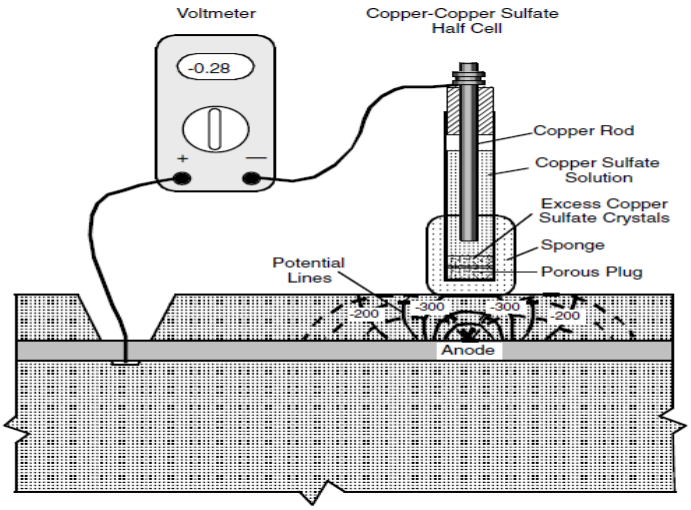

Figure 11: ASTM C876 Half-cell potential test set-up (ASTM, 2009)

Measurement of the half-cell potential of the reinforcement cannot be obtained directly due to the presence of the concrete cover. This is the reason for using the half-cell (Maierhofer, et al., 2010). Various

different half-cells can be used. Some of the more commonly used ones include the Copper-Copper Sulphate electrode, Silver-Silver Chloride electrode and the Standard Calomel electrode (Srinivasan, 2014). The type of reference electrode that is used will influence the numerical values, which are obtained from the test (Maierhofer, et al., 2010). Conversion factors, which allow readings to be converted from that of one type of half –cell to another, are available. Tables with such conversion factors can be found in ASTM C876, which standardizes the use of a copper-copper sulfate half-cell. The half-cell consists of a copper bar in a copper sulfate solution as seen in Figure 11 (Malhotra & Carino, 2004).

The locations of the reinforcement bars over which the half-cell is to be placed for recording measurements are determined by using a covermeter. This mapping of the reinforcement also provides possible locations for which the connection to the steel can be made. It is important to carry out resistance testing before measurements are taken to make sure that the reinforcement bars are continuous (Srinivasan, 2014). If the bar above which the test is being carried out is not electrically connected to the bar to which the voltmeter is connected, then this lack in continuity will affect the potential readings that are obtained (Malhotra & Carino, 2004). Once the above has been completed, an area or locations for testing should be marked out (Cheaitani & Collyer, 2002; Srinivasan, 2014). The area for investigation is usually marked out in a regular grid form with points for the locations of measurement (Elsener, 2001). The available budget and size of the structure under investigation guide to the spacing chosen for the measurement grid.

Spacing of measurements

The ASTM C876 (2013) standard says that there is no pre-defined minimum spacing requirement for half-cell potential measurements, but that the spacing depends on the member being investigated and the use for which these measurements are intended. When the spacing between test points is too large it is possible that the data obtained may be insufficient or active points may be missed. Using too small spacing is also not the best solution as it can prove to be costly, time-consuming and in cases where measurements are taken in locations which are very close to each other very little added value will be obtained (ASTM, 2009; Malhotra & Carino, 2004). A money-saving option would be to use a larger grid initially and then to make the grid smaller in areas where the possibility of reinforcement corrosion has been noted from the initial grid (Cheaitani & Collyer, 2002). Equipment with multiple electrodes and equipment with wheels are available to counter the challenges faced when using a close spacing or surveying large areas such as bridge decks or parking lots (Elsener, 2001; Malhotra & Carino, 2004).

Reinforcement connection

A connection point for the voltmeter to be connected to the reinforcement must be made through either coring or breaking out the concrete cover (FPrimeC, 2017; Mackechnie & Alexander, 2001). It is possible to use exposed rebar as the connection point provided that continuity is present between the rebar and the rest of the reinforcement under interest. In both cases, it is important to ensure that the reinforcement to which the voltmeter is to be connected is clean so that a high electrical resistance connection is not present. This can be achieved by scraping or brushing the reinforcement. There are numerous ways in which the connection to the reinforcement can be made including the use of a

compression-type clamp, by drilling a hole in the reinforcement into which a self-tapping screw is placed as well as through blazing or welding a protruding rod. The type of connection that is chosen will depend on whether the connection is to be permanent or temporary. An identical connection point should be used on each occasion when measurements for comparison purposes are to be taken in the same location over a long period (ASTM, 2009).

Pre-wetting the surface

It is very important that the concrete at the location being tested be sufficiently moist to provide electrical continuity between the half-cell and the concrete so that the circuit can be complete and valid measurements can be taken. Pre-wetting of the concrete surface becomes necessary if the half-cell is placed on the concrete and held still, and the potential values that are displayed vary with time. ASTM C876 suggests that an adequate moisture state and stability is reached when the measured potential does not change by more than 20 mV over a five-minute period (Malhotra & Carino, 2004). Often a wet sponge is placed between the concrete surface and the reference electrode to form a conductive bridge by ion transport. For the sponge to function optimally, it must remain wet and be cleaned or replaced on a regular basis. Excessive pre-wetting can, however, cause a forced negative shift in the potentials and lead to incorrect readings (Elsener, et al., 2003).

Two methods for pre-wetting the concrete surface are described in ASTM C876 (2009). The first method states that either the entire surface under investigation or just the point of interest must be sufficiently sprayed or wetted until the measured potentials vary by 20 mV or less over a five-minute period. The readings should not be taken when there is free surface water between the points of measurement. This method is suitable for locations that do not require a lot of pre-wetting. The second method requires a saturated sponge to be placed over the location of measurement for as long as it takes to meet the five-minute variation requirement mentioned for the first method. The half-cell and any sponge, which may be attached to the top of the half-cell, must then be placed firmly on top of the pre-wetting sponge for the length of a measurement. The standard says that the reference electrode method is not suitable should it not be possible to achieve the required stability in measurements by either method of pre-wetting. This may occur due to electrical interference or the electrical resistance of the circuit being too high (ASTM, 2009).

2.3.5.2. Displaying the data

The potential readings are usually found to be negative due to the way in which the system is set up, with the reinforcement being connected to the positive terminal of the voltmeter and the reference electrode to the negative terminal. It does occur that positive potential readings are found at times such as over passive reinforcement in drier concrete (Elsener, et al., 2003). Depending on the number of readings taken, the way of representing the data may vary. In cases where only a few readings have been taken or a large-sized grid has been used, it is often found that the data is presented in a table format or depicted on a point plan of the surveyed area. Large amounts of readings can be used to plot a potential map of the concrete or to provide a statistical representation. The data collected then forms the guideline for the prediction of possible locations of reinforcement corrosion (Andrade, et al., 2004).

Potential mapping is the more commonly used method for displaying larger amounts of data (Malhotra & Carino, 2004). The potential fields are usually displayed either in the form of a lined contour map or a colour map of the field (Elsener, 2001). The contours are generated by connecting measured points of equal voltages on a scaled plan view of the test surface. Software is available to generate these contour maps and some devices can use stored data to produce these maps by themselves. Concerning the statistical representations of data, the percentage of readings that are more negative than a certain value can be obtained using a cumulative frequency diagram (Malhotra & Carino, 2004).

2.3.5.3. Results and interpretation

The half-cell potential test has been standardised by several standard associations in works such as ASTM C876, UNI 10174 and RILEM TC 154. These standards provide ranges of values for interpreting results such as those from ASTM C876 shown in Table 3. Results can be evaluated numerically by comparing them to the prescribed values provided in the standards. The more negative the half-cell potential readings measured, the higher the risk of rebar corrosion having taken place and the higher the probability of increased severity of corrosion levels. This is, however, a measure of the likelihood of reinforcement corrosion and several factors can influence the numerical values (Malhotra & Carino, 2004).

Table 3: Half-cell potentials and associated risk of reinforcement corrosion (ASTM C876).

Measured potential (mV)		Risk of corrosion
Cu/CuSO4 electrode	Ag/AgCl electrode	Likely state of corrosion
> -200	> -106	Low (10% risk of corrosion)
-200 to -350	-106 to -256	Intermediate corrosion risk (uncertain)
< -350	< -256	High (> 90% risk of corrosion)

The potential difference technique is often used to provide a sense of the reinforcement corrosion problem instead of using a numerical evaluation. With this method, the presence of reinforcement corrosion is determined by using potential gradients. Large gradients tend to be indicative of the presence of anodic areas because of localised reinforcement corrosion. In a contour map, these large gradients can be seen in the form of closely spaced contours, where a large change in potential occurs over a short distance (Broomfield, 2007; Malhotra & Carino, 2004; Srinivasan, 2014). Potential values are influenced by a number of variables such as moisture content, temperature, carbonation and chloride content. Since absolute values of potential values are subject to change under various conditions, potential gradients are seen as a better option for interpretations (Elsener, et al., 2003).

The half-cell potential technique is better suited to reinforcement corrosion because of chloride attack as this type of corrosion tends to be characterised by macrocell corrosion, which is non-uniform with clearly defined corroding and passive areas. Fluctuations in the half-cell potential readings will thus point us in the direction of chloride-induced reinforcement corrosion (Alexander, et al., 2012). Should potential readings shift by several hundred millivolts over a short distance then this will be indicative of the high probability that reinforcement corrosion is taking place (Mackechnie & Alexander, 2001). The readings for

both chloride-induced and carbonation-induced reinforcement corrosion depends on the extent to which the reinforcement has depassivated. For carbonation-induced reinforcement corrosion, these readings will, however, be more constant due to the uniform nature of the induced corrosive action (Alexander, et al., 2012).

2.3.5.4. Advantages and limitations of the HCP test

The HCP test remains one of the most commonly used non-destructive techniques for determining whether reinforcement corrosion is occurring in reinforced concrete. It is however important that care is taken in applying the method and understanding the results since a lack of skill and experience has led to the failure of the technique in the past (Cheaitani & Collyer, 2002). The half-cell potential test is widely used as it is cost effective, easy and fast to carry out and a non-destructive condition assessment technique (Yodsudjai & Pattarakittam, 2017). Although the technique is a very popular one, it does not come without its constraints and flaws.

Environmental effects, the design of the structure and repair techniques can affect the potential readings obtained and thus lead to inaccuracies in reinforcement corrosion predictions. Factors such as humidity, temperature, moisture content, cover depths and surface coatings are a few factors which could lead to over or underestimations of potential readings, as they cause shifts in half-cell potential readings which may not be related to the actual severity of the reinforcement corrosion. It is therefore very important to understand the factors, which affect the test to assure that the best interpretations of the results can be made (Andrade, et al., 2004; Ping & Beaudoin, 1998). The effects on HCP readings caused by material inconsistencies and climatic conditions do not just vary from structure to structure or member to member, but can even vary locally due to locally varying humidity, aggregate contents etc. (Elsener, et al., 2003; Leelalerkieta, et al., 2004).

The following limitations of the technique are also mentioned in the literature:

I. Potential readings in delaminated areas are not possible as delaminations disrupt the potential field (Cheaitani & Collyer, 2002; Mackechnie & Alexander, 2001).
II. Less negative potentials can be shown on surface layers with high resistance levels (Malhotra & Carino, 2004).
III. The method is not applicable to water-saturated structures (ASTM, 2009).
IV. The accuracy of the results depends on the spacing between readings (Roberge, 2008).
V. Stray currents can lead to potential shifts (Broomfield, 2007).

2.3.5.5. Factors which influence HCP measurements

Oxygen concentration

Oxygen concentration impacts on the potential readings, such that low oxygen concentrations lead to a decrease in the measured potentials. Without the presence of oxygen, reinforcement corrosion is not possible and so the decreased potential readings may lead to misinterpretations concerning the state of corrosion (Maierhofer, et al., 2010). An indication of the possibility of low oxygen concentrations can be seen when potential values are relatively negative throughout the test region with little deviation in values (ASTM, 2009). Oxygen concentration in concrete may be low due to numerous reasons. Some of these reasons include the concrete being wet, dense or when polymer modified concretes are used (Raupach, et al., 2007).

Cover depth

Both the Utah department of traffic and the results of tests carried out by Yodsudjai & Pattarakittam (2017) suggest that concrete cover depth does not have a definitive effect on half-cell potential readings. It has however been found that thicker concrete cover depths result in a reduction in the gradients between potential lines, leading to less noticeable changes between the potentials of the anodic and cathodic regions. This flattening of the potential distribution may lead to more difficulty in ascertaining whether reinforcement corrosion is present or not (Maierhofer, et al., 2010; Yodsudjai & Pattarakittam, 2017). ASTM C876 (2009) states that the half-cell potential test method can be applied to all reinforced concrete members irrespective of the cover depth. The standard does, however, mention that for cover depths greater than 75 mm it may occur that an average of adjacent reinforcement potentials is given making it more difficult to notice changes in corrosion activity.

Electrical interference

External sources of stray currents can affect potential readings (Cheaitani & Collyer, 2002; Mackechnie & Alexander, 2001). Alternating current power lines and radio frequency transmitters, which are located near the area of measurement, can cause the occurrence of electromagnetic interference or induction and this will in turn cause errors in the measured values. A possible sign of such interference comes when the readings in a particular location tend to fluctuate even when the surface is sufficiently pre-wetted. The extent of the trouble caused by electrical interference can be determined with an oscilloscope (ASTM, 2009).

Repair techniques

Electrochemical restoration techniques such as electrochemical chloride extraction or electrochemical realkalinisation lead to the reinforcement being polarised to negative potential values, which may be misinterpreted as pointing to an active state of reinforcement corrosion. It is thus important to know the details of the structure and the repair techniques that may have been applied to it when assessing the

state of reinforcement corrosion or the success of a repair method, as some methods may decrease the HCP readings and others may increase these readings (Raupach, et al., 2007).

Moisture content

How wet or dry the surface on which half-cell potential measurements are being taken is can have a significant impact on the potential readings. Areas, which are subject to increased moisture content due to wetting, tend to display a negative shift in the measured potential values. The potential gradients have been found to remain the same with the change in moisture content even though the numerical values tend to shift (Elsener, et al., 2003). Half-cell measurements are weather-dependant such that in the dry season the corrosion cells shut down leading to higher potential values (Bungey & Grantham, 2006). Experiments conducted on one bridge deck showed a negative shift in potential values of 100 mV from measurements taken during a dry period to those taken after a period of rainfall had occurred (Elsener, et al., 2003).

The work of Gerardo Clemena (1992) refers to surveys that were conducted on a concrete deck in two separate months, the first of which was conducted soon after a period of rainfall. The results of the surveys showed that although the numerical values of the potential were less in the first survey, the potential maps and locations of concern from both surveys were similar with a few small differences. A superposition of the potential maps of the two surveys can be seen in Figure 12. These results support the idea that the potential maps which show the relation of potential values at different locations on a concrete surface serves as a better indication of the actual state of reinforcement corrosion of a structure than the ranges of values which are provided in the standards. Therefore, while the numerical value ranges that are provided may provide a useful source of information, these values should not be used as the sole guideline for drawing conclusions (Clemena, 1992).

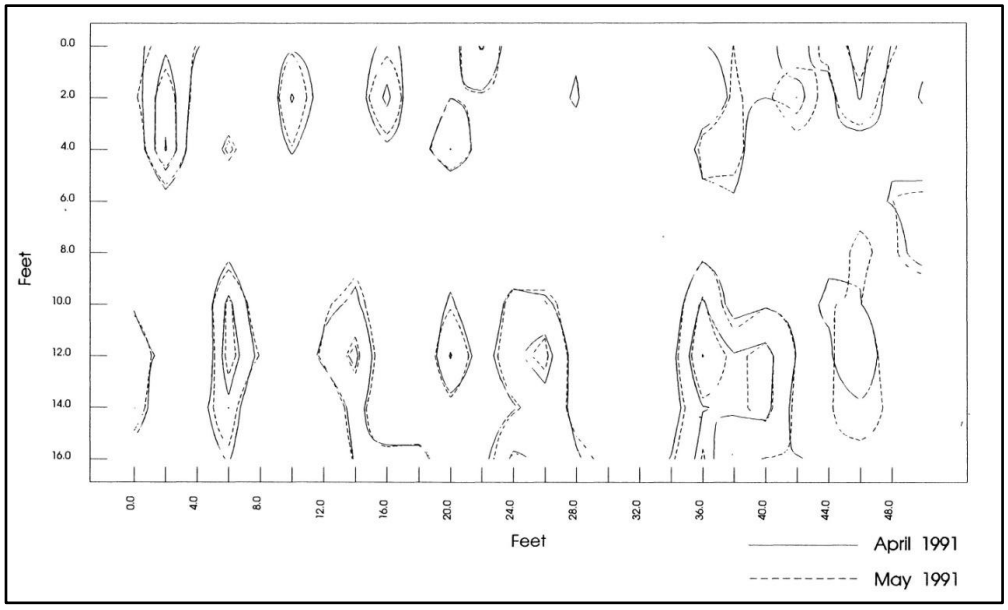

Figure 12: Superposition of half-cell potential maps from after a period of rain (April 1991) and from a dry period (May 1991) (Clemena, 1992).

In one set of experiments by Keßler & Gehlen (2016), three different methods for pre-wetting the concrete surfaces were tested to determine how this would affect the values of measured potentials. The first of the three methods involved wetting of a reference sponge prior to starting the test, the second, pre-wetting of the surface for 20 minutes and the third, intensive pre-wetting for two hours. The results of these tests can be seen in the probability plots of the potential values shown in Figure 13. These results show that the potential measurements shift to values that are more negative with the concrete surface being exposed to increased moisture. The shift between the results of the second and third methods is not as large as the shift between these two methods and the first method, which serves as an indication that HCP results can be misleading if an inadequate method for pre-wetting the surface is used.

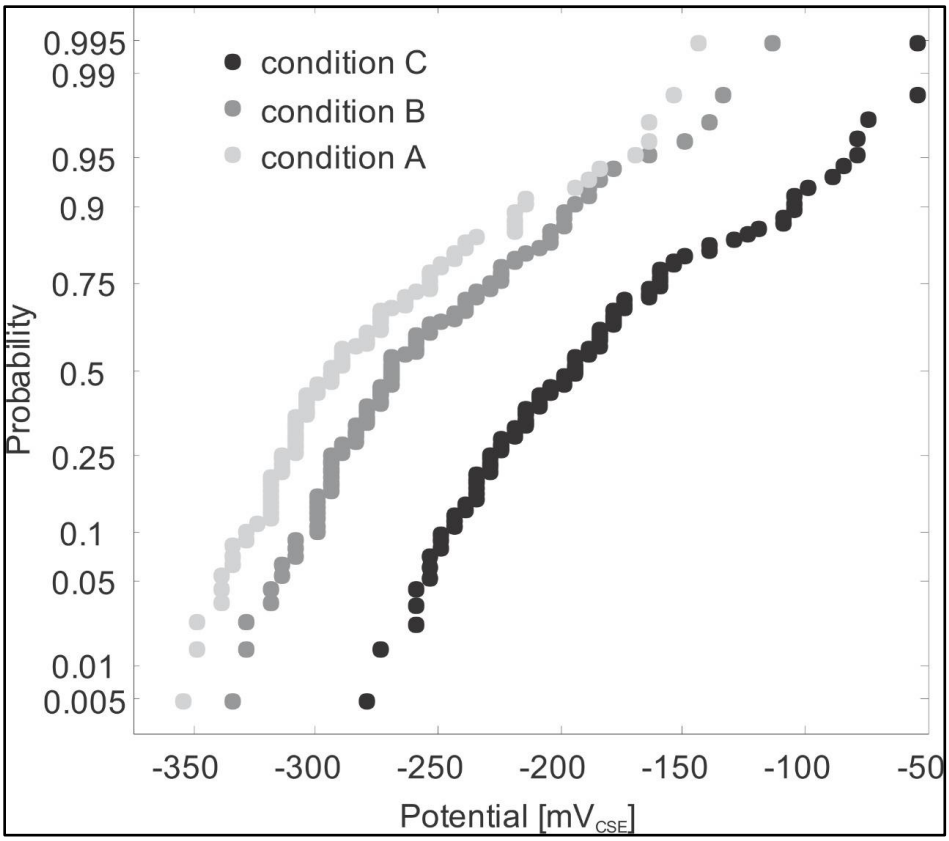

Figure 13: Probability plot of half-cell potential values under different pre-wetting conditions (Keßler & Gehlen, 2016)

A second set of experiments by Keßler & Gehlen (2016) involved half-cell potential tests, which were carried out during different weather conditions, namely dry and wet conditions as well as hot and cold conditions. The findings state that comparable potential gradients, values in a comparable range with no outliers and comparable outcomes were found. The variations in potential values were found to fall in an absolute range of 100 mV, with the measurements displaying the most positive values falling in periods of dry and cold weather and those displaying the most negative values falling in periods of wet and hot weather. These results point to similar findings concerning the effect of moisture content as was found from the set of experiments that involved changing the pre-wetting conditions.

It is clear that changes in the moisture content of a concrete surface lead to changes in the half-cell potential measurements. While changing weather conditions are one of the important causes of changing moisture contents, the effects of exposure conditions can also play an important part. The effects of moisture on a reinforced concrete structure will not necessarily be constant due to factors such as the location and form of the concrete surface as well as the direction of rainfall. Due to factors such as these, different locations on a particular element may be faced with varied exposure conditions, which can lead to flaws in potential maps (Elsener, et al., 2003; Keßler & Gehlen, 2016).

Temperature

Temperature changes have been shown to have an impact on the potential measurements taken on concrete structures (Clemena, 1992). An increase in temperature leads to a decrease in half-cell potential values as the higher temperatures facilitate an increased rate in electrolytic current flow (Guthrie, et al., 2008). Changes like these brought about by changing weather conditions make the numerical guidelines suggested in standards like ASTM C876 seem to be imprecise for use in drawing accurate conclusions (Clemena, 1992).

The experiments by Keßler & Gehlen (2016), which involved the measurement of half-cell potentials under varying weather conditions, as discussed in the previous section on moisture content, show that hotter temperatures lead to more negative potentials than colder weather. The effects of temperature are however less significant than those of moisture content.

The Washington State Department of Transportation conducted tests on two bridges to determine how variations in temperature effect half-cell potential measurements. The tests were carried out at 28 and 16°C for the first bridge and 24 and 5°C for the second bridge during different months of the year. From the results of both bridges, it was found that the half-cell potential values which were measured to be in an active state of corrosion according to the ASTM guideline (values less than -350 mV) showed very little shift in values due to the changes in temperature. The potential values which were found to fall in the ranges of values which ASTM C876 classifies as uncertain or a sign of a lack of reinforcement corrosion (values less than -350 mV) showed a slight shift in potential values to less negative potentials for the surveys conducted at the lower temperatures. This shift to less negative values was not found to be significant and so the work suggests that half-cell potential testing is only slightly influenced by temperature changes (Babaei, 1986).

2.3.6. Resistivity

While the half-cell potential test is more qualitative with regards to the reinforcement corrosion process, resistivity testing proves to be more quantitative as it helps to predict the corrosion rate and helps to give an understanding on how severe the problem is (Gowers & Millard, 1999; Malhotra & Carino, 2004). The rate of corrosion of reinforcement in concrete depends on how much electrical current is able to flow from the anodic region of the reinforcement to the cathodic region, through the concrete pore structure.

The ease with which current by ionic movement can flow through the concrete is governed by the resistivity of the concrete (Alexander, et al., 2012; Srinivasan, 2014).

Concrete with a higher resistivity can resist ion movement within the pore structure to a greater extent, resulting in lower rates of reinforcement corrosion than would take place in a lower resistivity concrete (Alexander, et al., 2012; Silva, et al., 2011; Layssi, et al., 2015). The electrical resistivity of the concrete depends on both the moisture content and pore structure of the concrete mixture (Malhotra & Carino, 2004). When concrete is both dry and of a high quality the resistivity readings are found to be higher, on the contrary when concrete is saturated and of a poor quality the resistivity readings tend to be lower (Mackechnie & Alexander, 2001).

In order to measure the electrical resistivity, an electrical current is applied to the concrete. As the current passes through the concrete, the potential difference is measured. The relationship between the electrical current and the potential difference in the form of Ohm's law can then be used to calculate the electrical resistance. A relationship between the electrical resistance and electrical resistivity is then used to obtain the resistivity values that are needed. Various relationships between the electrical resistance and electrical resistivity exist for the different techniques and devices used (Maierhofer, et al., 2010). It is usually necessary that the test location is pre-soaked before measurements can be taken on dry concrete surfaces so that a good electrical connection that allows the current to pass through the concrete can be established. It is suggested that the surface is pre-wetted for 20 minutes (Coimbatore, 2014).

There are a number of tests and resistivity meters available for measuring the resistivity of concrete. Commonly used methods work using electrodes which are placed on the concrete surface. Depending on the type and geometries of the devices used, the electrical resistivity can be calculated. Values obtained with these different methods are often not comparable as the different test methods and specimen geometries affect the readings in their own way. The Wenner method and the two-plate bulk resistivity method are the two most common methods used in resistivity measurements (Liu, et al., 2011; Silva, et al., 2011).

2.3.6.1. 2-plate bulk resistivity method

The bulk resistivity of the concrete is measured directly by the two-plate method. One plate is placed on either end of a specimen and a low-frequency current is passed between the electrodes. The drop in voltage that occurs as the current passes through the specimen is measured before calculating the bulk resistivity. The two-plate electrode method is used to measure resistivity values on concrete specimens that are usually cast in the lab or removed from site (Liu, et al., 2011; Silva, et al., 2011).

The contact between the plates and the concrete is very important as poor contact can lead to the development of a large resistance. It is often the case that a wet sponge or a conductive gel is placed between each plate and the concrete specimen in order to establish a strong electrical contact and prevent the development of this large resistance (Kevern, et al., 2015; Layssi, et al., 2015; Liu, et al., 2011).

The 2-plate method is simple, quick and reliable for measurement of the bulk resistivity in the lab and it is possible to use the same specimen that has been prepared for a compression test to measure the resistivity with this method (Layssi, et al., 2015). Both this method and surface resistivity measurements have been deemed suitable for tests on cylindrical samples, however, the surface resistivity measurements such as the Wenner method are found to be more suitable for field use (Kevern, et al., 2015). The different geometries found in the field, as well as the presence of reinforcement bars, make the use of the two-plate method impractical in field applications. It is possible to use this method to assess field structures, but this requires the removal of drilled cores on which the test can be performed (Layssi, et al., 2015; Liu, et al., 2011).

2.3.6.2. Wenner 4-probe meter

The 4-probe method is the most commonly used technique for measuring the resistivity infield, such as for the purpose of condition assessments (Silva, et al., 2011). This method of measuring the resistivity of the concrete is non-destructive, quick and simple to carry out and hand-held portable devices are available making the Wenner 4-probe meter well suited for practical field investigations (Layssi, et al., 2015). The devices have four probes/electrodes positioned in a straight line at equal distances from each other (Mackechnie & Alexander, 2001). A known alternating current of a low frequency is passed between the two outer probes. As the current travels through the concrete, a voltage drop occurs and the two inner probes measure this drop, which is then transformed to give resistivity values (Mackechnie & Alexander, 2001; Srinivasan, 2014). This method is the specified method in ASTM C1202 (Coimbatore, 2014). An illustration showing how the Wenner 4-probe meter works can be seen in Figure 14 and Equation 15 shows how the output surface resistivity is calculated.

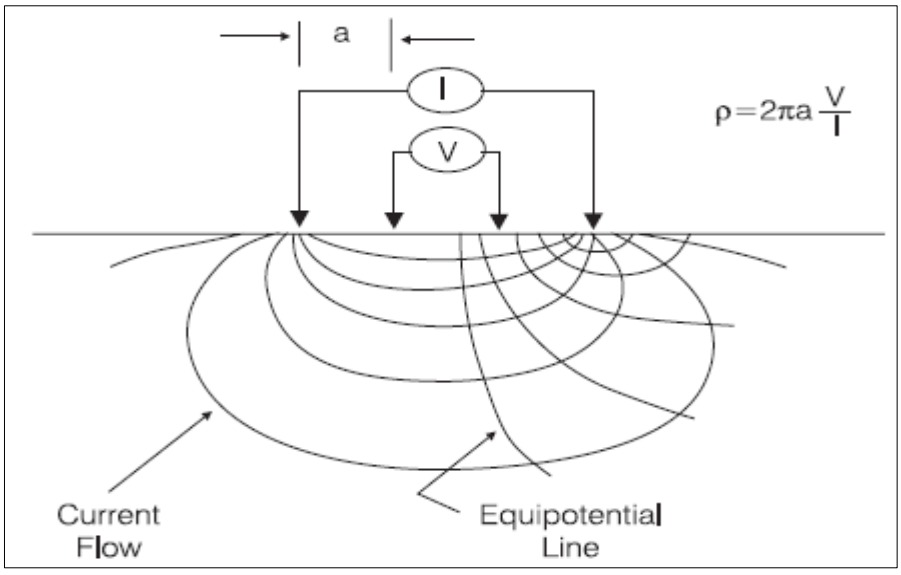

Figure 14: Illustration showing how the Wenner 4-probe meter functions (Srinivasan, 2014)

$\rho = \frac{2\pi aV}{I}$ (ACI, et al., 2002) … (15)

Where:

ρ : resistivity

a : probe spacing

V : measured potential

I : applied current

The resistivity, which is measured using the Wenner method, has been described as the apparent resistivity as the equation on which the method is based on makes the assumptions that the material is both semi-infinite and homogeneous. Should the assumptions not be true in the actual case of a measurement then there are likely to be errors between the measured resistivity and the actual resistivity (Liu, et al., 2011; Malhotra & Carino, 2004).

The assumption that the concrete is semi-infinite holds fairly well when the dimensions of the element under investigation are large in comparison to the probe spacing. Should this not be the case then the results may be overestimated due to current constriction. It has also been found that large errors in measurements can occur when readings are taken on thin concrete or near to an edge. Concrete is known to be an inhomogeneous material with larger aggregate particles and a fine cement paste. The resistivity of the cement paste tends to be low, while the aggregates generally show a high resistivity. When the particle sizes are small or the probe spacing is large, the impact of individual particles will be minimized. Large probe spacing allows the current to penetrate deeper into the concrete and this will mean that the measurements that are obtained will represent a larger volume of concrete (Gowers & Millard, 1999).

Research by Millard et al (1999) suggests a number of factors to obtain the best representative value of resistivity of the concrete when using the 4-probe technique. The works suggest that 50 mm spacing is adequate for typical concrete mixtures, the distance to the edge of a member from where the measurement is being taken should be greater than or equal to twice the probe spacing and that both the width and depth of a member should be greater than or equal to 4 times the probe spacing. Should the following factors be in place then Equation (15) on which the Wenner method is based will be satisfied and if not, the readings will be higher than the actual resistivity (Malhotra & Carino, 2004).

The method for measuring surface resistivity using a four-probe set-up often has the pins spring-loaded with water reservoirs in order to achieve the required electrical connectivity (Kevern, et al., 2015). An example of such a device is the Resipod, which can be seen in Figure 15. The Resipod is fast to use, stable and convenient for use under various conditions, as it is both robust and waterproof (Proceq, 2017).

Figure 15: Resipod Wenner 4-probe meter (Proceq, 2017)

Probe spacing

A smaller probe spacing results in the aggregates having a larger effect on readings (Gowers & Millard, 1999). The minimum spacing between probes thus increases with the maximum size of the coarse aggregate, as the use of a wider spacing helps to account for the inhomogeneities found in the concrete mixture (Malhotra & Carino, 2004; Proceq, 2017). The results of tests carried out by Millard et al (1999) found that should the probe spacing be at least 1.5 times greater than that of the largest aggregate particle, then the standard deviation in results would not exceed 5%. It is thus suggested a probe spacing of at least 1.5 times the maximum aggregate size should be used. A spacing of 38 mm or 50 mm between the probes is commonly used. When the spacing is too wide problems can also arise such as potential interference of measurements due to the presence of reinforcement bars below the areas where resistivity readings are being measured (Proceq, 2017).

Carrying out measurements

It is important to know the location of the reinforcement when carrying out resistivity measurements in order to minimise the interference that the reinforcement causes. When reinforcement bars are located directly below the area of measurement, the current field and thus resistivity measurements become distorted (Gowers & Millard, 1999). This interference occurs, as the reinforcement is a much better conductor of current than concrete. The reinforcement cover depth plays an important role in how much influence the reinforcement plays. The deeper the cover the less influence the reinforcement will have (Malhotra & Carino, 2004).

The map of the reinforcement can be used to find locations for measurements away from the reinforcement (Liu, et al., 2011). There are recommended orientations of the Wenner 4-probe meter to deal with the interference of rebars. When the reinforcement grid spacing is greater than the probe span, it is recommended that measurements be taken diagonally to the reinforcement as shown in Figure 16. Should the grid spacing be too small to avoid measurements over the reinforcement then taking measurements perpendicularly across the reinforcement has been found to minimise its influence (Proceq, 2017). Experimental tests and the use of a finite element analysis showed that errors were low

when measurements were taken perpendicular to the reinforcement (Gowers & Millard, 1999). Orientation perpendicular to the reinforcement is shown in Figure 17.

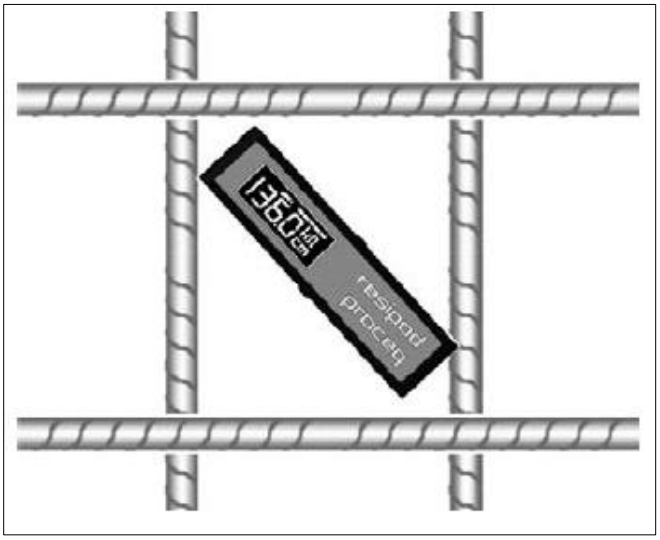

Figure 16: Measurements taken between the reinforcement with a diagonal orientation (Proceq, 2017)

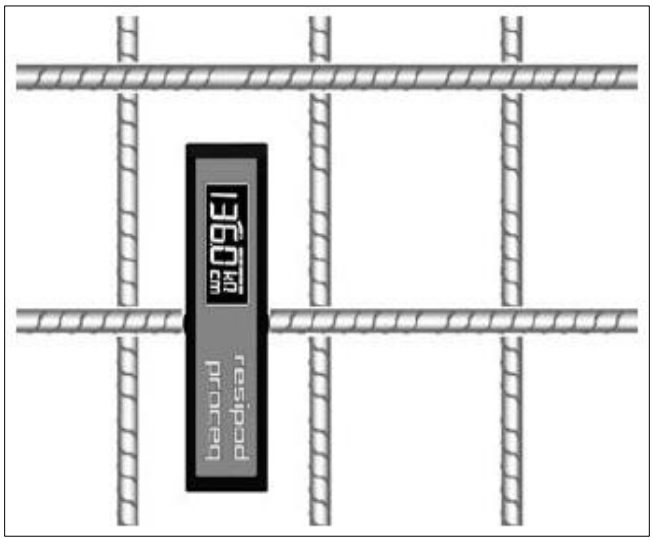

Figure 17: Measurements taken perpendicularly over the reinforcement (Proceq, 2017).

The Wenner probe technique is sensitive to the moisture, voids and other surface conditions. The resistivity that is measured may differ on the same specimen due to these many reasons. It is because of these effects that the taking of multiple measurements are recommended even on small samples. The AASHTO TP 95 test specification requires the taking of eight readings to provide a reliable average (Layssi, et al., 2015). RILEM TC154-EMC recommends that five measurements, a few millimeters apart, should be taken in the same location in order to obtain a median value (Proceq, 2017).

Interpreting results

Measurements of the surface resistivity may only be valid at the time of measurement as it is a measure of the pore continuity of the concrete and the amount of water that is contained in the pores (ACI, et al., 2002). Influencing factors such as temperature change can also have significant effects on the measured values. It is said that a decrease in temperature of approximately 20°C can lead to resistivity measurements doubling (Polder, et al., 2000). Theory and experimental tests have found resistivity to be linked to the rate and likelihood of reinforcement corrosion, once the passive layer of the steel has been destroyed (Proceq, 2017).

In general, it is known that the likelihood of reinforcement corrosion increases as the resistivity of the concrete decreases and vice versa. The relationship between concrete resistivity and reinforcement corrosion is still a subject of study; however, recommendations from empirical works are suggested and available for use as a guideline. Commonly used suggestions are shown in Table's 4, 5 and 6 (ACI, et al., 2002; Polder, et al., 2000; Proceq, 2017). The different criteria for the interpretation of resistivity measurements vary in both value ranges and the categories proposed. These variations in the empirically suggested criteria may be due to the use of different measurement techniques, the types of structures from which the data was collected and the cause of reinforcement corrosion. In practice, it is recommended to calibrate the technique by either exposing the reinforcement and assessing its condition or by correlating the measurements obtained to other available data (ACI, et al., 2002).

Table 4: Empirically found relationship between resistivity & the likely reinforcement corrosion rate (Proceq, 2017; Schiessel & Raupach, 1992).

Resistivity (Kohm.cm)	Likely corrosion rate
> 20	Low corrosion rate probable
10 to 20	Moderate/low corrosion rate probable
5 to 10	High corrosion rate probable
< 5	Very high corrosion rate probable

Table 5: Empirically found relationship between resistivity & the measured rate of reinforcement corrosion (Vassie, 1980).

Resistivity (Kohm.cm)	Likely corrosion rate
> 12	Corrosion unlikely to occur
5 to 12	Corrosion will probably occur
<5	Corrosion almost certain

Table 6: Empirically found relationship between resistivity and the risk of reinforcement corrosion (Polder, et al., 2000; Proceq, 2017; Rodriguez, et al., 1994).

Resistivity (Kohm.cm)	Risk of corrosion
< 10	High
10 to 50	Moderate
50 to 100	Low
< 100	Negligible

2.3.6.3. Factors which affect resistivity measurements

Surface contacts

The surface contact area has been found to be rather insignificant for the Wenner method, but the two-contact method is sensitive to deviations from the chosen area and so gels or moist sponges are used at the contact surface to ensure a good electrical contact.

For the Wenner method, it is important that the probes make good contact with the concrete surface. Should the two inner probes not make a good even contact then spurious common mode voltages can occur leading to errors in results. These effects can be reduced by using a low-frequency AC current instead of a DC current, which leads to polarization problems (Gowers & Millard, 1999).

Concrete mixture

The concrete mixture and the type of binder used influence the concrete resistivity and so the choice mixture and cement blend can play a significant role in fighting reinforcement corrosion (Alexander, et al., 2012; Ortega & Robles, 2014; Srinivasan, 2014). Blended cements have been found to possess higher resistivities than ordinary Portland cement concrete (regardless of cracking), making them very useful in slowing down both the initiation and propagation of reinforcement corrosion (Alexander, et al., 2012). The concrete pore structure and the resultant level of ease with which harmful substances can move through the concrete are important to resistivity measurements and the measurements tend to increase when the mixture results in smaller pore sizes (Malhotra & Carino, 2004).

Surface layer of different resistivity

When the resistivity of the surface layer differs from that of the bulk concrete, the flow of the current and resistivity measurements may be distorted. When the resistivity of the surface layer is lower than the rest of the concrete errors are found to be more significant when trying to assess the underlying concrete. Salt contamination is an example of a case where the surface resistivity may be lowered (Gowers & Millard, 1999; Malhotra & Carino, 2004).

The effects of carbonation influence the surface resistivity leading to a high resistivity surface layer (Gowers & Millard, 1999; Ortega & Robles, 2014). If the depth of the carbonated layer is small in relation to the probe spacing that is used, then the effects of this carbonated layer will be minor. In cases where the carbonated layer is thick, it may become necessary to increase the spacing between the probes in order to counter the effects of the carbonated layer and obtain results that are more accurate (Akhlaghi & Tronca, 2015). Measurement of the carbonation depth can thus help to determine the best resistivity values for reinforcement corrosion predictions. If the carbonation depth is found to be thin, then a probe spacing of 8 times this carbonation depth will help to minimize errors. If the carbonation depth has passed the reinforcement depth, then it is recommended that the probe spacing should be equal to or less than the depth of carbonation as the resistivity of the carbonated layer is what will influence the rate of reinforcement corrosion (Gowers & Millard, 1999; Silva, et al., 2011).

Moisture levels

As with the measurements of half-cell potentials, resistivity values can also vary with both location and time due to exposure conditions and seasonal changes. What this tells us is that the resistivity values, which are measured, may only be valid for the time during which the measurement is taken, so it is important to understand how variables such as moisture content and temperature affect the results in order to be able to draw good conclusions (Clemena, 1992).

Moisture content has a very significant influence on electrical resistivity (Azarsa & Gupta, 2017). Concrete, which is completely dry, behaves like an insulator preventing the movement of ions or charges (Osterminski, et al., 2012). Electrical current in the concrete is necessary to measure concrete resistivity and for this current to be able to flow through the concrete it needs interconnected pore water to be present. Since the flow of this current affects measured resistivities, it is found that the moisture content will affect resistivity values (Moreno & Liu, 2012). An increase in moisture allows current to be carried more easily and hence results in a decrease in the resistivity (Layssi, et al., 2015). Humidity levels have a similar effect as they influence the amount of water found in the concrete pore structure (Silva, et al., 2011).

The surface layers of the concrete are directly exposed to weather conditions, while deeper layers are not and so they will be less affected by short-term rain and moderate length dry periods. The level to which changes in moisture content as a result of weather conditions impact on resistivity measurements depends on the ability of the concrete to absorb water during periods of rain and to release water during dry periods. The cement type and water/cement ratio are the two parameters that have the largest influence on this (Osterminski, et al., 2012).

Experiments by Larsen, et al. (2006) found that the change in moisture content could have a varying degree of change on resistivity values depending on how much the moisture content changes by. The results of these experiments showed that when the degree of moisture changed from 88 to 77% in comparison to 88 to 66%, the average resistivity increased from 2 times to 6 times respectively (Azarsa & Gupta, 2017).

The decrease in resistivity values caused by a change in moisture content can be seen after taking measurements with different levels of pre-wetting (Keßler & Gehlen, 2016). Experiments have shown that poor surface saturation through the use of static ponding or pressurized water can lead to a difference in resistivity values of over 30% in comparison to laboratory tests under full saturation. Research on how to obtain a good moisture level through the bulk concrete on-site is still lacking. So additional investigations are necessary in order to be able to achieve the best results in practical conditions (Azarsa & Gupta, 2017).

Temperature

The resistivity of concrete is influenced by the temperature to which it is exposed because changes in temperature lead to changes in ion mobility, the concentration of ions in the pore solution, ion-solid interactions and ion-ion interactions (Azarsa & Gupta, 2017; Moreno & Liu, 2012). Since the flow of

electric current depends on ionic movement, the temperature will affect the ability of electric current to flow through the concrete. A temperature increase leads to increased movement of ions and thus increased flow of current and reduced resistivity measurements (Kevern, et al., 2015; Layssi, et al., 2015). It is noted that extremes in variation can be seen when changes in air temperature occur, as opposed to changes in internal concrete temperature (Gowers & Millard, 1999).

Several studies show that temperature changes can have a significant effect on resistivity measurements. Spragg, et al. (2013) stated that the resistivity of a sample could change by as much as 80% when the temperature of the sample varies between 10-40°C. One report suggests that for concrete with low saturation levels (<30%) the resistivity changes by 5% for every °C change in temperature when compared to a temperature of 21°C. A 3% change in resistivity occurs per °C for concrete with saturation levels between 30% and 70%. This suggestion is also put forward by Proceq, the manufacturers of the commonly used Resipod Wenner 4-probe meter (Akhlaghi & Tronca, 2015). It has been suggested as a simplification that a change of 3-5% per °C be used to adjust resistivity values when the temperature falls in a range of 0-40°C (Azarsa & Gupta, 2017; Moreno & Liu, 2012).

A proposed linear relationship, which describes the effect which temperature has on resistivity, can be seen in Equation 15. Using this equation, a measured resistivity can be standardised to the resistivity at a reference temperature of for example 21°C. This Equation has however been found to only work in a narrow range of temperatures from the reference temperature (T0 ± 5°C) (Azarsa & Gupta, 2017; Moreno & Liu, 2012). There are however currently no publications which provide a practical correlation for the relationship between temperature and resistivity in real-world conditions (Azarsa & Gupta, 2017).

$$p = p_0(1 + \alpha.\Delta T) \quad \text{... (15)}$$

Where:

p : resistivity at the required temperature

p_0 : resistivity at the reference temperature

α : temperature coefficient

ΔT : temperature difference between the reference temperature and the required temperature

The results of tests performed on saturated specimens under a range of temperatures during 2 cycles, 2 months apart can be seen in Figure 18. These tests were performed on saturated specimens so that the temperature parameter could be the only parameter of concern. The results show that the resistivity increases as the temperature decreases. What can also be observed from the results is that an increase

in moisture content also leads to a decrease in resistivity. Cycle 1 was performed two months before cycle 2 and although the specimens were saturated, they were not fully saturated, which is why a small decrease in resistivity can be seen as the specimens became more saturated with time. Tests on concrete specimens with different intrinsic resistivities showed that the effect of temperature is greater on concrete with higher intrinsic resistivities. It has also been found that at higher temperatures the temperature effects have less of an impact on measured resistivities (Liu, et al., 2011).

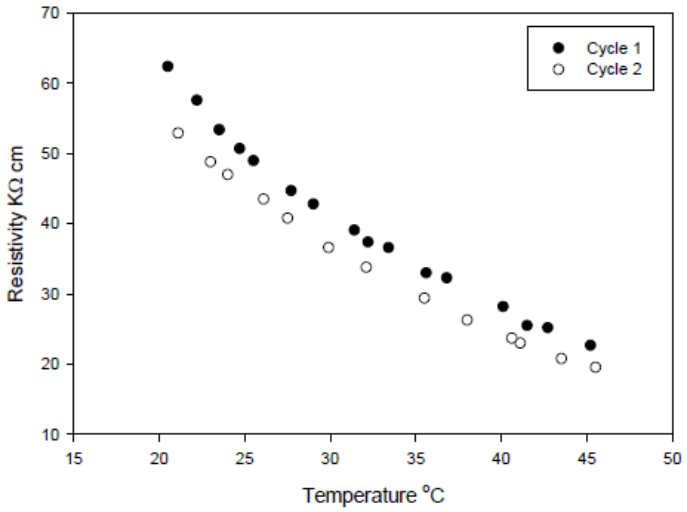

Figure 18: Resistivity variation with temperature from 2 sets of measurements in 2 different cycles (Liu, et al., 2011)

Other factors that influence resistivity

I. Conductive layers on the surface of the concrete influence readings (Mackechnie & Alexander, 2001).
II. Concentration of harmful ionic substances (Mackechnie & Alexander, 2001).
III. Chloride levels (Srinivasan, 2014).
IV. Geometrical limitations in test locations or on test specimens (Liu, et al., 2011; Silva, et al., 2011).

2.4. Summary

There are several different types of tests that are used to assess the state of corrosion of reinforced concrete structures, each providing some sort of guidance when drawing conclusions. It is often suggested that a combination of tests should be used in order to make well-informed decisions. ASTM C876 suggests that HCP results are of most value in reinforcement corrosion determination when accompanied by other tests such as the resistivity test and tests for chloride contents and carbonation depths. The choice of which test or combination of tests should be used will depend on a number of factors such as structural features and environmental conditions amongst others (Concrete Society, 2009; Elsener, et al., 2003).

A number of factors including moisture content and temperature play a role in the occurrence of reinforcement corrosion. The moisture content and temperature to which a structure is exposed can be influenced to a large degree by environmental conditions. From the different environmental conditions that have been found to affect reinforcement corrosion, moisture content has been deemed to be the most influential. An increase in the temperature to which a structure is subject to can speed up the reactions that are necessary for corrosion to occur but can also have an inhibiting effect on corrosion due to the reduction that it causes in moisture content (Vavpetic, 2008).

Different intensities and durations of rainfall result in different levels of moisture ingress into a structure. High and medium intensity rainfalls don't show a great difference in the ingress of moisture when compared to each other but do show greater ingress when compared to low-intensity rainfalls. Longer duration of rainfalls also results in greater ingress of moisture. When it comes to intensity duration combinations high-intensity rainfalls that fall over a shorter period show less ingress than the same amount of low-intensity rainfall that falls over a longer period (Sarkar & Bhattacharjee, 2014).

For the half-cell potential test value ranges have been defined for the prediction of the risk of reinforcement corrosion (Malhotra & Carino, 2004). Value ranges that define criteria for the interpretation of resistivity measurements have also been proposed in different works of literature (ACI, et al., 2002). Both half-cell potential and resistivity measurements are however influenced by the effects of changing moisture content and temperature (Clemena, 1992). It is thus very important to understand how these factors influence the results that are obtained so that more accurate conclusions can be made when interpreting test results.

Concrete cover depth influences the rate of reinforcement corrosion as moisture, oxygen and aggressive chemical species that cause reinforcement corrosion to occur and progress must first pass through the cover layer before reaching the reinforcement (Arito, 2017; Otieno, et al., 2010). Cover depth testing is thus an important part of a condition assessment for the effects of reinforcement corrosion as it indicates where the distance through which substances need to pass to reach the reinforcement is less and can also serve as an immediate indication of the risk of corrosion initiation when compared to carbonation depths or chloride ingress profiles. When carrying out a cover depth assessment on a structure it can become too time-consuming to survey the entire structure. It thus becomes necessary to make a choice as to how much of the structure needs to be assessed in order to draw appropriate conclusions (PCTE, 2014). While

standards and guidelines provide information on the minimum required cover depths and how to carry out cover depth measurements, there is a lack of information on how to assess these measurements. Some guidelines do however exist for assessing cover depth measurements for the purpose of quality assessments such as RILEM suggested methods and methods by the German Concrete & Construction association (Corbett, 2015).

The results of the different condition assessment tests can be influenced by a number of factors and so it is important to understand the effects that these factors can have. Not all the tests are easy to carry out or easy to understand and for this reason, it is often suggested that specialist individuals or groups should carry out the tests or interpretations of the tests (Mackechnie & Alexander, 2001). These tests are very important when it comes to prolonging the lives of structures and protecting both people and the environment and so continuous research into condition assessments can prove to be crucial.

3. Methodology

3.1. Test procedures

3.1.1. Visual assessment

The locations that were chosen for the purpose of the field investigations were selected after carrying out a visual analysis of the buildings at the University of Cape Town's Upper Campus while taking several limitations into consideration. The University was selected for the purpose of this investigation as the equipment which was used for testing belongs to University's Civil Engineering department and needed to be collected on the days when tests were to be carried out. Together with the convenience of carrying out tests at UCT, the location also provides a safe environment for tests being carried out early in the morning and in the evenings due to the security presence and regular passing by of both staff and students.

The great majority of buildings at UCT are covered with plaster, which influences the half-cell potential and resistivity tests as these tests rely on an electric current passing through the concrete. Both the half-cell probe and resistivity meter need to be applied directly to the wet concrete surface to allow for a good flow of current through the concrete and the plaster layers create difficulty in doing so. The layers of plaster would also cause challenges when recording the cover depths as the depth of the plaster layer is not known and this depth adds an extra value to the measured cover depth. The plaster which is used is in general not smooth, which can also hinder the use of the covermeter. These plastered buildings were thus deemed unsuitable for the purpose of these investigations. Three buildings, namely the Rachel Bloch House, Hoerikwaggo Building and Neville Alexander building were found to have suitable locations of reinforced concrete that were not plastered and found to be adequate for the investigations. Images of the three buildings can be seen in Figures 19-21. Locations 2-4 were on the face of the building and had no shelter. Locations 1 and 5 had some shelter but were still largely exposed to the environmental conditions in the areas where the measurements were taken. This could be seen on rainy days as both Locations 1 and 5 were wet.

The locations that were chosen on the above mentioned three buildings, for comparing the results of the different test methods and carrying out the half-cell potential and resistivity testing, all showed visual signs of reinforcement corrosion at the selected location or close to the selected location. The five test locations are shown in Figures 22-26 and zoomed out images of each location can be seen in Figures 76-80 in Section 1 of the Appendix. Signs of visual damage at 4 of the 5 tests locations included spalling and exposed corroded reinforcement. The fifth location had delamination and repair works for reinforcement corrosion-induced problems occurring nearby. Locations which displayed visual signs of reinforcement corrosion were selected as this would allow for a comparison of the results of the different test methods when a state of corrosion is present, creating consistency in the investigation. The half-cell potential

measurements that were obtained were close to the range of uncertainty from the ASTM C876 standard and thus did not only indicate the presence of reinforcement corrosion or a complete lack thereof within the locations that were chosen. With values within these ranges, it becomes clearer to assess whether the changing weather conditions can lead to changes in the interpretation of the state of reinforcement corrosion based on the prescribed value ranges.

For the purpose of the half-cell potential tests, a connection to the reinforcement is necessary. The locations with exposed reinforcement were also selected for this reason, as they allow for the reinforcement connection to be made without having to remove any extra concrete from the buildings. Only the rust from the exposed reinforcement needs to be brushed off to make an adequate connection and so no damage to any buildings was necessary to carry out the half-cell potential tests.

The fifth location that showed signs of reinforcement corrosion nearby was found to show no indication of the presence of reinforcement corrosion under the different condition assessment tests. For this test, the half-cell potential values were found to be high with all values falling outside of the range of risk of corrosion as prescribed by the ASTM C876 standard. The resistivity values were also high, all falling well out of the range of risk of corrosion as prescribed in the literature. It was decided to use this location as a control location to determine whether the changing weather conditions have a similar effect on the measured values for a location where reinforcement corrosion is present and a location where it is not present.

- Buildings on which the tests were carried out:

Figure 19: Rachel Bloch House

Figure 20: Hoerikwaggo building

Figure 21: Neville Alexander building

- Five test locations which were chosen:

Figure 22: Location 1 (Rachel Bloch House)

Figure 23: Location 2 (Hoerikwaggo building)

Figure 24: Location 3 (Hoerikwaggo building)

Figure 25: Location 4 (Hoerikwaggo building)

Figure 26: Location 5 (Neville Alexander building)

3.1.2. Carbonation

Carbon dioxide from the atmosphere moves into concrete and reacts with the alkalinity of the cement leading to the formation of calcium carbonate and a drop in the concrete's pH levels. The reactions which occur cause the protective passive layer which surrounds the reinforcement to be destroyed and this allows for the occurrence of corrosion (Otieno, et al., 2010). Carbonation testing is used to determine how deep into the concrete the carbonation front has progressed in relation to the reinforcement depth. This allows for a prediction on whether corrosion due to carbonation is likely to be occurring or how likely it is that it may occur in the future. The phenolphthalein indicator test is a commonly used test for predicting the depth of the carbonation front. The indicator is sprayed on freshly exposed concrete samples and changes colour on uncarbonated concrete to a pink/purple colour, while remaining clourless on concrete that has undergone carbonation. Measuring the depth of the colourless layer gives the carbonation depth (Chandra Paula, et al., 2018; Lee, et al., 2012).

I. Locations for removing cores:
   - The 5 locations shown in Figures 22-26, that were selected for comparing the results of the different tests.
   - Four cores from different locations along the Neville Alexander building. Cores were taken from each face of the building. The locations from which these cores were taken are shown in Figures 27-30.
   - An additional core from a location on the west side of the Hoerikwaggo building as shown in Figure 31.

Figure 27: Location from which a core was extracted on the ground floor of the South side of the Neville Alexander building

Figure 28: Location from which a core was extracted on the ground floor of the East side of the Neville Alexander building

Figure 29: Location from which a core was extracted on the ground floor of the West side of the Neville Alexander building

Figure 30: Location from which a core was extracted on the ground floor of the North side of the Neville Alexander building

Figure 31: Location from which a core was extracted on the ground floor of the West side of the Hoerikwaggo building

II. The concrete core drill was set to drill cores of a 15 mm diameter. The depth of each core that was drilled was approximately 70 mm. The core dimensions were chosen in order to cause the least amount of damage to the structures while remaining adequate for carbonation testing.

III. Each core was wiped down to remove the dust.

IV. Once wiped down the phenolphthalein indicator was sprayed onto each sample.

V. The depth of carbonation in millimeters was measured using a ruler. Measurements were taken from different sides of each core so that an average depth of carbonation per core could be determined.

3.1.3. Cover depth

The depth of reinforcement cover plays an important role in protecting against the occurrence of reinforcement corrosion. For reinforcement corrosion to occur, harmful substances need to move through this layer of cover to reach the reinforcement (Otieno, 2014). Cover depth tests are important to determine what the actual cover depth on-site is and whether locations are at risk of reinforcement corrosion damage due to insufficient cover. The location of the reinforcement is also necessary for determining the appropriate locations for carrying out half-cell potential, resistivity and carbonation tests (Sivasubramanian, et al., 2013).

The cover depth survey was conducted in 2 parts. The first part involved mapping of the reinforcement and recording of cover depths at the locations chosen for the comparisons of the different test methods. The second part involved a more comprehensive analysis of cover depths carried out at several locations on the Neville Alexander building.

3.1.3.1. Part 1

These tests were carried out at the very beginning of the fieldwork procedures for each of the five test locations shown in Figures 22-26 as well as all the locations from which the cores for carbonation were to be drilled. The mapping of reinforcement was carried out first as the location of the reinforcement feeds into all the other tests that were carried out. The map of the reinforcement is necessary to provide the locations for taking both half-cell potential and resistivity measurements as well as to provide locations from which it would be safe to remove cores for the carbonation testing. For each of the five test locations cover depth measurements were recorded in the locations where the reinforcement had been mapped out for both the vertical and horizontal reinforcement.

3.1.3.2. Part 2

Cover depth measurements were taken at 8 locations along the 4 different faces of the Neville Alexander building. The purpose of these tests was to assess variability in cover depth measurements due to changes in location along a building and changes in the measurement sample size that is used. The locations included locations along the ground, first and third floors of the building. These measurements were all taken on the same member type, namely the walls of the building, to allow for consistency in comparisons. Details on the location along the building and sizes of the measurement locations that were used for the analysis are given in Section 3.2.2. Images of the different locations care shown in Figures 33-40. Zoomed out images of these test locations can be seen in Figures 81-88 of Section 2 of the Appendix.

3.1.3.3. Test equipment

Elcometer 331 Concrete Covermeter. This covermeter is used as a gauge for determining the location of reinforcement bars and metal pipes and for measuring the thickness of the concrete cover above the reinforcement and pipes. The covermeter uses interchangeable search heads, such as for measurements in locations where the concrete cover is deep. The covermeter can be used in accordance with a number of standards including British and ASTM standards. An image of this covermeter can be seen in Figure 32 (Elcometer, 2012).

Figure 32: Elcometer 331 covermeter (Elcometer, 2012)

3.1.3.4. Test procedure

The procedure for measuring the reinforcement cover depths was carried out as follows:

I. The location of the vertical reinforcement was determined by first zeroing the covermeter and then passing the search head over the concrete surface in the horizontal direction, parallel to the vertical reinforcement. The location of the reinforcement is indicated by the covermeter when the reinforcement depth displayed reaches a local minimum value before it begins to increase again. When approaching the minimum, the covermeter emits a high-pitched sound and displays a red LED light. At the location of the reinforcement, the sound will be at its highest pitch and the

LED light will shine brightest. It is at these locations that markings were made to map the vertical reinforcement.

II. Finding the location of the horizontal reinforcement was carried out in the same manner as was followed for the vertical reinforcement, except that the search head was now passed over the concrete surface in the vertical direction parallel to the reinforcement.

III. A full map of the reinforcement in each location was then drawn on the building by connecting the markings that had been made.

IV. The size of the reinforcement bars was determined by exposing a small section of the reinforcement.

V. The reinforcement bar size was input into the covermeter and cover depth measurements in both the vertical and horizontal directions were recorded at each intersection along the drawn-out maps.

Figure 33: Location for the cover depth assessment on the ground floor of the south side of the Neville Alexander building

Figure 34: Location for the cover depth assessment on the ground floor of the east side of the Neville Alexander building

Figure 35: Location for the cover depth assessment on the 1st floor of the east side of the Neville Alexander building

Figure 36: Location for the cover depth assessment on the ground floor of the west side of the Neville Alexander building

Figure 37: Large location for the cover depth assessment on the ground floor of the west side of the Neville Alexander building

Figure 38: Location for the cover depth assessment on the 1st floor of the west side of the Neville Alexander building

Figure 39: Location for the cover depth assessment on the ground floor of the north side of the Neville Alexander building

Figure 40: Location for the cover depth assessment on the 3rd floor of the north side of the Neville Alexander building

3.1.4. Half-cell potential

The half-cell potential test is commonly used in the prediction of reinforcement corrosion. This test method is suggested for use in a number of standards and guidelines and is considered a non-destructive test. Corrosion causes a potential difference to exist between actively corroding areas and passive zones. A current flows between these areas and leads to the development of potentially differentiated fields around the reinforcement. It is through measurement of these potentials that the half-cell potential test forms a guide for predicting whether corrosion is present or not (Maierhofer, et al., 2010; Malhotra & Carino, 2004).

The half-cell potential measurements were carried out over a 4-month period under different exposure conditions. These exposure conditions included dry periods, periods after different levels of rain and days with different temperatures ranging from 13-35°c. This was done with the intention of testing for variations in measurements due to the effects of rain (moisture content) and temperature. Two days of test results were used for the comparison of the different test methods, namely the day with the highest and the day with the lowest measured values that were obtained across the testing period at each location.

3.1.4.1. Test equipment

Elcometer 331 Concrete Covermeter with half-cell probe. The Elcometer 331 can be used as a half-cell gauge that measures half-cell potential values in millivolts. The covermeter comes with a half-cell kit that contains a half-cell probe with a silver electrode in a silver chloride solution as well as a crocodile clip extension for connection to the rebar. The covermeter can be used in accordance with a number of standards including the ASTM C876 standard. An image of the covermeter with the half-cell probe connection can be seen in Figure 41.

Figure 41: Elcometer 331 covermeter with half-cell probe connection (Elcometer, 2012)

3.1.4.2. Test procedure

Exposed reinforcement was selected for the metallic connection where possible. In the one location where no exposed reinforcement was present, a small amount of cover was removed in order to make the necessary connection. The following procedure was then carried out:

I. A steel brush was used to remove the rust layer from the top of the exposed reinforcement. This was necessary in order to make a good metallic connection to the reinforcement.

II. The connection to the reinforcement bar was made using a crocodile clip.

III. The head of the half-cell probe was wetted by placing water in the probe cap and placing the head of the probe into the cap for a few minutes.

IV. The surface of the concrete was also wetted by pouring water over the concrete surface.

V. The half-cell was then placed on each location of the reinforcement map where the vertical and horizontal reinforcement met. At each location, the half-cell potential measurements were recorded.

VI. Measurements were then taken in the same locations after 5 minutes and these results were compared with those that were previously taken. When the values had not changed by more than 20 mV over a 5-minute period then the initial values were deemed as a sufficient representation of the actual half-cell potential at that measurement point. When the values changed by more than 20mV then the concrete surface had to be wetted again. This process was repeated until the change over a 5-minute period was found to be less than or equal to 20 mV.

3.1.5. Resistivity

The corrosion rate depends on how much electrical current is able to move through the concrete pore structure between the anodic and cathodic region. The resistivity of the concrete governs the ease with which current by ionic movement passes through the concrete (Alexander, et al., 2012; Srinivasan, 2014). Concrete with a higher resistivity allows less ionic movement to occur. The Wenner 4-probe meter is a commonly used tool for measuring resistivity infield. The Proseq Resipod is an example of such a resistivity meter and works by passing an alternating current between the 2 outer probes and measuring the voltage drop which occurs as the current travels through the concrete. This voltage drop is measured by the 2 inner probes and is converted to obtain the surface resistivity of the concrete.

The resistivity measurements were carried out at the same time and under the same conditions as the half-cell potential measurements. This was also done to test for variations in measurements brought about by rain and temperature changes. As with the half-cell potential measurements, the days with the highest and lowest measurements that were obtained across the testing period were used to carry out the comparisons of the different test methods.

3.1.5.1. Test equipment

Proseq Resipod 4-probe Resistivity meter. The Resipod functions on the basis of the Wenner probe principle to measure the electrical resistivity of the concrete. The version of the Resipod that was used has a 50 mm probe spacing that conforms to the industry accepted standard. The resistivity measurements are shown on a display screen in units of kilo Ohm-centimeter. An image of the Proseq Resipod can be seen in Figure 42 (Proceq, 2017).

Figure 42: Proceq resipod 4-probe Resistivity meter (Proceq, 2017)

3.1.5.2. Test procedure

The procedure for measuring resistivity was carried out as detailed below:

I. The Resipod was tested against the test strip before taking measurements at each location.

II. Each location was then wetted over a period of time.

III. The Resipod was then used to take measurements diagonally between the grid squares of horizontal and vertical reinforcement as shown in Figure 16 of the literature review.

IV. If the reading was stable, then it was recorded. If a stable reading was not obtained, then the surface was further wetted until stable readings were be obtained.

V. At each location, the Resipod was moved 5 times by a few millimeters in order to calculate an average value per grid square.

3.2. Analysis procedures

3.2.1. Half-cell potential & resistivity across varying weather conditions

The measurements collected at the different locations for each day of testing are to be displayed in table form for both the half-cell potential and resistivity results as well as in the form of contour plots for the half-cell potential results. The details of the exposure conditions for the different days of testing is based on weather data obtained from the South African Weather Service. The measurement data and the weather data are to be compared to each other to determine how the absolute values and contour plots may have changed due to varying exposure conditions.

The comparison of absolute values was done by relating the values that have been measured to the prescribed value ranges for the prediction of the presence of reinforcement corrosion from ASTM C876 for half-cell potential measurements and experimentally determined ranges for the resistivity measurements. These prescribed value ranges can be seen in Tables 3-6. The aim is to determine whether changes in environmental conditions will lead to a big enough shift in absolute measurements causing the value to fall in a different range and thus leading to a change in the predicted state of reinforcement corrosion. Data pertaining to the change in value per measurement across the testing period will take the form of the minimum value, maximum value, the difference between the minimum and maximum values and the standard deviation per measurement location. These values will then be used to calculate the average maximum change and average standard deviation per location for each of the five test locations.

The comparison of the potential plots will be used to determine whether the shift in values due to the exposure conditions leads to any significant change in the contour patterns or whether the changes are limited to absolute measurements, thus supporting the use of a contour analysis instead of the prescribed value ranges.

3.2.2. Variation in cover depth

The variation in cover depth due to changes in location, the number of measurements taken, and analysis procedure used was determined by using general statistics as well as RILEM and German suggested methods (Monteiro, et al., 2015) for assessing the minimum achieved cover depths. When it comes to taking cover depth measurements for the purpose of a condition assessment it is very rarely possible to survey the whole building or even a large percentage of the building. It is often the case that only a few measurements are taken in a particular location or from a number of random locations. This analysis aims to determine if and by how much cover depth statistics will change if a small or large amount of measurements are taken from a particular location, if the measurements are taken from one side of a

building or another or from locations at different heights along the building. The analysis was performed on the Neville Alexander building.

For the purpose of assessing variations in location for both the different sides of the building and different floors of the building, the following cases were considered:

I. Measurements were taken across equal surface areas of approximately 1.5 m^2 for the following seven locations:

- North face ground floor
- South face ground floor
- East face ground floor
- West face ground floor
- East face 1st floor
- West face first floor
- North face 3rd floor

II. The second case considered involved taking measurements from a large 7.5 m^2 area and then two 1.5 m^2 areas from both the right and left top corners of the same 7.5 m^2 area. This location was located on the west side of the ground floor of the building. This was also done for a 3 m^2 area on the ground floor of the south side of the building.

To assess how variations in sample sizes affect the cover depth results, the following cases were considered:

I. The same 7.5 m^2 area from the west side of the building that was used to assess changes due to variations in location was assessed for this purpose. For this location, a difference in sample size was considered by using the 190 measurements across the full 7.5 m^2 area as well as random samples of 100, 50 and 20 randomly selected values from the 7.5 m^2 area.

II. A second analysis for variation in sample size involved using all 245 measurements from the seven 1.5m^2 areas from around the building as well as 200, 100, 50, 20, 10 and 5 randomly selected values from these locations.

III. Seven runs for both 100 and 10 randomly selected values from the seven 1.5 m^2 areas were also carried out to aid in the assessment of variations caused by sample size.

* Note: The random selection of cover depth values was carried out by using the Microsoft Excel sampling tool

3.2.2.1. RILEM quantitative analysis

The RILEM quantitative analysis is described in detail in section 2.3.4.3 of the literature review. For the analysis that was carried out it was assumed that the cover depth population was normally distributed. The assumption of a normal distribution is recommended when the mean cover depth value is greater than 20 mm and this was found to be the case for all the measurement locations that were chosen. The minimum cover depth values for each of the above-mentioned cases were then determined using Equation 7. This required the calculation of both the mean and standard deviations for each case as well as the selection of the tolerance factor k from Table 1. All the cases were assessed for both the 5^{th} and 10^{th} percentiles and 50, 75, 90 and 95% confidence levels for both percentiles.

3.2.2.2. German (DBV-Merkblatt) quantitative analysis:

The German quantitative analysis is described in detail in Section 2.3.4.4. of the literature review. The minimum achieved cover depths for both the 5^{th} and 10^{th} percentiles were calculated for each of the above-mentioned analysis cases using Equations 11 and 12 respectively. Equations 11 and 12 required the calculation of the input variables r and m which were determined using Equations 13 and 14 respectively. In order to solve for Equations 13 and 14 the standard deviation, mean and median of the cover depth samples had to be calculated for each case.

3.2.3. Comparison of the different test methods

The half-cell potential and cover depth tests and half-cell potential and resistivity tests is compared in this analysis. This comparison is carried out based on the results of the tests which were conducted at Locations 1-5, which are shown in Figures 22-26. Scatter plots of the results for HCP vs Cover Depth and HCP vs Resistivity were graphed. The plots were output for each location to determine whether a relationship between the variables exists and if so, whether the relationship remains the same or varies from location to location.

The relationship between HCP and cover depth is likely to be affected by variations in the concrete's material properties and variations in the exposure conditions which can both influence the rate of reinforcement corrosion. The material properties of the concrete will not remain constant in all locations and this can influence the ability of corrosion inducing substances being able to reach the depth of the reinforcement. Variations in exposure conditions due to location, surrounding obstacles and the effects of weather can also speed up the onset of reinforcement corrosion in certain locations. The HCP results are expected to decrease as the resistivity results decrease and vice versa as both of these tests are somewhat affected by the same factors such as moisture content and temperature.

The results of the carbonation tests will not be statistically compared to the results of the other tests as only a few carbonation measurements were taken in comparison to the number of measurements taken for each of the other tests. The number of half-cell potential and cover depth values at each location are equal and so these values will be compared directly.

Resistivity measurements were taken in the area between two horizontal and vertical reinforcement bars, while half-cell potential measurements were taken at the intersection of horizontal and vertical reinforcement bars. This means that for every resistivity measurement there are four surrounding half-cell potential measurements. For this reason, the average of the four-half-cell potential measurements surrounding the resistivity measurement was calculated so that the number of values could be equal to those of the resistivity tests and a comparison of the test results could be carried out.

4. Results & interpretation of results

4.1. Results

4.1.1. Carbonation depth

The depth of carbonation for each of the core samples taken from the different locations is shown in Table 7. The measurements represent the average depth of the uncoloured layer of each core after the core was removed, wiped down and sprayed with the phenolphthalein indicator. All the carbonation depths are given in millimeters.

Table 7: Table of the average measured carbonation depths (mm).

Locations	Average carbonation depth (mm)
Rachel Bloch House Column	2
Neville Alexander South Face Ground	3
Neville Alexander West Face Ground	3
Neville Alexander East Face Ground	3
Neville Alexander North Face Ground	4
Neville Alexander North Face Top	2
Hoerikwaggo West wall	17
Hoerikwaggo North wall	26
Hoerikwaggo retaining wall	8
Hoerikwaggo North Column	7

4.1.2. Cover depth

The cover depth measurements were read and recorded from the display screen of the Elcometer 331 covermeter. There were however too many cover depth measurements to record in this report and so the results were recorded statistically in the form of the mean, median, range and standard deviation for each of the different measurement cases mentioned in Section 3.2.2. Cover depth measurements were also taken for the five measurement locations that were used for the half-cell potential and resistivity measurements and are displayed in the comparison graphs for the HCP and cover depth results shown in Figures 56-65. Cover depth results for the seven 1.5 m^2 areas from around the Neville Alexander building in the form of general statistics can be seen in Table 8. Further cover depth statistics are shown in Tables 29-34 and Tables 35-90 of Section 4 of the Appendix.

Table 8: General cover depth statistics for the seven 1.5 m^2 areas from around the Neville Alexander building.

All 1.5m^2 locations							
Data	Vertical Cover Depth Measurements (mm)						
	North Ground	North 3rd Floor	South Ground	East Ground	East 1st Floor	West Ground	West 1st Floor
Number of measuremnts	28	30	28	42	40	30	49
Median	57	49	45	40	47	42	60
Range	35-75	35-55	32-57	26-50	27-60	25-52	33-82
Mean	57	48	44	39	47	42	61
Standard deviation	10.5	48.0	5.8	6	6.5	5.6	10.6

4.1.3. Half-cell potential

The half-cell potential results were recorded from the measurement screen of the Elcometer 331 covermeter. The half-cell potentials were recorded in millivolts. Potentials were recorded for eight days during the months of August to November. The results for each of the five test locations are shown in Tables 9-13.

Table 9: Half-cell potential results for location 1.

Location 1															
Date	Half-cell potential (mV)														
7th Aug	41	-20	81	174	94	70	130	183	75	27	137	205	77	78	99
13th Aug	28	-46	62	160	88	64	122	152	80	16	121	213	81	84	92
27th Aug	20	-74	30	64	71	45	48	83	44	2	54	120	38	38	40
6th Sep	15	-76	31	96	49	51	44	61	51	14	61	121	41	58	48
28th Sep	-171	-136	16	35	-19	-32	15	-25	-50	-50	-9	45	-34	-31	-40
27th Oct	-362	-333	-223	-122	-162	-149	-214	-121	-171	-207	-200	-60	-162	-140	-187
19th Nov	-350	-326	-207	-130	-159	-130	-197	-119	-173	-198	-192	-39	-150	-147	-186
23rd Nov	-327	-312	-196	-113	-146	-119	-170	-98	-157	-155	-150	10	-123	-98	-125

Table 10: Half-cell potential results for location 2.

Location 2										
Date	Half-cell potential (mV)									
7th Aug	-182	-150	-89	-97	-114	-116	-77	-115	-50	-103
13th Aug	-202	-185	-110	-110	-121	-131	-85	-141	-69	-129
27th Aug	-260	-236	-160	-175	-177	-169	-177	-166	-130	-151
6th Sep	-290	-293	-193	-200	-212	-182	-187	-184	-152	-196
28th Sep	-204	-193	-128	-150	-117	-142	-115	-155	-120	-133
27th Oct	-205	-175	-95	-140	-106	-126	-98	-140	-94	-135
19th Nov	-201	-169	-90	-121	-101	-106	-92	-121	-73	-122
23rd Nov	-198	-152	-79	-106	-82	-99	-67	-128	-55	-114

Table 11: Half-cell potential results for location 3.

Location 3												
Date	Half-cell potential (mV)											
7th Aug	-300	-309	-348	-217	-337	-289	-313	-210	-280	-189	-251	-152
13th Aug	-356	-369	-377	-256	-379	-347	-427	-255	-306	-213	-304	-205
27th Aug	-417	-480	-447	-391	-420	-433	-450	-304	-384	-314	-430	-350
6th Sep	-419	-471	-433	-422	-424	-390	-450	-292	-370	-282	-377	-322
28th Sep	-403	-451	-418	-332	-405	-364	-422	-284	-364	-303	-362	-311
27th Oct	-375	-399	-390	-317	-386	-330	-405	-269	-350	-284	-350	-286
19th Nov	-372	-390	-378	-270	-376	-299	-376	-263	-328	-270	-338	-279
23rd Nov	-365	-379	-347	-276	-348	-276	-358	-245	-310	-262	-319	-240

Table 12: Half-cell potential results for location 4.

Location 4																
Date	Half-cell potential (mV)															
7th Aug	-166	-142	-105	-83	-96	-78	-66	-45	-60	17	14	59	55	45	51	64
13th Aug	-139	-132	-95	-68	-56	-50	-51	-35	-50	17	20	64	70	59	68	82
27th Aug	-220	-185	-172	-152	-144	-107	-103	-115	-96	-41	-27	-22	-15	-20	-11	-7
6th Sep	-215	-194	-170	-151	-135	-115	-100	-72	-94	-57	-26	-21	-5	-5	-1	3
28th Sep	-206	-193	-158	-142	-136	-113	-97	-60	-90	-36	-22	-24	-11	-10	-6	6
27th Oct	-186	-169	-127	-106	-85	-69	-56	-36	-49	-12	-7	-3	6	8	4	12
19th Nov	-173	-157	-114	-92	-72	-55	-48	-39	-34	6	12	14	26	23	19	34
23rd Nov	-176	-162	-134	-90	-68	-58	-43	-42	-30	-3	-1	5	15	11	9	17

Table 13: Half-cell potential results for location 5.

Location 5														
Date	Half-cell potential (mV)													
7th Aug	227	230	223	172	257	237	236	144	251	240	267	242	184	240
13th Aug	197	194	180	123	215	206	202	96	213	197	218	207	145	197
27th Aug	147	154	143	81	168	168	162	56	170	120	151	190	90	148
6th Sep	150	155	142	82	173	171	160	59	169	124	153	182	92	150
28th Sep	141	139	139	77	160	170	155	54	163	126	157	176	93	144
27th Oct	193	193	188	149	205	216	211	102	195	181	207	217	157	201
19th Nov	195	190	197	170	211	222	226	107	212	220	226	232	187	227
23rd Nov	212	212	217	178	224	234	241	115	228	243	240	226	181	139

4.1.4. Resistivity

The resistivity results were recorded from the measurement screen of the Proseq resipod. These results were recorded in units of kilo Ohm-centimeters. The resistivity results were recorded for the same eight days of testing during the months of August to November as was the case for the half-cell potential measurements. These results for each of the five tests locations are shown in Tables 14-18.

Table 14: Resistivity results for location 1.

Location 1									
Date	Resistivity (kohm.cm)								
7th Aug	127	114	160	124	173	217	117	205	285
13th Aug	108	91	144	82	137	223	95	178	245
27th Aug	70	69	60	61	117	175	63	118	219
6th Sep	57	49	60	75	108	170	65	140	216
28th Sep	84	80	83	88	119	185	82	160	219
27th Oct	89	85	88	82	134	215	87	163	281
19th Nov	111	92	110	93	149	241	99	170	321
23rd Nov	113	93	115	96	164	234	111	186	333

Table 15: Resistivity results for location 2.

Location 2												
Date	Resistivity (kohm.cm)											
7th Aug	469	436	603	605	296	332	551	259	247	533	361	360
13th Aug	446	395	556	575	290	236	511	254	170	491	341	372
27th Aug	314	200	254	410	122	126	232	106	123	378	215	233
6th Sep	340	230	260	427	156	150	300	120	131	385	226	248
28th Sep	319	217	255	415	137	138	284	104	144	455	214	256
27th Oct	412	401	610	585	322	288	540	213	184	500	337	366
19th Nov	423	400	627	601	345	295	552	240	198	515	345	380
23rd Nov	442	429	642	580	325	306	571	358	213	536	351	394

Table 16: Resistivity results for location 3.

Location 3						
Date	Resistivity (kohm.cm)					
7th Aug	1206	1415	1424	1009	850	763
13th Aug	1100	1238	1394	975	673	737
27th Aug	980	1185	1292	856	597	636
6th Sep	1025	1156	1340	880	632	654
28th Sep	1047	1180	1367	876	616	678
27th Oct	1183	1256	1412	925	643	724
19th Nov	1223	1273	1480	1004	705	752
23rd Nov	1302	1367	1533	1102	770	806

Table 17: Resistivity results for location 4.

Location 4									
Date	Resistivity (kohm.cm)								
7th Aug	408	532	457	742	1135	1217	1523	1231	1512
13th Aug	393	546	472	794	1248	1244	1550	1264	1581
27th Aug	267	387	343	594	960	1035	1306	1134	1359
6th Sep	285	442	356	623	1014	1082	1350	1163	1382
28th Sep	280	401	376	611	1044	1077	1364	1070	1377
27th Oct	352	498	479	689	1094	1180	1460	1223	1429
19th Nov	363	514	493	679	1078	1205	1443	1039	1480
23rd Nov	360	486	509	693	703	1223	1511	1235	1505

Table 18: Resistivity results for location 5.

Location 5									
Date	Resistivity (kohm.cm)								
7th Aug	1374	1409	1274	1249	833	791	745	1103	1439
13th Aug	1245	1280	1104	1180	857	949	968	942	1342
27th Aug	1073	1115	892	976	546	557	577	519	1100
6th Sep	1142	1184	964	1055	622	680	602	608	1167
28th Sep	1050	1126	937	1011	579	528	538	495	1087
27th Oct	1165	1237	1042	1091	674	693	704	734	1267
19th Nov	1178	1252	1033	1136	698	743	652	761	1202
23rd Nov	1197	1267	1068	1150	711	726	678	793	1321

4.2. Interpretation of results

4.2.1. Half-cell potential & resistivity across varying weather conditions

When comparing the measurements taken across the different days of testing to the weather data obtained from the South African Weather Service, it was found that rain and the impact it has on concrete moisture content can have a notable impact on both the half-cell potential and resistivity measurements. The weather data was from the closest weather station to the university, located at the Kirstenbosch Botanical Gardens. The gardens are approximately 6.1 kilometers away from UCT and so the weather data may not fully represent the conditions at university but was deemed suitable for the purpose of these tests. Bar graphs showing a comparison between rainfall, average HCP and average resistivity for the different days of testing at each of the five locations are shown in Figures 43-47. The rainfall in these graphs are exaggerated by a factor of 10 to illustrate the change more clearly. From Figure 43 rainfall appears to have a direct correlation with the resistivity at Location 1, but not with HCP. The change in HCP measurements from positive to negative at Location 1 is discussed in Section 4.2.1.1.

The City of Cape Town had been experiencing a drought prior to the period during which the testing was carried out. During June and July rain had started to fall again and continued to fall significantly up to the month of October. The results show that over the period of testing as more and more rain fell the results became more negative and during the drier months of October and November the results started to increase again. These findings are supported by the theory and experimental works dealing with the effect of moisture content on half-cell potential and resistivity measurements that are discussed in Sections 2.3.5.5 and 2.3.6.3 respectively. During the months of October and November, the total rainfall that was recorded was 22.6 and 32 mm respectively, which is significantly less than the 120, 209 and 206.4 mm that fell during the respective months of July, August and September.

The rainfall in the week leading up to and including the first two days of testing, namely the 7th and 13th of August were 46.2 and 49.2 mm respectively. Both the half-cell potential and resistivity results on these days were found to be significantly higher than the results that were recorded over the next three days of testing on the 27th of August, 6th of September and 28th of September. This can be attributed to the rainfall prior to and including the first two days of testing being 20-40 mm less than that of the next three days of testing as well as a build-up of the effects of rainfall as the rainy season progressed.

The three days of testing that showed the most negative measurements were the days of the 27th of August, 6th of September and 28th of September. The amount of rain which was recorded in the week prior to and including each of these days of testing was 88.6, 71.8 and 81 mm for the three respective days of testing. The most negative day of results for all the locations (with the exception of the half-cell potential results at location 1) was found to be on one of these 3 days, but not the same date for all the locations. This can be attributed to variables such as the direction that the locations face, surrounding obstructions and the direction and intensity with which the rain was falling. In the week prior to and including the day of testing for the days of the 27th of October, 19th of November and 23rd of November the amount of rain

recorded was 0, 2.4 and 5.2 mm respectively. This is very little rain when compared to the days of testing at the end of August and during September and this can be seen to cause an increase in both the half-cell potential and resistivity measurements.

A higher temperature is known to speed up reactions leading to half-cell potential and resistivity values becoming more negative. During the first five days of testing the temperatures were very similar, ranging from 13-17°c. The similar temperatures combined with these days of testing falling within a period of high rainfall makes it difficult to isolate the relationship between temperature and half-cell potential or resistivity measurements. For the test days of the 27th of October, 19th of November and 23rd of November the average temperatures were 35, 29 and 25°c respectively. These three days showed more negative measurements on the days when the temperature was higher.

The difference in measurements between the last three days of testing is not as notable as those between the days of testing with large amounts of rain and small amounts of rain. This shows that the effect of temperature change in comparison to the effect that rainfall has on half-cell potential and resistivity measurements is not significant. The change in measurement values for the 27th of October, 19th of November and 23rd of November may also not be solely due to the effects of temperature change and may also be brought about by the increase in the time since the occurrence of the period of significant rainfall. This is supported by the results during the first two days of testing at the beginning of August being higher than the results of the last three days of testing, showing that the effects of rainfall may still be in play for a period after the rainy season ends and that the effects reduce as time passes. To try and isolate the effect of temperature change on these measurements it is recommended that tests be carried out during a period of drought so that the effects of rainfall do not influence results.

When it comes to the effects of temperature change on half-cell potential measurements the results of this works is supported by the findings of Keßler & Gehlen (2016), who's experiments under varying weather conditions showed that hotter temperatures lead to more negative half-cell potential measurements than colder weather. These changes were however found to be less significant than those caused by changing moisture content. Tests by the Washington State Department of Transportation on two bridges also found that a decrease in temperature resulted in slightly more positive half-cell potential measurements, but that this shift was not significant (Babaei, 1986). When it comes to the effect of temperature on resistivity several studies have found that temperature change can have a significant effect on resistivity measurements. As discussed in Section 2.3.6.3 studies have found that resistivity can change by 3-5% for every °C change in temperature (Akhlaghi & Tronca, 2015).

The findings of this works differs from the findings of other researchers when it comes to the effects of temperature change on resistivity. The reason for this may be due to this works being carried out infield and the other studies being carried out under controlled conditions within a lab. Infield measurements are subject to varying exposure conditions and so the effects of temperature change alone cannot be isolated. For the dry test days of the 27th of October, 19th of November and 23rd of November the average temperatures changed by a maximum of 10°c. In order to better assess the effect of temperature change on resistivity measurements taken infield a wider range of temperature changes would need to be tested. This was not possible due to time constraints and the occurrence of rainfall that would impact on results.

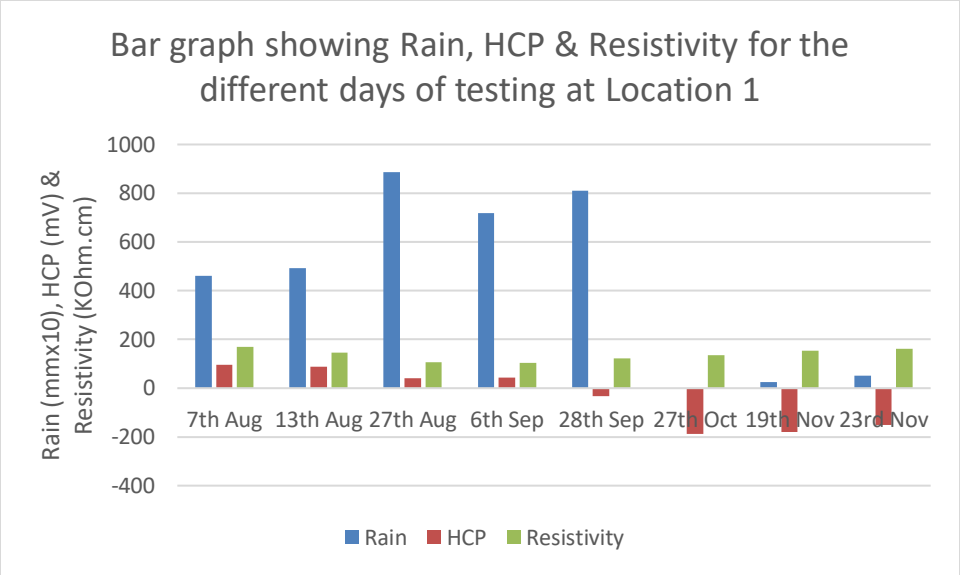

Figure 43: Bar graph showing the rainfall, average HCP & average resistivity for the different days of testing at Location 1.

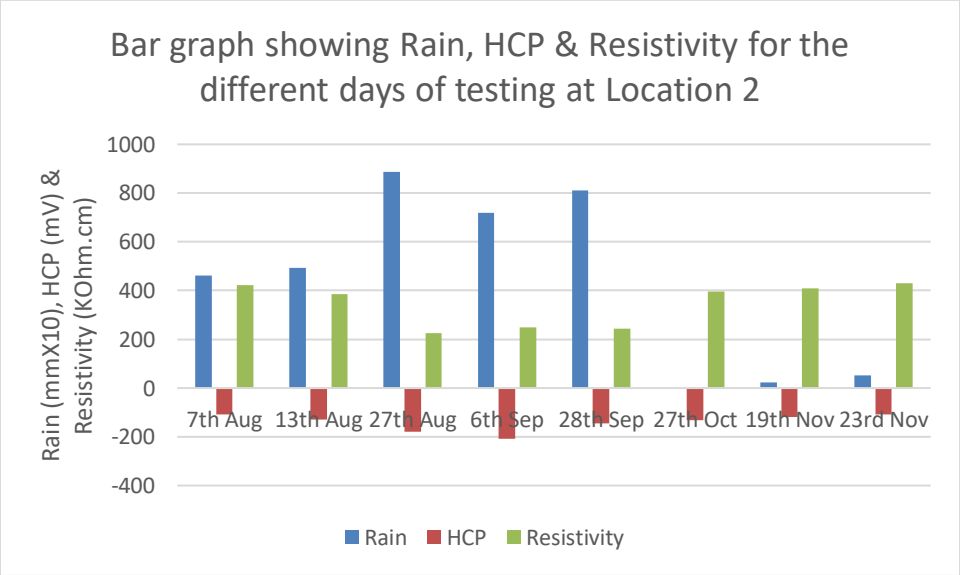

Figure 44: Bar graph showing the rainfall, average HCP & average resistivity for the different days of testing at Location 2.

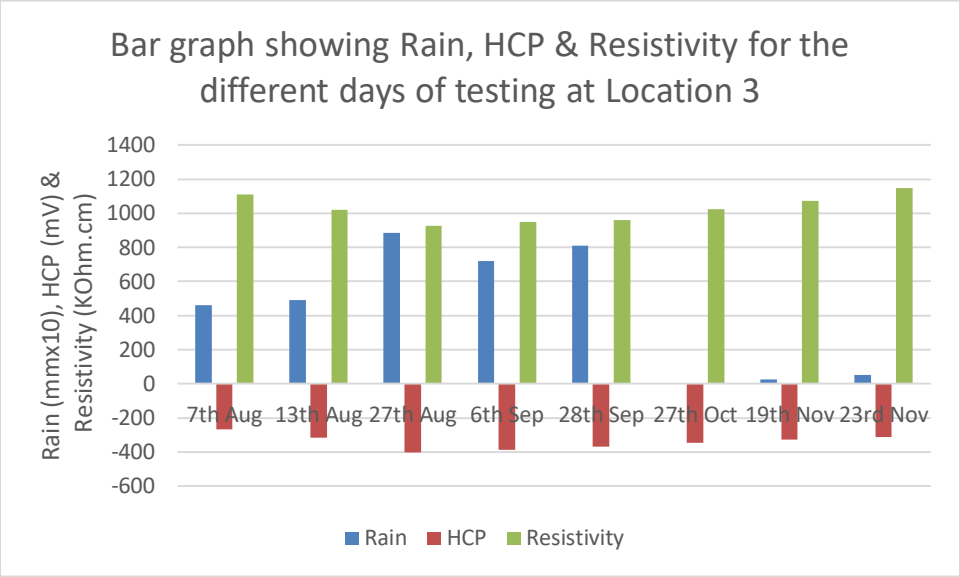

Figure 45: Bar graph showing the rainfall, average HCP & average resistivity for the different days of testing at Location 3.

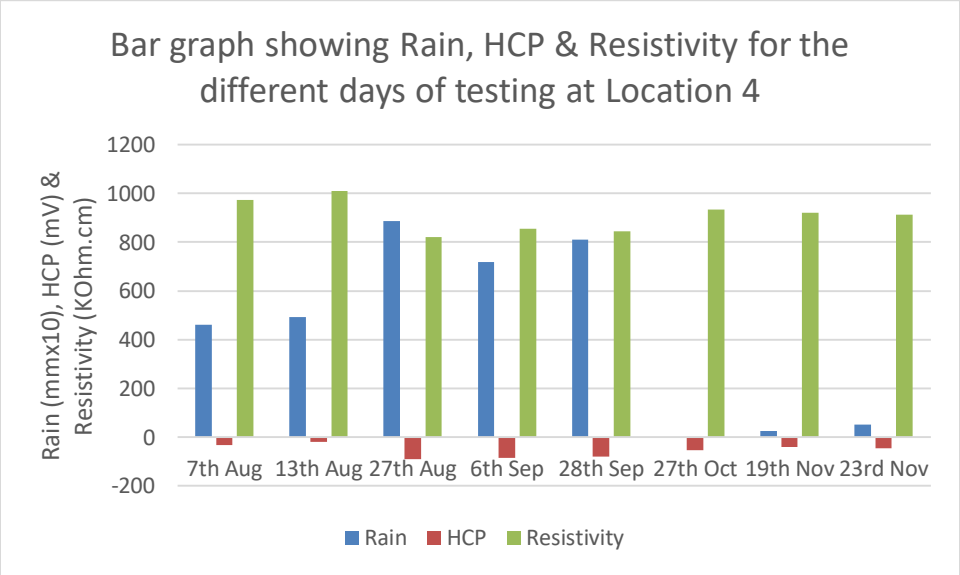

Figure 46: Bar graph showing the rainfall, average HCP & average resistivity for the different days of testing at Location 4.

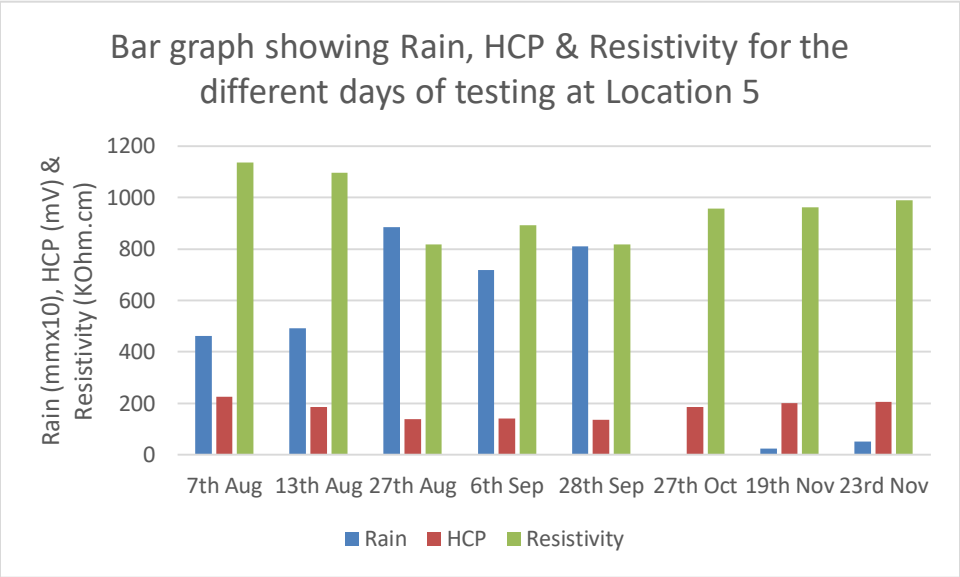

Figure 47: Bar graph showing the rainfall, average HCP & average resistivity for the different days of testing at Location 5.

4.2.1.1. Half-cell potential

Locations 1-4 which showed clear signs of corrosion in the form of delamination and exposed rusted reinforcement all displayed negative measurements which indicate a high risk or uncertain risk of the presence of corrosion as per the risk categories suggested in the ASTM C876 guideline. The results for Location 5, which did not show any clear signs of corrosion, were high in value and falling in the range of a low risk of corrosion. Location 5 was used as a control test location. The results show that the half-cell potential test can be valuable in the assessment of the corrosion state of a reinforced concrete structure.

The minimum and maximum value at each measurement point for each location over the testing period were calculated in order to determine what the maximum change in half-cell potential was for the testing which was carried out. This change was determined by subtracting the maximum value from the minimum value. The average of the maximum change per location was also calculated and these results can be seen in Tables 19-23.

Locations 1-5 show a maximum change in half-cell potential values of 403, 143, 198, 89 and 123 mV respectively. The average maximum change for locations 2-5 was found to lie between 75 and 140 mV, while location 1 had an average change of 287 mV. The large maximum and average maximum change for location 1 are believed to be due to corrosion initiation taking place during the testing period. The measurements at this location underwent a significant change from the measurements being notably positive to being notably negative.

From the bar graph shown in Figure 43 there seems to be a delay in the influence that rainfall and the consequent change in moisture content has on the half-cell potential values for Location 1. The increase

in rain seems to cause HCP values to become more negative and once corrosion had been initiated this became more evident and the trend continued into the next few months. Initially it was believed that corrosion was already taking place throughout Location 1 due to the exposed corroded rebar at a location with very low cover depth. The HCP values nearest to the exposed rebar were low from the time testing started, but as time went by all the measurements began to shift to much more negative values. This supports the idea that corrosion had started in the area where the rebar was exposed and then progressed throughout the location due to the exposure conditions. Location 1 was also the location with the lowest resistivity, which may have contributed to this location undergoing a large change in HCP values. The lower resistivity coupled with the increased moisture content that was brought about by the rain would have made it easier for the onset of corrosion to take place.

The standard deviation in half-cell potential values for each measurement point was also calculated and can be seen in Tables 12-16 together with an average standard deviation per location. The average standard deviation for locations 1-5 were found to be 114, 35, 44, 27 and 34 mV respectively. The maximum change, average maximum change and average standard deviation for all the locations were found to be different from each other, but all large in value. This indicates that a half-cell potential measurement could easily move between levels of low and uncertain risk of corrosion and high and uncertain risk of corrosion based on the value ranges provided in ASTM C876 (2009). Experiments by both Elsener (2003) and Keßler & Gehlen (2016) also found half-cell potential values to vary to a large degree when comparing test results taken during dry and wet periods with shifts of up to 100mV recorded.

For a silver/silver chloride electrode as was used for these tests, the ASTM C876 standard suggests that measurements above -106 mV indicate a low risk of corrosion, measurements between -106 and -256 mV indicate an uncertain risk of corrosion and measurements below -256 mV indicates a high risk of corrosion. Movement of measurements between the ranges of low and uncertain risk of corrosion and high and uncertain risk of corrosion can be seen to occur several times in the half cell potential results tables for locations 1-4 (Tables 10 & 32-35). All measurements at location 5, which was the control location remained in the range of uncertain risk of corrosion for the full period during which the tests were carried out. The average maximum change of 93 mV and average standard deviation of 34 mV at location 5 show that the change in half-cell potential measurements due to the impact of changing weather conditions can be large enough to cause values to move between recommended ranges of risk. The control location also shows that even when corrosion is not likely to be occurring, half-cell potential values still fluctuate due to changing weather conditions.

For locations 3-4 the measurements only move between the low and uncertain risk range and high and uncertain risk range. There are no measurements at these locations where the change has been between the high and low-risk range. The results at location 3 show a large average maximum change of 140 mV and a number of maximum change values over 150 mV (the difference in value between the range of high and low risk as prescribed in ASTM C876), which shows that it is possible for measurements to move between the high and uncertain risk range and that this may depend on factors such as the location, how intense the exposure conditions are and what the actual state of corrosion of the reinforcement at the measurement location is. Location 1's results show a couple of measurements that move between the

high and low-risk ranges, but the changes which occurred at this location were drastic and are likely caused by some form of interference as previously mentioned.

Table 19: Half-cell potential statistics for Location 1.

Location 1															
	Half-cell potential (mV)														
Min value at measurement point	-362	-333	-223	-130	-162	-149	-214	-121	-173	-207	-200	-60	-162	-147	-187
Max value at measurement point	41	-20	81	174	94	70	130	183	80	27	137	213	81	84	99
Max change at measurement point	403	313	304	304	256	219	344	304	253	234	337	273	243	231	286
Std Deviation at measurement point	173	126	123	118	108	89	134	114	107	95	130	98	96	91	112
Average max change at location	287														
Average std deviation at location	114														

Table 20: Half-cell potential statistics for Location 2.

Location 2										
	Half-cell potential (mV)									
Min value at measurement point	-290	-293	-193	-200	-212	-182	-187	-184	-152	-196
Max value at measurement point	-182	-150	-79	-97	-82	-99	-67	-115	-50	-103
Max change at measurement point	108	143	114	103	130	83	120	69	102	93
Std Deviation at measurement point	35	45	37	34	41	27	42	22	35	27
Average max change at location	107									
Average std deviation at location	35									

Table 21: Half-cell potential statistics for Location 3.

Location 3												
	Half-cell potential (mV)											
Min value at measurement point	-419	-480	-447	-422	-424	-433	-450	-304	-384	-314	-430	-350
Max value at measurement point	-300	-309	-347	-217	-337	-276	-313	-210	-280	-189	-251	-152
Max change at measurement point	119	171	100	205	87	157	137	94	104	125	179	198
Std Deviation at measurement point	36	54	35	65	29	50	45	28	34	40	50	61
Average max change at location	140											
Average std deviation at location	44											

Table 22: Half-cell potential statistics for Location 4.

Location 4																
	Half-cell potential (mV)															
Min value at measurement point	-220	-194	-172	-152	-144	-115	-103	-115	-96	-57	-27	-24	-15	-20	-11	-7
Max value at measurement point	-139	-132	-95	-68	-56	-50	-43	-35	-30	17	20	64	70	59	68	82
Max change at measurement point	81	62	77	84	88	65	60	80	66	74	47	88	85	79	79	89
Std Deviation at measurement point	26	22	28	31	32	25	24	25	25	26	18	33	29	26	27	29
Average max change at location	75															
Average std deviation at location	27															

Table 23: Half-cell potential statistics for Location 5.

Location 5														
	Half-cell potential (mV)													
Min value at measurement point	141	139	139	77	160	168	155	54	163	120	151	176	90	139
Max value at measurement point	227	230	223	178	257	237	241	144	251	243	267	242	187	240
Max change at measurement point	86	91	84	101	97	69	86	90	88	123	116	66	97	101
Std Deviation at measurement point	30	29	32	41	31	27	33	30	29	49	41	23	41	38
Average max change at location	93													
Average std deviation at location	34													

Contour plots

The contour plots of the half-cell potential values have been found to undergo changes in shape for the different days during which testing was carried out. Contour plots for location 3 are shown in figures 48-55 below, while plots for the remaining 4 locations can be seen in figures 89-120 in Section 3 of the Appendix. The discussion in this section relates to all five locations, but only the plots of location 3 are shown due to the number of pages that the plots take up. There are days of testing where the contour plots look very similar in shape and days where the shapes vary from one day of testing to the next. This change in shape may be attributed to the variability in weather conditions to which the measurement locations are exposed. Variability in exposure conditions includes variability in rainfall intensity, rainfall direction, wind conditions, temperature conditions and exposure to sunlight. The variability can be due to both natural variability only or natural variability combined with obstructions from surrounding objects. A second possible cause of the change in contour shape may be due to the amount of prewetting which is needed to record a stable measurement. The amount of prewetting needed was not the same on every day of testing. The prewetting method involved pouring water over the location with a bottle and so complete consistency in the amount of prewetting over each measurement point was also not possible.

It can also be seen from the scales of the contour plots that the absolute half-cell potential values undergo shifts across the different days of testing, with the contour maps for measurement days after significant periods of rain displaying a more negative range of values. Although both the value ranges of the contour plots and the shape of the contour lines undergo changes across the different days of testing, it is evident that for all 5 test locations the regions of the contour plots showing the more negative values remain more negative and the regions showing more positive values remain more positive across all the days of testing. Location 1 shows the most variation in the contour plots, but the behaviour of this location suggests that the initiation of corrosion had occurred during the test period.

The half-cell potential survey that was carried out by Gerardo Clemena (1992), showed similar findings with numerical values measured after a period of rain being more negative than those after a dry period, but the half-cell potential maps and locations of concern remained similar for the two test periods. The shape of the two potential maps in Clemena's works showed less variation than the potential maps in this works. This can also be attributed to factors such as varying exposure conditions and the presence of obstructions seeing as these works were carried out on buildings while Clemena's works were carried out on a bridge deck.

The results of these contour plots support the idea that mapping of potential gradients is a more accurate method than comparing measured values to prescribed value ranges when it comes to making interpretations on the corrosion state of a reinforced concrete structure based on half-cell potential measurements. This is because the absolute measurements of half-cell potentials are more subject to misinterpretation, as the change in absolute values are more significant than the change in potential maps across different weather conditions. It sometimes occurs in practice that a single half-cell potential measurement or a handful of half-cell potential measurements are taken to make interpretations about the state of a structure. This may prove to be highly inaccurate due to the high variability in measurements. Potential maps require a good number of measurements to be taken in order to make a valuable interpretation and as a result may force a larger number of measurements to be taken than might otherwise be the case, thus further supporting the use of these plots as a more effective analysis tool.

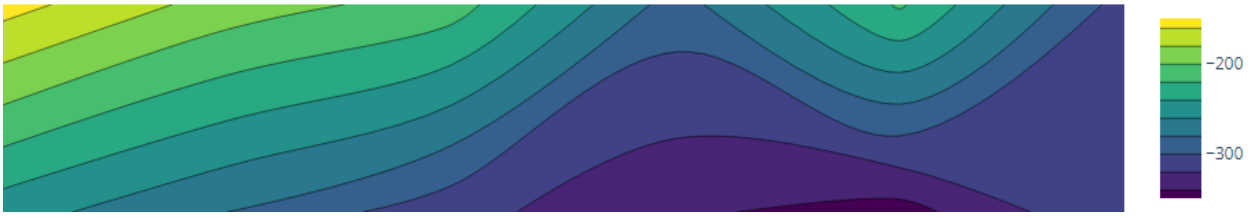

Figure 48: Location 3 contour plot on the 7th of August.

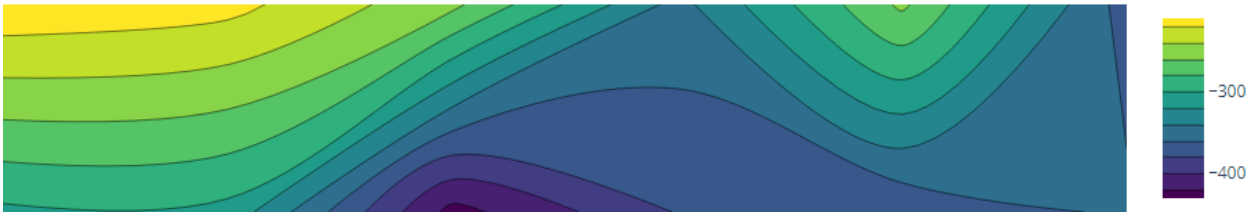

Figure 49: Location 3 contour plot on the 13th of August.

Figure 50: Location 3 contour plot on the 27th of August.

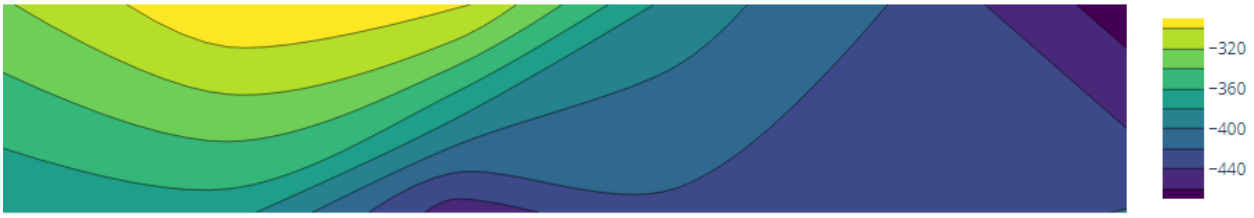

Figure 51: Location 3 contour plot on the 6th of September.

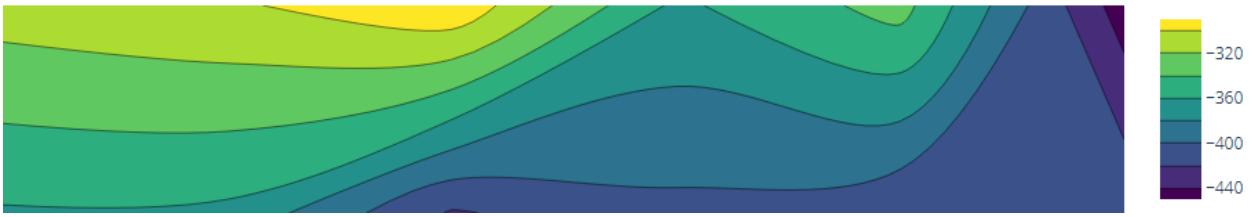

Figure 52: Location 3 contour plot on the 28th of September.

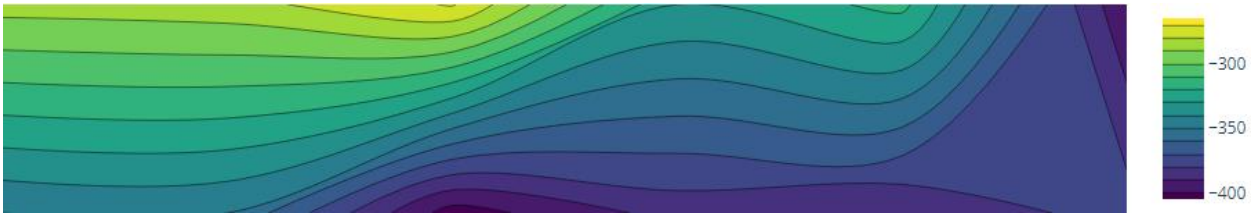

Figure 53: Location 3 contour plot on the 27th of October.

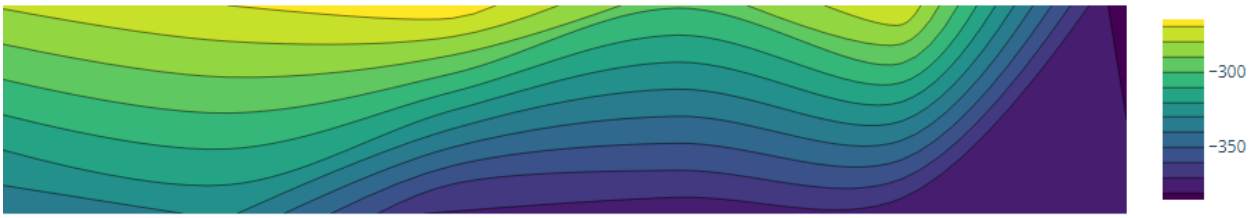

Figure 54: Location 3 contour plot on the 19th of November.

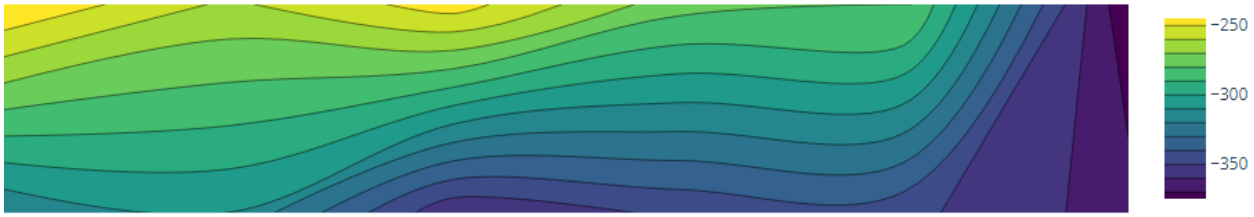

Figure 55: Location 3 contour plot on the 29th of November.

4.2.1.2. Resistivity

The resistivity values at each of the 5 test locations were found to be high. When compared to the suggested ranges for predicting the corrosion rate and the risk of corrosion as shown in Tables 3-5. These measurements indicate that the corrosion rate should be low and that the risk of corrosion occurring is low to negligible. Corrosion is however clearly visible at locations 1-4 and this indicates that the suggested ranges can be unreliable. A number of factors can impact on corrosion and the risk of corrosion which may lead to the occurrence of corrosion over time even though the resistivity may be found to be high.

The buildings on which the tests were carried out are old buildings. The Hoerikwaggo building is the oldest of the three buildings, while the Neville Alexander building & Rachel Bloch House are approximately 50, 30 and years old respectively. The old age of the buildings could indicate that the corrosion that has occurred could have happened slowly over this long period of time. Resistivity measurements provide information about the corrosion activity at the time of measurement but cannot provide information about corrosion activity that may have occurred over a period of time.

Location 1 which is the youngest of the three buildings on which the testing was performed (Rachel Bloch House) was found to have a lower average group of resistivity measurements than any of the locations from the two other buildings. This together with the results from the other locations shows that the age of a structure is an important consideration to take into account when corrosion assessments using resistivity measurements are carried out. The value ranges suggested in Tables 3-5 may be considered to be less useful in predictions on the state of older buildings. Other factors such as inconsistent cover depths and changing exposure conditions also play a role in the rate of corrosion and can be reasons for corrosion occurring even though the resistivity of the concrete is high.

There is an evident change in resistivity values due to changing weather conditions. This can be seen in Tables 24-28, which show the maximum change and standard deviations in resistivity values at each measurement point as well as the average maximum change and average standard deviation for each location. The average maximum change and average standard deviations at locations 2-5 were very high, ranging from 216-377 KOhm.cm and 79-116 KOhm.cm respectively. Experiments by Larsen, et al. (2006) also showed large changes in resistivity values depending on how much the moisture content changes by with a larger change in moisture content leading to a larger change in resistivity values. Osterminski, et al. (2012) states that the surface layers of concrete structures are directly exposed to weather conditions and so these layers on which the measurements are taken will undergo the largest changes.

The changes at location 1 were high, but low in comparison to the other locations. The change at location 1 shows that lower resistivity values may undergo a smaller change due to fluctuating weather conditions. The changes that occurred, although smaller than that of the other locations are still a large fraction of the values measured at the location. Although the measurements do not compare well with the ranges of values suggested for the assessment of corrosion in Tables 4-6, they do indicate that exposure conditions can have an impact on the interpretation that is drawn from these tables. This is due to the large change which is seen to occur under the influence of fluctuating exposure conditions.

Table 24: Resistivity for Location 1.

Location 1									
	Resistivity (kohm.cm)								
Min value at measurement point	57	49	60	61	108	170	63	118	216
Max value at measurement point	127	114	160	124	173	241	117	205	333
Max change at measurement point	70	65	100	63	65	71	54	87	117
Std Deviation at measurement point	22	18	34	17	22	25	18	25	44
Average max change at location	77								
Average std deviation at location	25								

Table 25: Resistivity statistics for Location 2.

Location 2												
	Resistivity (kohm.cm)											
Min value at measurement point	314	200	254	410	122	126	232	104	123	378	214	233
Max value at measurement point	469	436	642	605	345	332	571	358	247	536	361	394
Max change at measurement point	155	236	388	195	223	206	339	254	124	158	147	161
Std Deviation at measurement point	58	96	172	84	88	79	134	85	40	59	63	63
Average max change at location	216											
Average std deviation at location	85											

Table 26: Resistivity statistics for Location 3.

Location 3						
	Resistivity (kohm.cm)					
Min value at measurement point	980	1156	1292	856	597	636
Max value at measurement point	1302	1415	1533	1102	850	806
Max change at measurement point	322	259	241	246	253	170
Std Deviation at measurement point	105	86	72	79	81	54
Average max change at location	249					
Average std deviation at location	79					

Table 27: Resistivity statistics for Location 4.

Location 4									
	Resistivity (kohm.cm)								
Min value at measurement point	267	387	343	594	703	1035	1306	1039	1359
Max value at measurement point	408	546	509	794	1248	1244	1550	1264	1581
Max change at measurement point	141	159	166	200	545	209	244	225	222
Std Deviation at measurement point	51	56	62	64	149	75	84	78	74
Average max change at location	235								
Average std deviation at location	77								

Table 28: Resistivity statistics for Location 5.

Location 5									
	Resistivity (kohm.cm)								
Min value at measurement point	1050	1115	892	976	546	528	538	495	1087
Max value at measurement point	1374	1409	1274	1249	857	949	968	1103	1439
Max change at measurement point	324	294	382	273	311	421	430	608	352
Std Deviation at measurement point	95	88	111	85	104	124	125	194	116
Average max change at location	377								
Average std deviation at location	116								

4.2.2. Variation in cover depth

The cover depth results shown in Tables 29-34 include the median, range, mean, standard deviation and minimum cover depth values calculated according to German and RILEM suggested methods. Only the results of the 5th percentile calculations for both the German and RILEM methods are shown in these tables, but the results for the 10th percentile can be seen in Tables 35-90 of section 4 of the Appendix. The RILEM results shown are for calculations using a 50% confidence interval as these are more comparable to the results of the German method, whereas the results for larger confidence intervals are more conservative. Results for calculations using a 75, 90 and 95% confidence interval can also be seen in section 4 of the Appendix. All the results are not shown in these tables as the aim of the analysis is to assess variations according to location and sample size and not calculation parameters per se. These tables present the results for the primary reinforcement cover depth measurements. Tables showing cover depth statistics for the secondary reinforcement cover depth can also be found in Section 4 of the Appendix.

The results of Table 29 show cover depth statistics for cover depth measurements taken at random from seven 1.5 m^2 locations along the Neville Alexander building. These locations include 1 location on the ground floor from each face of the building, 2 locations on the east and west side of the 1st floor of the building and one location from the North side on the 3rd floor of the building. In total 245 cover depth measurements were taken from these 7 locations. Random samples of 200, 100, 50, 20, 10 and 5 measurements were obtained from the total amount of 245 measurements. The statistics which are shown in the table were calculated for the total 245 measurements and each of the groups of random samples in order to assess variability in cover depth measurements for different sample sizes.

In general, the results show that the measurements tend to deviate more from the results of the total number of measurements as the sample size begins to get smaller. This is however not a given due to the randomness associated with the samples which can be seen with the results of the 100 and the 20 randomly selected samples being similar. The randomness of the sample allows for the sample to be similar to the population or misrepresentative of the sample. A more comprehensive statistical analysis would help to deal with the issue that arises due to the randomness of the sample. The more comprehensive analysis would entail taking at least a hundred randomly selected runs of 5, 10, 20, 50,

100 and 200 measurements from a larger population and then using the average of each of the hundred randomly selected groups to carry out a comparison as was done in Table 29.

To carry out the more comprehensive analysis would however require a substantial amount of statistical analysis which would fall out of the scope of this research due to time constraints and the number of different aspects that this work aims to cover. It is proposed that such an analysis be carried out as a separate future work of research. A less comprehensive analysis which follows this principle was carried out by comparing seven random runs of 10 and 100 measurements from the population of 245 measurements. These results are shown in Tables 30 and 31 and make it clearer to see that greater sample sizes show less variability from the population. The analysis that was carried out has its limitations as the effects of the randomness may still not be completely minimised as it is not a very comprehensive analysis and it does not look at multiple measurement runs for a wider range of measurements such as 5, 20, 50 or 200 measurements. It does however paint the picture of how greater sample sizes show less variability from the overall population than is the case for smaller sample sizes and was deemed acceptable for the scope of this work.

Table 29: Cover depth statistics for random samples taken from seven 1.5 m^2 locations.

All 1.5m^2 locations							
Data	Vertical Cover Depth Measurements (mm)						
	All	200 Randomly Selected	100 Randomly Selected	50 Randomly Seleccted	20 Randomly Selected	10 Randomly Selected	5 Randomly Selected
Number of measuremnts	245	200	100	50	20	10	5
Median	48	48	46	45	45	47	55
Range	25-81	25-76	25-76	31-76	32-72	32-81	36-72
Mean	49	49	47	45	47	51	55
Standard deviation	10.8	10.9	10.6	9.9	9.7	13.7	12.2
German DBV-Merkblatt minimum (5th percentile)	34	33	32	31	32	31	38
Rilem minimum (5th percentile)	31	31	30	29	30	29	35

Table 30 shows cover depth statistics for 7 different runs of 10 randomly selected cover depth measurements from a group of 245 measurements. The 245 measurements are from the 7 previously mentioned 1.5 m^2 locations along the Neville Alexander building. The mean and median values obtained for the 7 runs range from 41-55 mm and 43-54 mm respectively. The difference is greater than 10 mm in both cases and shows that the variability can be large when a smaller amount of cover depth measurements are taken. This is evident when looking at the minimum cover depths obtained from both the German and RILEM methods. Run 2 shows a minimum cover depth of 26 mm and 23 mm according to the German and RILEM methods respectively and this is the lowest from the 7 runs. Run 4, on the other hand, has the highest minimum cover depth from the 7 runs with values of 40 and 38 mm according to the German and RILEM methods. The results show that when a small group of measurements are taken at random from a large group of measurements there can be a significant difference in the results obtained depending on where the measurements are taken from. This may be the case when a building is being assessed and a quick or less in-depth cover depth assessment is carried out.

Table 31 shows the results of an analysis carried out in the same way for the same locations, except in this case the random samples consisted of 100 measurements and not 10. It is clear that with this larger

sample size, the variations in the calculated statistics work out to be less. In the table, it can be seen that the median ranges from 46-49 and the mean from 47-51. The range of the minimum cover depths for the 7 runs according to the German and RILEM methods are 32-34 and 30-32 respectively. When looking at the range of values covered by the 7 runs for the 100 random measurements in comparison to the ranges which were covered by the 10 random measurement runs it can be seen that a larger sample size is more likely to detect a wider range of values. This shows that larger samples are more likely to better represent the true information about the cover depth of a structure.

Table 30: Cover depth statistics for seven runs of 10 randomly selected cover depth measurements taken from seven 1.5 m^2 locations.

All 1.5m^2 locations							
Data	10 Random Vertical Cover Depth Measurements (mm)						
	Run 1	Run 2	Run 3	Run 4	Run 5	Run 6	Run 7
Number of measuremnts	10	10	10	10	10	10	10
Median	41	47	46	55	44	43	47
Range	25-61	32-81	34-71	40-70	35-72	25-60	34-55
Mean	43	51	49	54	47	42	45
Standard deviation	11.9	13.7	11.4	10	10.8	10.1	6.7
German DBV-Merkblatt minimum (5th percentile)	26	31	32	40	30	29	36
Rilem minimum (5th percentile)	23	29	30	38	29	26	34

Table 31: Cover depth statistics for seven runs of 100 randomly selected cover depth measurements taken from seven 1.5 m^2 locations.

All 1.5m^2 locations							
Data	100 Random Vertical Cover Depth Measurements (mm)						
	Run 1	Run 2	Run 3	Run 4	Run 5	Run 6	Run 7
Number of measuremnts	100	100	100	100	100	100	100
Median	46	46	48	48	47	48	49
Range	25-76	30-81	25-76	30-81	25-75	25-81	31-81
Mean	47	48	49	51	49	48	51
Standard deviation	10.6	10.6	10.2	12	10.3	10.2	11.8
German DBV-Merkblatt minimum (5th percentile)	32	33	34	33	34	34	34
Rilem minimum (5th percentile)	30	31	32	31	32	31	32

Table 32 compares 54 measurements taken from a 3 m^2area on the south side of the ground floor of the building to 28 measurements taken from 1.5 m^2 areas to the top left and right sides of the larger area. The mean and minimum cover depth values from both the German and RILEM methods were found to be a few millimeters less than that of the full area for the smaller area on the top right side, but a few millimeters greater than the full area for measurements on the top left side of the full area. This shows how variation can occur within a small space and shows that the location from which measurements are taken can influence the conclusions that are made. These results also support the idea that in order to make the best decisions with regards to cover depth and draw conclusions that are more representative, the values which are recorded should be more spread out and taken from a larger area. Areas of concern can then be determined and focussed on to a greater degree.

A similar comparison can be seen in Table 33. In this case, a larger area with a total of 196 measurements on the ground floor of the West side of the building was analysed. The results were also found to be similar

with the mean, median and minimum cover depth values being lower than that of the full area for the 1.5 m^2 area to the left side and greater than that of the full area for the 1.5 m^2 to the right side. For this location, the variation from the results of the full area was however greater, which further supports the conclusions that were mentioned for the results in Table 32.

Table 32: Cover depth statistics for measurements taken from a full 3 m^2 location and 1.5 m^2 areas from the top right- and left-hand sides of the 3 m^2 location.

Ground Floor Location on the South Side of the Building			
Data	Vertical Cover Depth Measurements (mm)		
	All	1.5m^2 Area on Right Side	1.5m^2 Area on Left Side
Number of measuremnts	54	28	28
Median	49	45	49
Range	32-57	32-57	43-57
Mean	47	44	49
Standard deviation	5.2	5.8	3
German DBV-Merkblatt minimum (5th percentile)	40	36	44
Rilem minimum (5th percentile)	38	34	44

Table 33: Cover depth statistics for measurements taken from a full 7.5 m^2 location and 1.5 m^2 areas from the top right- and left-hand sides of the 7.5 m^2 location.

Large location on the west side of the building			
Data	Vertical Cover Depth Measurements (mm)		
	All	1.5m^2 Area on Right Side	1.5m^2 Area on Left Side
Number of measuremnts	190	49	49
Median	50	41	54
Range	27-81	31-53	35-58
Mean	50	42	53
Standard deviation	8.7	5.5	3.6
German DBV-Merkblatt minimum (5th percentile)	38	33	48
Rilem minimum (5th percentile)	35	33	47

The same seven 1.5 m^2 areas that were used to get the statistics in Tables 29-31 were used in Table 34. In this table, the statistics were calculated for each of the seven locations individually. The variation in mean and median values between the seven locations is large with the mean and median values ranging from 40-60 mm and 39-61 mm respectively. The minimum cover depth values calculated using the German and RILEM methods were also subject to large variability. For the German method, the location on the ground floor of the East face of the building had a minimum cover depth of 31 mm, whereas the location on the 1st floor of the West face of the building had a minimum cover depth of 45 mm and all other locations had values between these two extremes. With such large variation in the statistics the wrong conclusion could easily be drawn should a cover depth survey be focussed on a particular area.

There is no clear relationship between the face of the building and the results that were determined. For example, the results on the ground floor of the East face of the Building were lower than that on the ground floor of the South side of the building, while the results on the 1st floor of the East side were higher than the results on the ground floor of the South side. There is also no clear relationship between the

cover depth and the floor from which the depths were measured. The first floor of the East and West sides showed greater depths than the ground floor on the East and West sides, while the 3rd floor on the North side showed lower depths than the ground floor on the North side. In order to determine whether a relationship exists between the floor of the building or the face of the building and the cover depths measured, a more detailed investigation will need to be carried out. What is however clear from the results is that cover depth values can easily vary with location along a building showing that measurements taken in one location along a building are not necessarily representative of the whole structure. The perceived durability of a structure based on mean measurements for example, would be very different for a mean cover depth of 35 mm when compared to a mean of 62 mm.

Table 34: Cover depth statistics for measurements taken from seven 1.5 m^2 locations.

All 1.5m^2 locations							
Data	Horizontal Cover Depth Measurements (mm)						
	North Ground	North 3rd Floor	South Ground	East Ground	East 1st Floor	West Ground	West 1st Floor
Number of measuremnts	28	30	28	42	40	30	49
Median	52	51	44	35	42	37	61
Range	37-59	35-61	30-50	23-43	30-56	29-49	44-81
Mean	51	50	43	35	43	38	62
Standard deviation	5.4	6.7	6	5.1	5.6	4.8	9.1
German DBV-Merkblatt minimum (5th percentile)	39	40	35	28	34	30	48
Rilem minimum (5th percentile)	36	39	33	27	34	30	47

4.2.2.1. Recommendations for analysing cover depth results

Variation in cover depth measurement with sample size or location can easily occur. This variation may be very dangerous or costly should it occur close to a depth based on which decisions are to be made as it could lead to the wrong choice being made. The range of cover depth values in all cases shows that there are low and excessively high cover depth values. This is likely to be due to the construction process. If a large enough survey is not conducted, then misinterpretations can easily be made due to for example low values being missed or too many high values being measured. For this reason, the mean and median values alone may not be deemed suitable for drawing conclusions. The RILEM and German methods for calculating the minimum cover depth gives more conservative values than the mean and median values and so these values may prove to be a safer option on which to base an analysis. This being said, the method of conducting the survey may be more important than the statistical analysis as it is the values from the survey which feeds into this analysis.

4.2.2.2. Recommendations for conducting a cover depth survey

The results of these tests have shown that in order to take cover depth measurements that are more representative of the structure a larger amount of measurements should be taken which are spread around the structure. Based on the measurements of concern which are identified in this initial widespread analysis a more in-depth and focused analysis can be carried out in zones which are identified as high risk for the presence of corrosion. It is also recommended to carry out a more in-depth analysis in

structurally critical locations as these are the locations which would pose the greatest risk of harm should they be subject to corrosion.

4.2.2.3. Incorporating the cover depth analysis into the corrosion assessment

Should the cover depth be found to be low in areas which pose a threat to the state of the structure then an analysis using multiple methods is recommended. From the section to follow, it was found that a good relationship between cover depth and half-cell potential measurements exists and so carrying out half-cell potential tests in the areas of concern will complement the condition assessment analysis for determining whether corrosion is present or not. Other tests which will complement the analysis include carbonation and chloride depth tests. These tests are used to determine how far into the concrete corrosion inducing substances have progressed and should the depth be determined to be close to or greater than the cover depth then these areas are very likely to be subject to corrosion. In a case like this, the cover depth analysis should no longer be based on the mean, median or minimum cover depth as the carbonation and chloride penetration depths will be of greater importance.

4.2.3. Carbonation assessment

All the core samples that were taken from the Neville Alexander building showed low carbonation depths which varied between 2 and 4 mm. The cores were taken from the ground floor of each face of the building as well as Location 5 which is on the third floor of the building. These results suggest little variation in carbonation depth with location or sample size. All the cores which were taken from the Hoerikwaggo building showed different carbonation depth results with cores from locations 2, 3 and 4 showing measurements of 7, 26 and 8 mm respectively. A further core from the ground floor of the west side of the building showed a carbonation depth of 17 mm. These results contradict the results from the Neville Alexander building and suggest that carbonation depth can vary significantly with location. The reasons for the differing variance between the two buildings may be down to the construction and materials used. From the results of the carbonation tests, it can be seen that the risk of variation with location and sample size exists and so it is recommended that cores are taken from different locations along a structure with more cores being taken in areas of concern.

The cores from Locations 1, 2 and 4 showed low carbonation depths even though visual areas of exposed corroding reinforcement were present. The core from location 3 showed a carbonation depth of 26 mm which was greater than the cover depth near the location from which the core was taken. This core thus indicated that corrosion was present and supported the clear visual signs of corrosion in the form of spalling and exposed corroding reinforcement at this location. These results point to the need for accompanying test methods to be carried out together with the carbonation depth tests in order to draw more accurate conclusions and prevent any misinterpretations on the state of the structure from being made.

4.2.4. Comparison of the different test methods

4.2.4.1. Half-cell potential vs cover depth

From the graphs shown in Figures 56-65 it can be seen that for the majority of the more negative half-cell potential measurements, the cover depth measurements fall within the lower range of cover depth measurements for that location. The trend lines shown in the graphs indicate that there is an overall trend of HCP values becoming more negative with decreasing cover depths. The trend lines that are presented in these graphs have been inserted as an indication for the trend although no particular type of trend line can really be justified based on both the results of these experiments or information that is available in existing literature. A linear trend line has been opted for here just to make the point that from these experiments it has been found that overall HCP measurements decrease as cover depth decreases. The lack of a stronger relationship between the two variables can be due to factors such as variance in the resistivity of the concrete and the exposure conditions of the different measurement points.

The overall trend that can be seen in most of the graphs shows that the relationship between half-cell potential and cover depth measurements can be very useful in predicting whether reinforcement corrosion is present. This relationship shows that lower cover depths reduce the amount of time that is needed for corrosion inducing substances to reach the depth of the reinforcement and cause the onset of reinforcement corrosion. It also shows that corrosion propagation is sped up in locations with lower cover depths due to more wetting/drying cycles and the higher availability of moisture and oxygen. It must however be considered that even if the reinforcement is located at a different cover depth and has the same level of corrosion activity occurring, the HCP results are likely to show a difference in value. This difference occurs because the HCP test which is carried out on the surface of the concrete measures the potentially differentiated fields that are formed as a result of the corrosion activity, and the iso potential lines of these fields become less negative with distance away from the reinforcement. These results may thus not only be due to rebar located at a lower cover corroding more, but may be more due to equipotential lines reaching the surface better when the surface is close (at lower cover depths) as is mentioned in works by Maierhofer, et al. (2017), and Yodsujai & Pattarkittam (2017).

Location 5 which is the control location does not follow the overall trend. This is because the half-cell potential measurements remain fairly constant due to a lack of reinforcement corrosion, while the cover depth varies due to the construction. This indicates that a variance in half-cell potential measurements gives a good indication of the presence of corrosion and that the correlation between half-cell potential and cover depth measurements will be fairly strong when reinforcement corrosion is occurring.

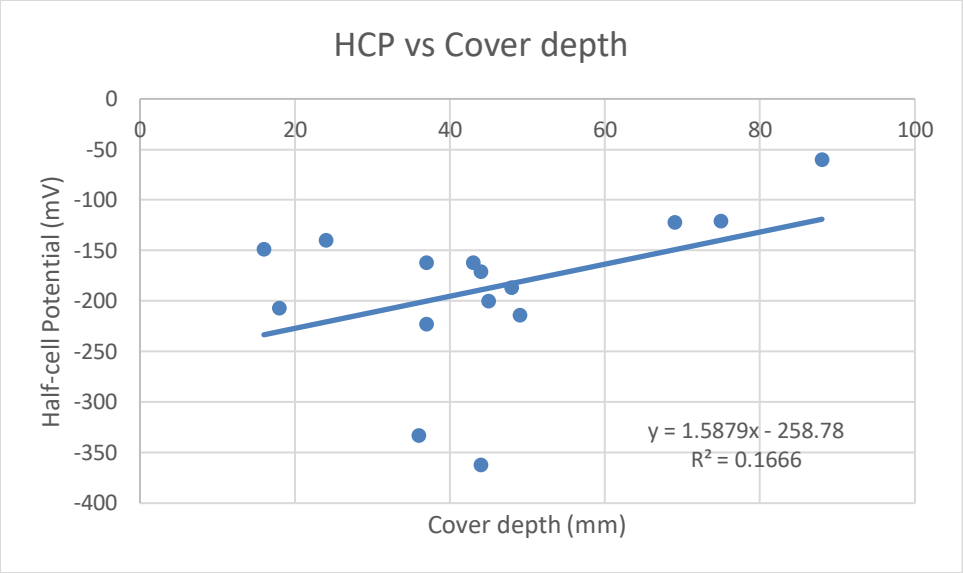

Figure 56: Graph of the minimum measured Half-cell potential (mV) vs Cover depth (mm) for location 1

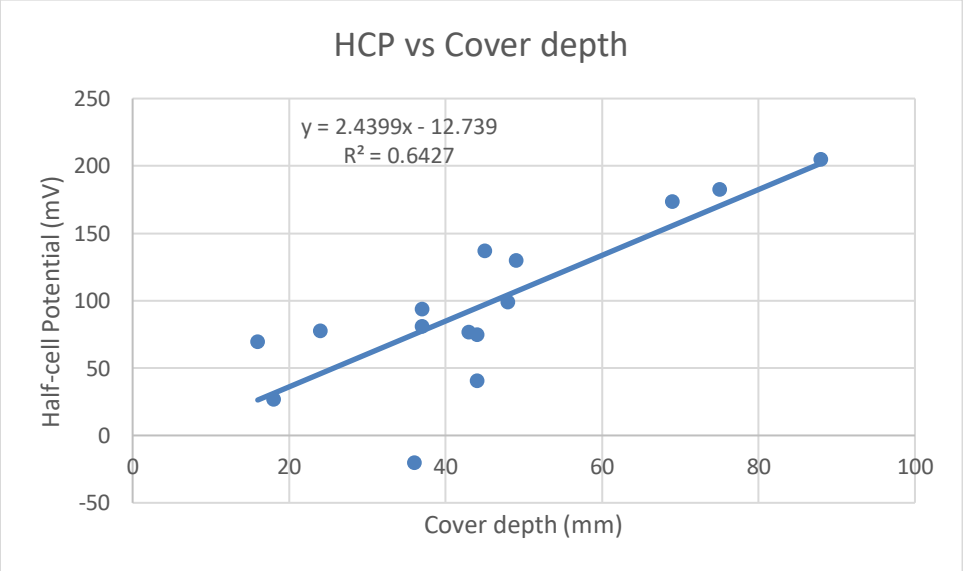

Figure 57: Graph of the maximum measured Half-cell potential (mV) vs Cover depth (mm) for location 1

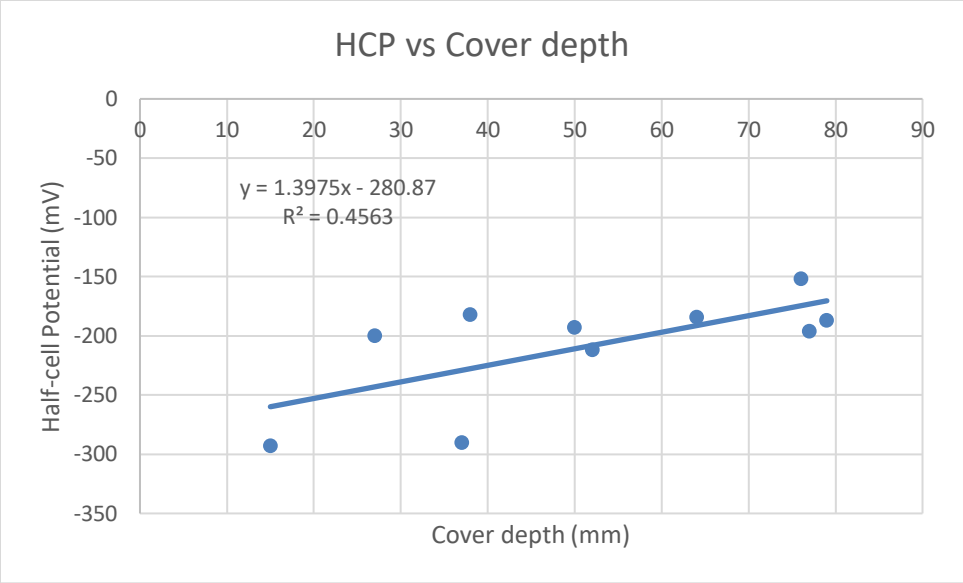

Figure 58: Graph of the minimum measured Half-cell potential (mV) vs Cover depth (mm) for location 2

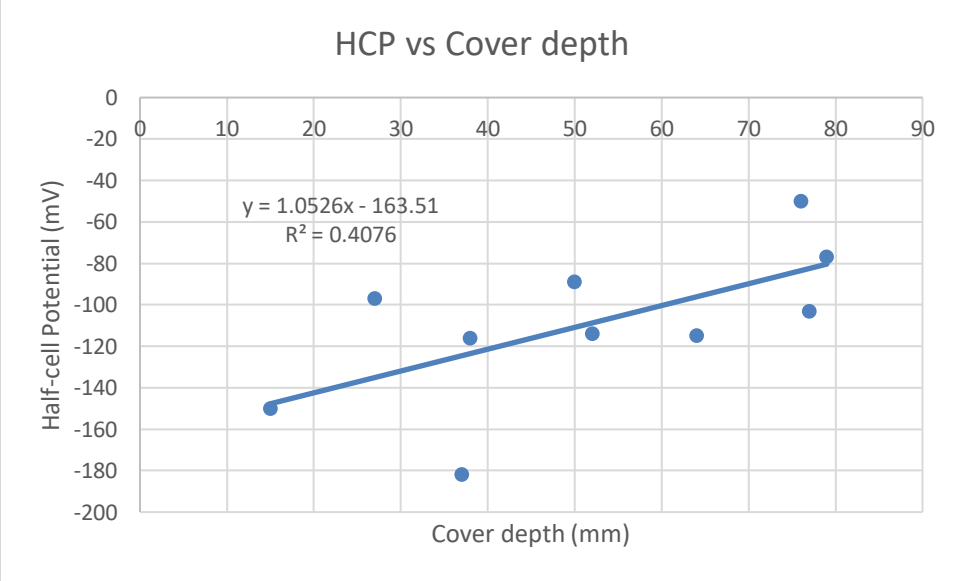

Figure 59: Graph of the maximum measured Half-cell potential (mV) vs Cover depth (mm) for location 2

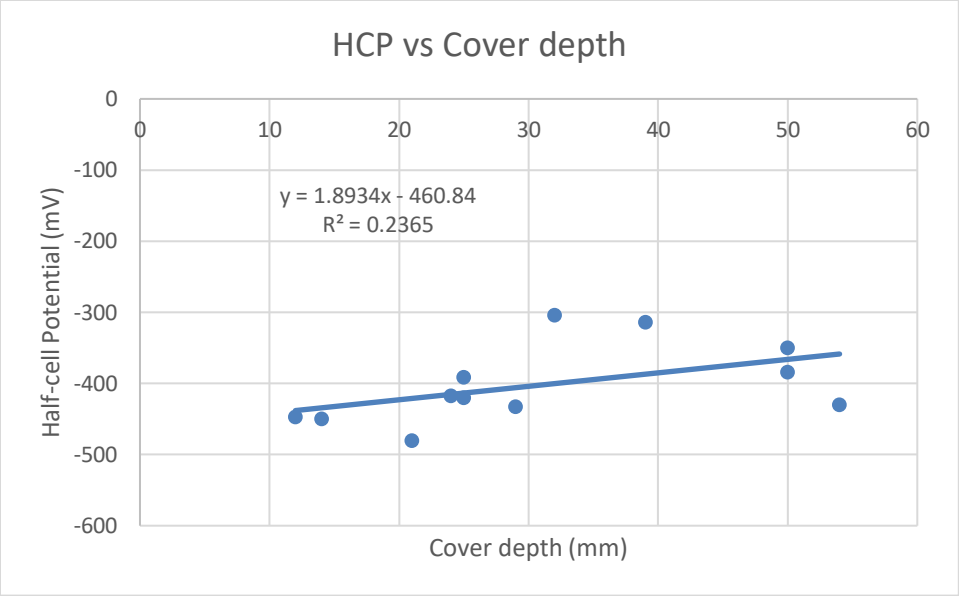

Figure 60: Graph of the minimum measured Half-cell potential (mV) vs Cover depth (mm) for location 3

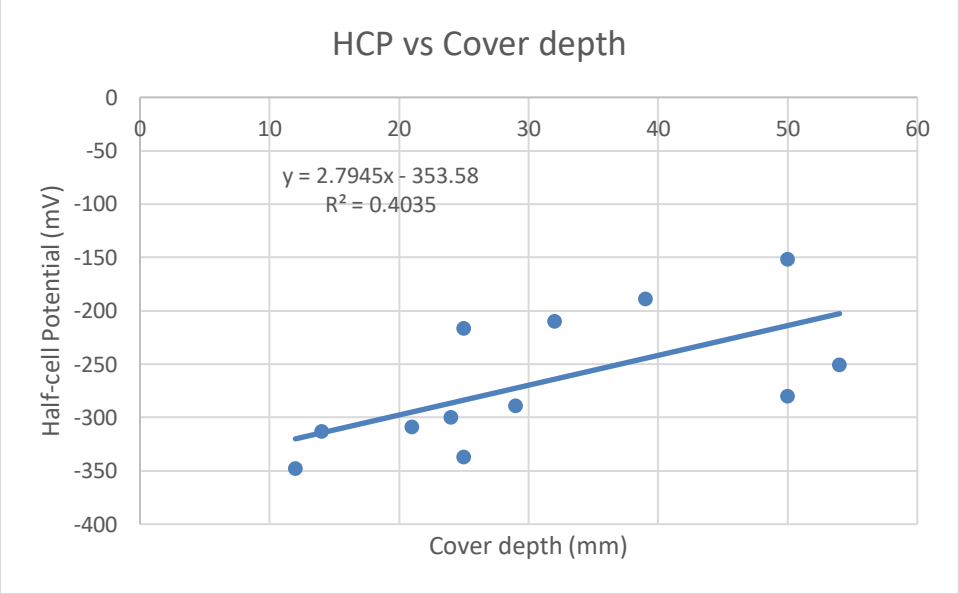

Figure 61: Graph of the maximum measured Half-cell potential (mV) vs Cover depth (mm) for location 3

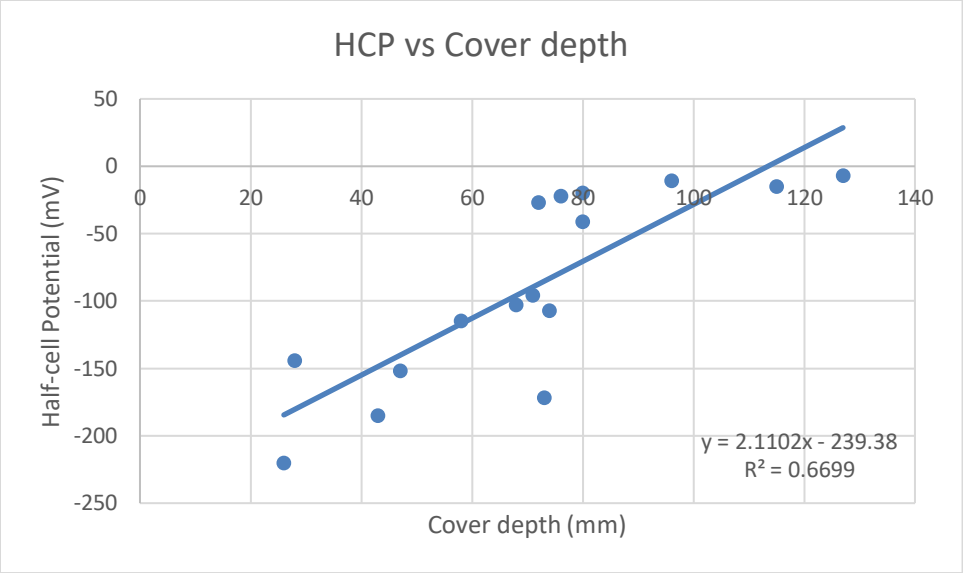

Figure 62: Graph of the minimum measured Half-cell potential (mV) vs Cover depth (mm) for location 4

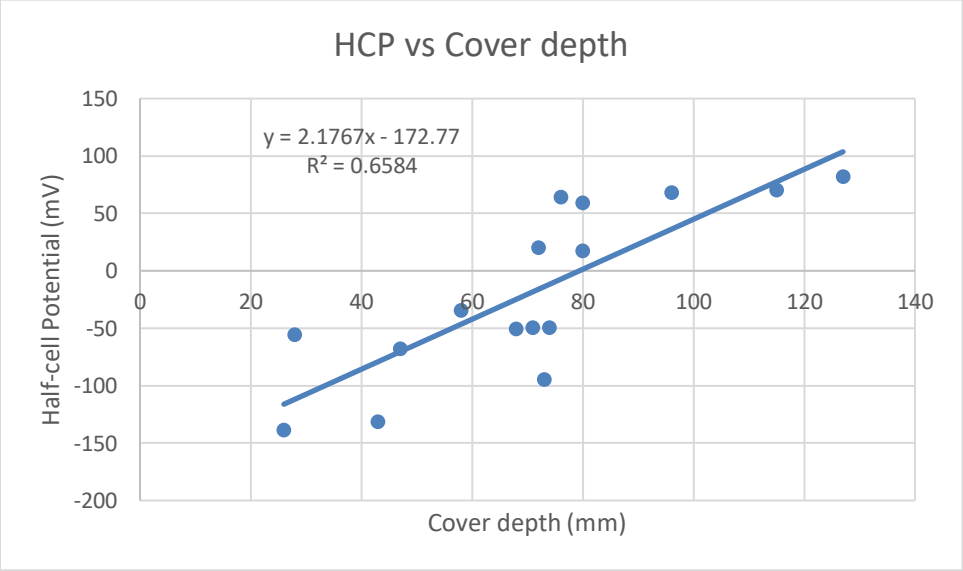

Figure 63: Graph of the maximum measured Half-cell potential (mV) vs Cover depth (mm) for location 4

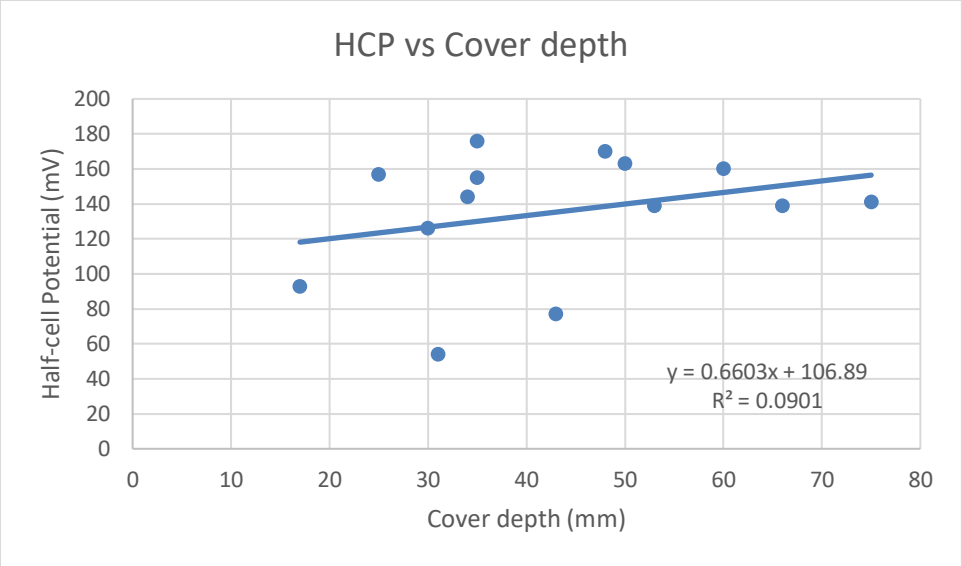

Figure 64: Graph of the minimum measured Half-cell potential (mV) vs Cover depth (mm) for location 5

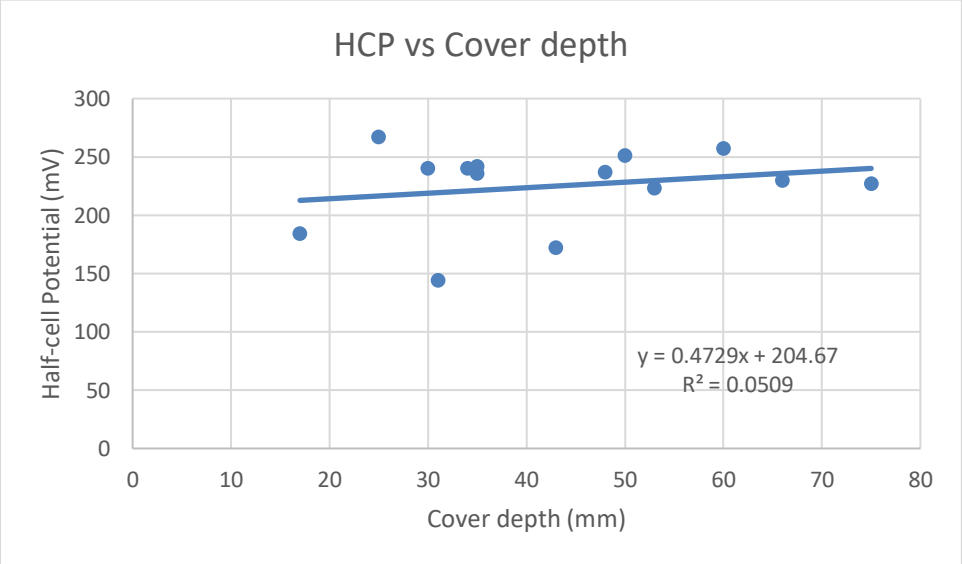

Figure 65: Graph of the maximum measured Half-cell potential (mV) vs Cover depth (mm) for location 5

4.2.4.2. Half-cell Potential vs Resistivity

The different locations show different relationships between half-cell potential and resistivity measurements, as can be seen in the graphs shown in Figures 66-75. As was the case for the comparison between HCP and cover depth measurements, the trend lines that are presented in these graphs have been inserted simply as an indication for the trend. A linear trend line has been opted for here to try and illustrate that HCP measurements decrease as resistivity decreases. HCP measurements are expected to decrease as resistivity measurements decrease according to existing theory. This is because these tests are somewhat affected by the same factors.

HCP measurements are merely related to a certain probability that the reinforcement may or may not be corroding, while resistivity is an actual material property of the concrete. The expected relationship between the two tests is thus only valid in cases where reinforcement corrosion is actually occurring. This is evident from the results of Location 5 where the resistivity varies to a significant degree, but the half-cell potential measurements remain fairly constant. This location did not show clear visual signs of corrosion and the reinforcement that was exposed to make the connection for the half-cell potential test also showed no corrosion. These results also suggest that contour maps of resistivity may not offer value in corrosion prediction as these measurements vary when corrosion is present or not.

At locations 1-4 there were clear visual signs that corrosion was occurring in the form of delaminations and exposed corroded reinforcement. Locations 3 and 4 show a strong positive trend between half-cell potential and resistivity measurements, thus supporting the expected relationship. Locations 1 and 2 on the other hand show almost no trend between these measurements. The trend between the measurements of the maximum half-cell potential and maximum resistivity at location 2 even shows a trend that contradicts the expected relationship. The weak relationship between the HCP and resistivity results is likely to be due to the resistivity values being generally high. At such high resistivity values little correlation is expected with HCP results.

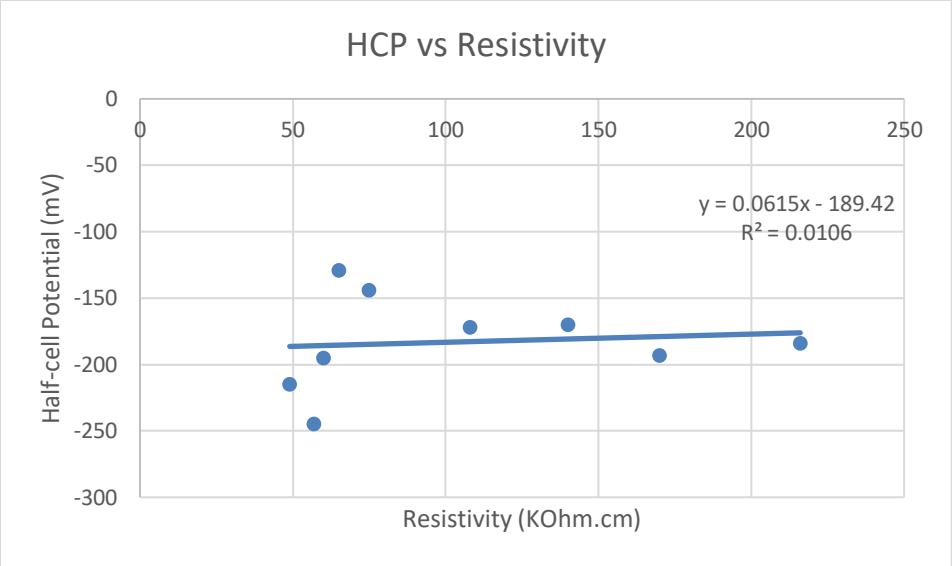

Figure 66: Graph of the minimum measured Half-cell potential (mV) vs minimum measured Resistivity (KOhm.cm) for location 1

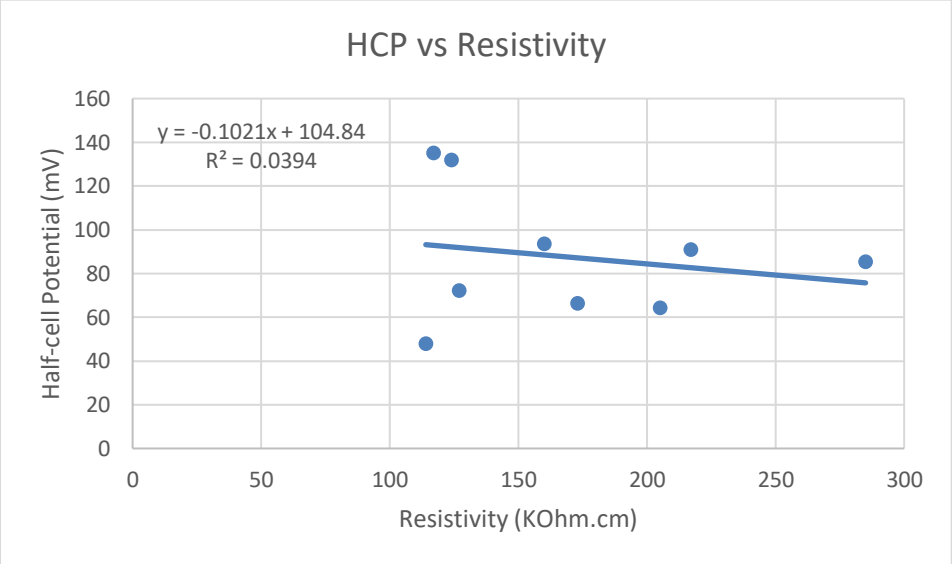

Figure 67: Graph of the maximum measured Half-cell potential (mV) vs maximum measured Resistivity (KOhm.cm) for location 1

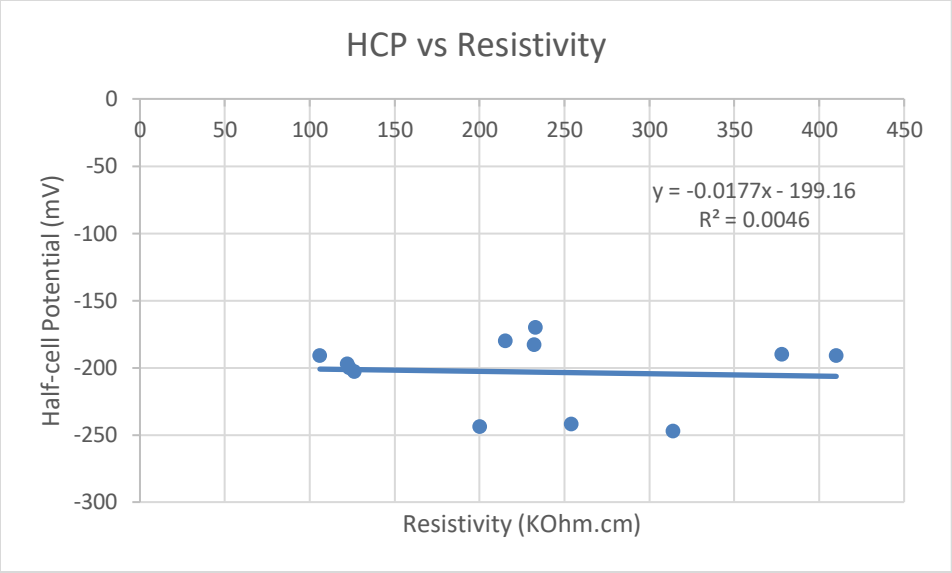

Figure 68: Graph of the minimum measured Half-cell potential (mV) vs minimum measured Resistivity (KOhm.cm) for location 2

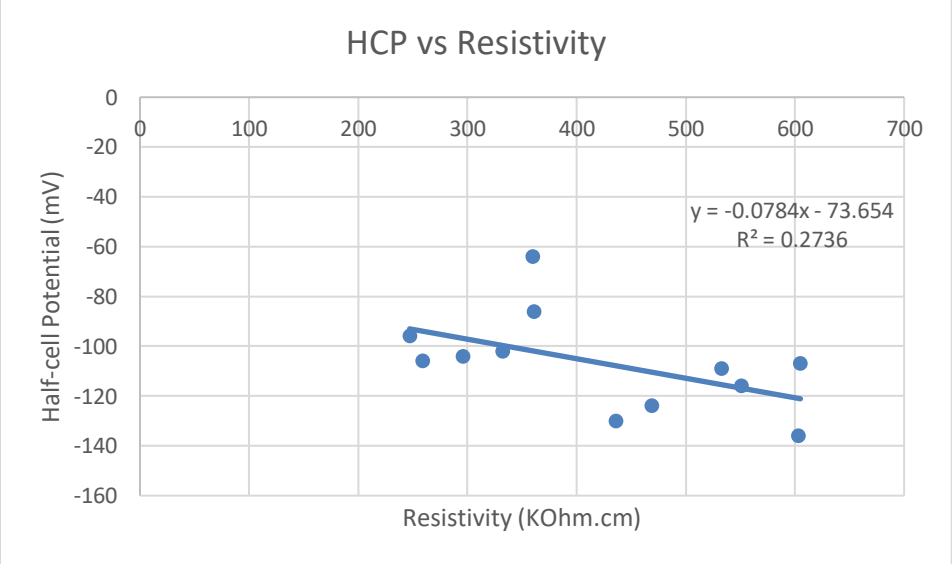

Figure 69: Graph of the maximum measured Half-cell potential (mV) vs maximum measured Resistivity (KOhm.cm) for location 2

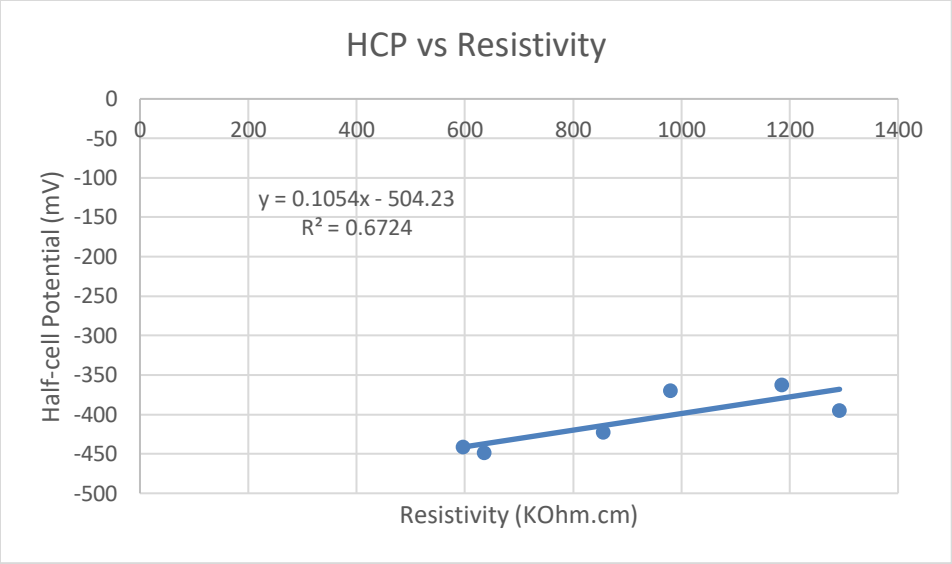

Figure 70: Graph of the minimum measured Half-cell potential (mV) vs minimum measured Resistivity (KOhm.cm) for location 3

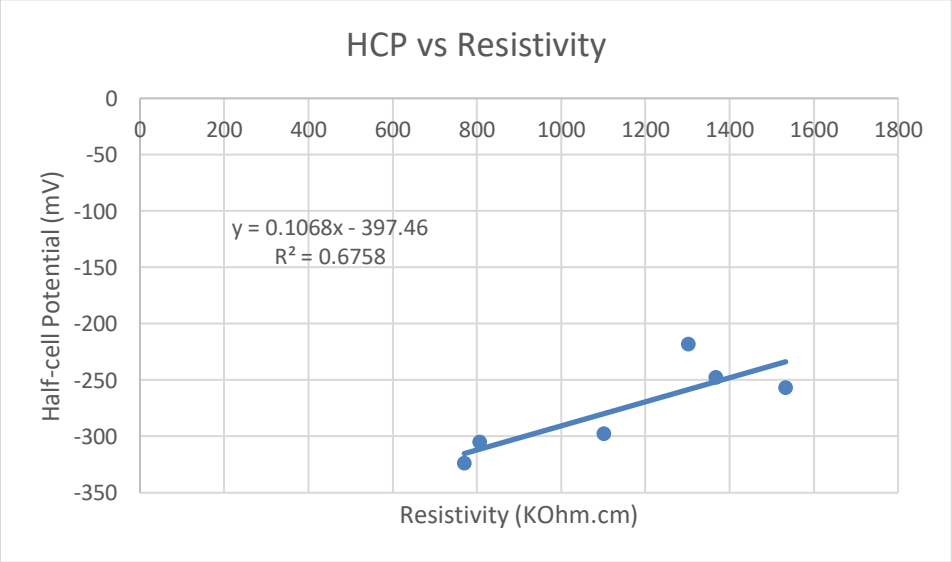

Figure 71: Graph of the maximum measured Half-cell potential (mV) vs maximum measured Resistivity (KOhm.cm) for location 3

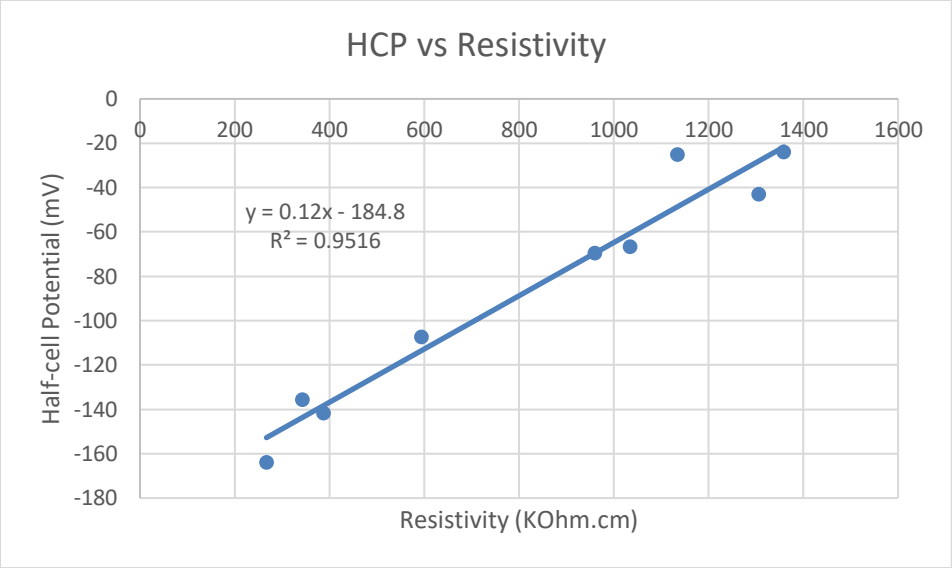

Figure 72: Graph of the minimum measured Half-cell potential (mV) vs minimum measured Resistivity (KOhm.cm) for location 4

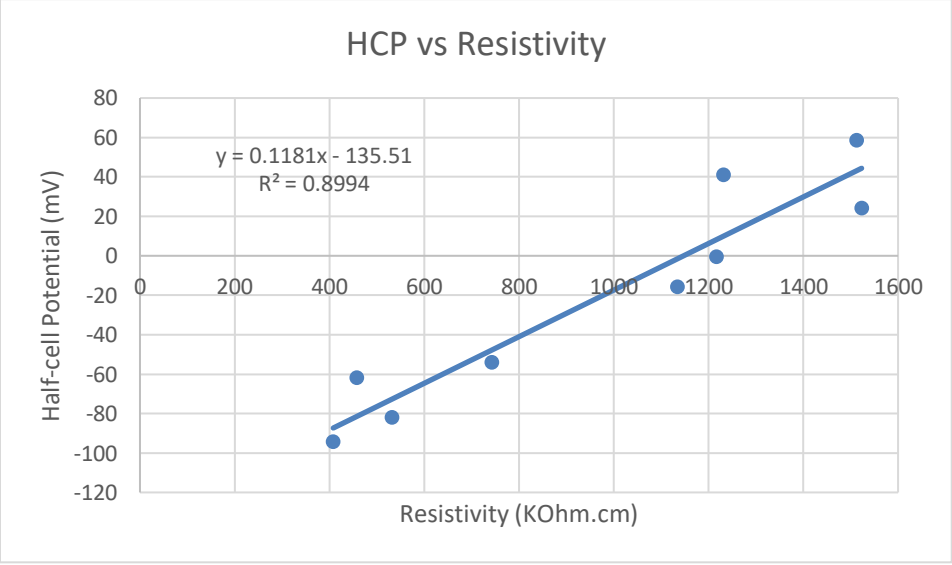

Figure 73: Graph of the maximum measured Half-cell potential (mV) vs maximum measured Resistivity (KOhm.cm) for location 4

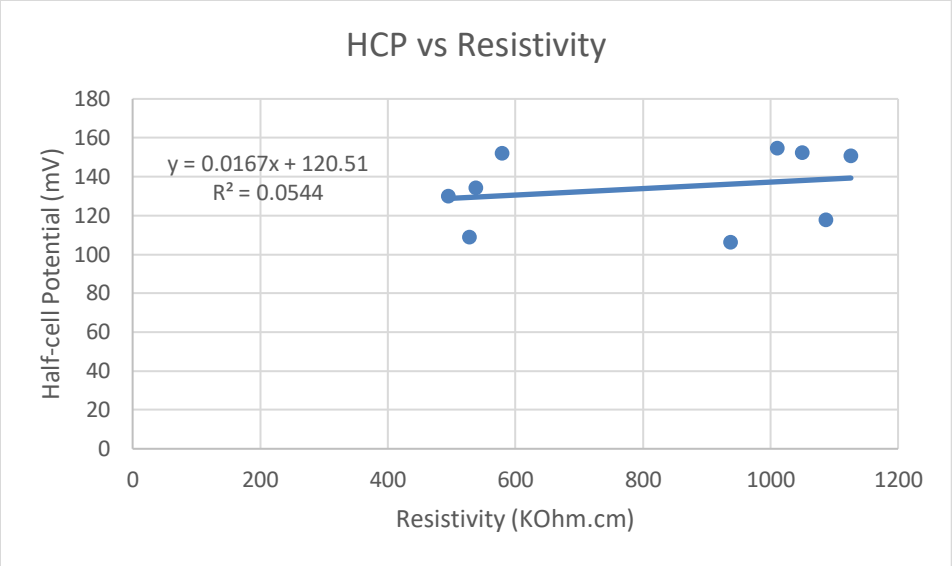

Figure 74: Graph of the minimum measured Half-cell potential (mV) vs minimum measured Resistivity (KOhm.cm) for location 5

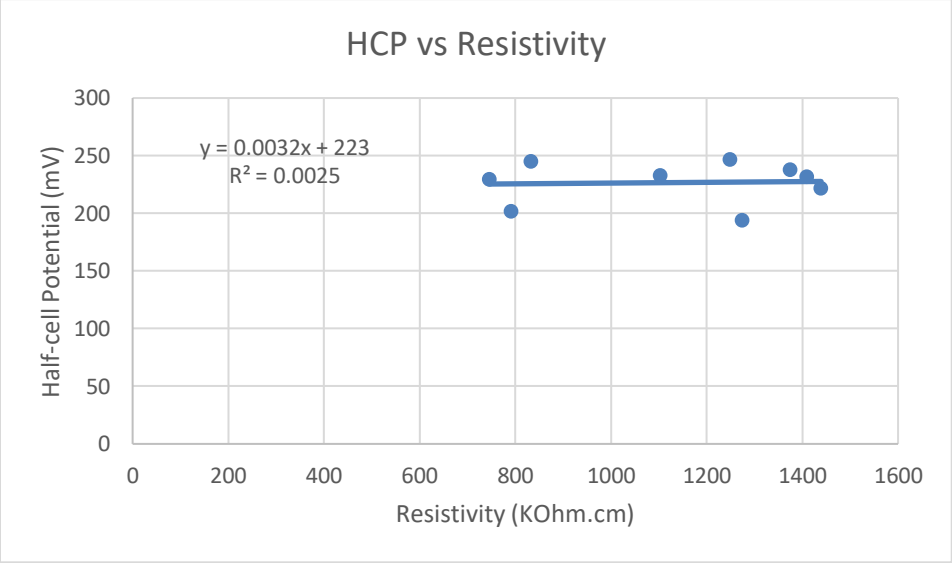

Figure 75: Graph of the maximum measured Half-cell potential (mV) vs maximum measured Resistivity (KOhm.cm) for location 5

5. Conclusions & Recommendations

5.1. Summary

Reinforcement corrosion is the main cause of deterioration in concrete structures. The effects of reinforcement corrosion can have several serious consequences such as harm to people, the environment and major financial implications. To prevent the occurrence of such consequences, condition assessment tests have been developed to predict whether reinforcement corrosion is occurring or not. Some of these tests include cover depth, carbonation, half-cell potential & resistivity testing.

The main objective of this research was to carry out the above-mentioned tests and determine how the results of the different tests will be influenced when certain factors changed. These tests were carried out following well-known procedures that have been standardised. Moisture content and temperature play a role in the occurrence of reinforcement corrosion and the moisture content and temperature to which a structure is exposed can be largely influenced by environmental conditions (Vavpetic, 2008). Environmental factors in the form of rainfall and temperature fluctuation were thus selected as the factors of influence that were tested for the half-cell potential (HCP) and resistivity tests. The factors of influence that were tested for the cover depth and carbonation tests were the number of measurements that are taken and the locations from which these measurements are taken. The other objectives were to determine if and how the results from HCP and cover depth and HCP and resistivity tests relate to each other and to provide guidance on how to carry out a cover depth analysis for the purpose of a condition assessment.

The results of the half-cell potential and resistivity tests showed significant variations under the influence of changes in moisture content brought about by the occurrence of rainfall. Wet weather caused the values to become more negative, while dry weather led to more positive values. Experiments by Sarkar & Bhattacharjee (2014) showed that high intensity and longer duration rainfalls led to higher levels of moisture ingress into a structure. Although rainfall intensity and duration were not measured during these tests, the most negative results that were recorded for both the half-cell potential and resistivity tests were found to occur on the days of testing following more significant periods of rainfall.

The half-cell potential measurements changed by over 100 mV on a number of occasions, with values moving between the ranges of low and uncertain risk of corrosion and high and uncertain risk of corrosion, as defined in ASTM C876 (2009). In some instances, changes in half-cell potential measurements of over 150 mV which is equal to the difference between the low and high-risk ranges were found to occur after the occurrence of significant rainfall. The half-cell potential contour plots proved to be a more stable method of interpreting results under the variations of moisture as the relation between the more negative and more positive locations on the plots hardly changed under the influence of rain. The resistivity values that were measured were all highly positive and so did not move between any of the risk ranges prescribed

in the literature (ACI, et al., 2002), but still underwent significant negative changes due to the occurrence of rain.

The effects of temperature were difficult to isolate from the effects of rain, but the results appear to show a slight negative shift in the values of both the half-cell potential and resistivity measurements with an increase in temperature. Vavpetic (2008) states that moisture content is the most influential of the environmental factors that influence reinforcement corrosion. These tests have shown that the effect that rain has on the moisture content of a structure has a much more significant influence on both half-cell potential and resistivity measurements than the effects caused by temperature fluctuations.

Core samples taken for carbonation depth tests from 2 different buildings showed contradictory results concerning variations in measurements with location along a building and sample size. One building showed very little variation, while the second building showed variations of over 10 mm. The chance of variation of results with measurement location was thus found to be possible and so taking a limited number of cores may lead to a misinterpretation of the state of a structure.

Carrying out a cover depth assessment on a full structure can be too time-consuming. It thus becomes important to make decisions on how much of a structure needs to be analysed in order make adequate conclusions (PCTE, 2014). To do this a good understanding of the factors that influence cover depth assessments are needed. The cover depth analysis showed cover depths to vary to a large degree with both the location from which the measurements were taken and the size of the sample that was used. The average and median cover depths showed differences of over 15 mm when comparing 1.5 m^2 areas from different locations along the same building. The changes with sample size were not as significant as the changes with location, but these changes did, in general, grow in magnitude as the sample size decreased. With the large variations that were found it was recommended that a cover depth assessment should cover more locations from around a structure and include more measurements in order to better represent the state of a structure. A more general assessment representing the different faces and levels of a structure should be followed by detailed focused assessments in areas of concern.

Available standards and guidelines provide information on how to carry out cover depth measurements and what the minimum required cover depths are, but there is a lack of information on how to assess these measurements. Some guidelines for assessing cover depth measurements for the purpose of quality assessments such as the RILEM suggested methods and methods by the German Concrete and Construction association do exist (Corbett, 2015). The large variations that were found in the results of the cover depth tests indicate the need for a more conservative analysis. The RILEM and German methods both proved to be more conservative than using general statistics like the mean and median of the results to conduct an analysis.

Concrete cover depth influences the rate of reinforcement corrosion as moisture, oxygen and aggressive chemical species that cause reinforcement corrosion to occur and progress must first pass through the cover layer before reaching the reinforcement (Arito, 2017; Otieno, et al., 2010). The overall relationship between half-cell potential and cover depth measurements from the results of the testing that was carried out showed that half-cell potential measurements decrease as cover depth measurements decrease. For

the control location the correlation was however low, showing that cover depth and half-cell potential measurements only show a relationship when corrosion is present. Half-cell potential results are expected to become more negative as resistivity results become more negative since both these tests are somewhat affected by the same factors. The results for the comparison between half-cell potential and resistivity results are however contradictory for the different locations. Some of the locations show a poor relationship between the two sets of measurements, while other locations show the expected relationship. There is evidence from these tests that suggest that a relationship between the different tests exist, but this is inconclusive as not all the locations show the same results.

5.2. Conclusions

Condition assessment tests are very important when it comes to prolonging the life of all types of structures. These tests allow for conclusions on the current state of a structure to be drawn and can thus be used to inform on where and when repair and rehabilitation on a structure need to be carried out. The more timeously the tests are performed, the better the chances are of maintaining the safety of the structure and reducing the costs of dealing with deterioration. When it comes to assessing the state of reinforcement corrosion of a concrete structure, tests such as the carbonation, cover depth, half-cell potential and resistivity tests are commonly used. The choice of which test or combination of tests should be used depends on a number of factors such as structural features and environmental conditions amongst others.

The results of these different tests are subject to change due to a number of variables. Half-cell potential and resistivity test results can change due to the effects of fluctuating weather conditions, with the effect that rain has on the moisture content of a structure leading to significant changes. Cover depth and carbonation results can also vary significantly due to factors such as the choice of measurement location and sample size. It is often suggested that a combination of tests should be used in order to make well-informed decisions. Understanding the influence of the variables that affect the different tests as well as how and why the results of the different tests may relate to each other will guide in choosing which test or combination of tests should be used when carrying out a condition assessment. This understanding will help to minimise the chance of misinterpreting the results and to allow for more accurate conclusions on the state of reinforcement corrosion of a structure to be made.

5.3. Recommendations

5.3.1. Recommendations for performing a condition assessment

The testing that was performed provided insight into how to carry out and interpret the results of a few condition assessment tests. Based on these findings following list of recommendations for carrying out a condition assessment of reinforced concrete structures for the assessment of the state of reinforcement corrosion are proposed:

I. Contour plots should be used as the main source for interpreting half-cell potential results as they vary less under fluctuating weather conditions. Prescribed value ranges can then be used as a secondary source for interpretation.

II. Should information from both the contour plots and prescribed value ranges still lead to uncertainty as to what the state of reinforcement corrosion is then small areas of cover should be removed from above the reinforcement. The concrete should be removed where the most negative potentials are found, and the exposed reinforcement can then be analysed.

III. A few cores to interpret the state of carbonation of a structure may provide misleading and varying results. Cores should thus be taken from a number of locations around a structure so as to account for a range of locations which are exposed to different conditions due to for example the direction they face or the presence of obstructions.

IV. A cover depth survey should be carried out at a number of locations along a structure to be able to account for inconsistencies in construction. The locations should come from different faces of the structure as well as different heights along a structure. The number of measurements that are taken per location will depend on the intensity of the investigation. The tests that were carried out showed that 1.5 m^2 areas can be sufficient enough to identify variances. This may however vary from structure to structure.

V. When carrying out a cover depth assessment a broader search should be carried out first and should areas of concern be identified then a more focussed assessment should be done in these areas.

VI. Since cover depth measurements can vary a lot with both location and sample size it is recommended that a more conservative analysis of the results should be done. For this purpose, the RILEM and German methods have proven to be more conservative than the use of general statistics.

VII. The overall trend that was found between HCP and cover depth results supports the idea that the identification of areas with low cover can be used as a guide for where the best locations would be to carry out HCP testing.

VIII. The expected relationship between HCP and resistivity results where the HCP results will increase as resistivity results increase may not always be the case even when reinforcement corrosion is present. This relationship should therefore be interpreted with care.

5.3.2. Recommendations for future research

The following are recommended areas for future research that will help to improve and add to the knowledge that was gained from this piece of work:

I. **Conduct tests on more locations:** the results of the half-cell potential and resistivity tests were carried out at 5 locations along three different buildings, all of which are located at the University of Cape Town. The locations were selected due to material and time constraints. In order for the results of such tests to be more conclusive, it is recommended that the tests be carried out at a variety of different locations, as a greater sample size will mean more accurate findings or allow for location-dependent variables to be sought out. The same applies to the cover depth tests which were carried out on one building at UCT. A look into the assessment of variations of cover depth with respect to floor levels was restricted to a few locations due to access limitations and therefore a more in-depth analysis in this regard could prove valuable.

II. **A proper comprehensive statistical analysis should be carried out:** for the different areas of testing a comprehensive statistical analysis should be carried out. This can be done to get a clearer understanding of how weather conditions impact on half-cell potential and resistivity results and how variations in measurement location and sample sizes impact on cover depth results.

III. **A similar study should be carried out for chloride-induced corrosion:** this work was carried out on buildings that are subject to carbonation induced corrosion. A similar work on buildings subject to chloride-induced corrosion will provide information on this type of corrosion and allow for a comparison between the two types of corrosion to be made.

IV. **Assess structures with higher carbonation depths and more rebar corrosion damage:** the carbonation depths that were found on the buildings that were tested were in general low. In order to further this research structures showing higher carbonation depths and more reinforcement corrosion should be assessed.

V. **Carry out tests during a dry period:** the half-cell potential and resistivity tests should be carried out during a drier period in order to get a more accurate indication of how temperature variations in-field influences the results of these tests. Should the tests be carried out during a drier period, then the results are less likely to be influenced by the effects of the changes in moisture content which are brought about by the influence of rain.

VI. **Test for a possible relationship which dictates if and when cover depth or resistivity are more influential on the occurrence of corrosion:** from the test results it was found that sometimes the resistivity results would support the half-cell potential results and sometimes the cover depth results would support the half-cell potential results. This indicates that there may be a relationship which determines whether resistivity or cover depth is more influential when it comes to the occurrence of corrosion. The half-cell potential results were taken to be accurate as corrosion was visible at the four locations from which high negative measurements were obtained. If such a relationship exists, then it will help to determine which of the two tests will lead to drawing a more accurate conclusion under different circumstances.

I. References

Abbas, Y. et al., 2018. Non-destructive measurement of chloride ions concentration in concrete– A comparative analysis of limitations and prospects. *Construction and Building Materials,* Volume 174, pp. 376-387.

ACI, 2008. *Guide for Conducting a Visual Inspection of Concrete in Service,* Conneticut: The American Concrete Institute Committee 201.

ACI, BRE, ConcreteSociety & ICRI, 2002. *Concrete Repair Manual.* 2nd ed. s.l.:American Concrete Institue; BRE; The Concrete Society; International Concrete Repair Institue.

Ahlström, J., 2014. *Corrosion of steel in concrete at various moisture and chloride levels,* Lund: Lund University Faculty of Engineering Division of Building Materials.

Akhlaghi, A. & Tronca, G., 2015. *Proceq Webinar: Resistivity measurements for quality inspection of new structures,* s.l.: Proceq.

Alexander, M., Beushausen, H. & Otieno, M., 2012. *Corrosion of steel in reinforced concrete: Influence of binder type, water/binder ratio, cover and cracking,* Cape Town: Concrete Materials and Structural Integrity Research Unit, Department of Civil Engineering, University of Cape Town.

Al-Neshawy, F. & Sistonen, E., 2015. *Condition Assessment of Structures (Visual inspection & non-destructive testing of structures).* s.l., Aalto University School of Engineering.

Alsharqawia, M., Zayeda, T. & Abu Dabousb, S., 2018. Integrated condition rating and forecasting method for bridge decks using Visual Inspection and Ground Penetrating Radar. *Automation in Construction,* Volume 89, pp. 135-145.

Andrade, C., 2007. Corrosion of steel reinforcement. *Transactions on State of the Art in Science and Engineering,* Volume 28, pp. 185-216.

Arito, P., 2017. *REBAR CORROSION: Principles, mechanisms and influencing factors.* s.l., The University of Cape Town.

Arndt, R. & Jalinoos, F., 2009. *NDE for corrosion detection in reinforced concrete structures.* Nantes, Non-Destructive Testing in Civil Engineering.

Arya, A. & Agarwal, A., 2007. *CONDITION ASSESSMENT OF BUILDINGS FOR REPAIR AND UPGRADING,* New Delhi: National Disaster Management Division Ministry of Home Affairs, Government of India.

ASTM, 2009. *ASTM C876: Standard Test Method for Corrosion Potentials of Uncoated Reinforcing Steel in Concrete,* s.l.: ASTM International.

Azarsa, P. & Gupta, R., 2017. Electrical Resistivity of Concrete for Durability Evaluation: A Review. *Advances in Materials Science and Engineering,* Volume 2017, pp. 1-30.

Babaei, K., 1986. *Evaluation of Half-cell Corrosion Detection Test For Concrete Bridge Decks,* Wahington: Washington State Department of Transportation .

Barnes, R. & Zheng, T., 2008. Research on Factors Affecting Concrete Cover Measurement. *The e-Journal of Nondestructive Testing.*

BEG, 2002. *Building Performance.* [Online]
Available at: http://www.civil.uwaterloo.ca/beg/building_performance.htm
[Accessed 2 January 2019].

Beushausen, H., 2017. *Damage assessment and diagnostic testing.* Cape Town, The University of Cape Town.

Broomfield, J., 2007. *Corrosion of Steel in Concrete.* 2nd ed. New York: Taylor & Francis.

Brownlee, J., 2018. *How to Use Correlation to Understand the Relationship Between Variables.* [Online]
Available at: https://machinelearningmastery.com/how-to-use-correlation-to-understand-the-relationship-between-variables/
[Accessed 15 DECEMBER 2018].

BS-1881, 1988. *British Standard Testing Concrete Part 204. Recommendations on the use electromagnetic covermeters,* London: British Standards Institution.

BS-1881, 1988. *Testing concrete Part 124. Methods for analysis of hardened concrete,* London: British Standards Institution.

Bungey, J. & Grantham, M., 2006. *Testing of Concrete in Structures.* 4th ed. New York: Taylor & Francis.

Chandra Paula, S. et al., 2018. An empirical model design for evaluation and estimation of carbonation depth in concrete. *Measurement,* Volume 124, pp. 205-210.

Cheaitani, A. & Collyer, A., 2002. Half-Cell Potential Mapping Of Reinforced Concrete. *Corrosion & Materials,* 27(5), pp. S1-S4.

Choi, J., Lee, Y., Kim, Y. & Lee, B., 2017. Image-processing technique to detect carbonation regions of concretesprayed with a phenolphthalein solution. *Construction and Building Materials,* Volume 154, pp. 451-461.

Clemena, G., 1992. *Benefits of Measuring Half-Cell Potentials and Rebar Corrosion Rates in Condition Surveys ofConcrete Bridge Decks,* Virginia: Virginia Transportation Research Council In Cooperation with the U.S. Department of Transportation Federal Highway Administration.

Coimbatore, V., 2014. *Inspection Guidelines for Condition Assessment of Concrete Structures,* Leederville: Water Corporation.

ConcreteSociety, 2009. *Technical Report No. 69: Repair of concrete structures with reference to BS EN 1504,* Surrey: The Concrete Society.

ConcreteSociety, 2018. *Concrete @ your Fingertips Reinforcement depth.* [Online]
Available at: http://www.concrete.org.uk/fingertips-nuggets.asp?cmd=display&id=459
[Accessed 29 April 2018].

Corbett, D., 2015. STATISTICAL ASSESSMENT OF CONCRETE COVER IN THEORY AND PRACTISE. *REINFORCED CONCRETE AND MASONRY STRUCTURES – THEORY AND PRACTICE,* 48(12), pp. 249-256.

Costa, J., 2011. *Corrosion Assessment of Reinforced Concrete Structures Using NDE Techniques.* Houston, Electrotech CP.

Dayaram, K., 2010. *The Recarbonation of Crushed Concrete from a New Zealand Perspective,* Christchurch: The University of Canterbury.

Elcometer, 2012. *Elcometer 331 Concrete Covermeter Operating Instructions,* s.l.: Elcometer Limited.

Elsener, B., 2001. Half-cell potential mapping to assess repair work on RC structures. *Construction and Building Materials,* Volume 15, pp. 133-139.

Elsener, B. et al., 2003. RILEM TC 154-EMC: Half-cell potential measurements – Potential mapping on reinforced concrete structures. *Materials and Structures,* Volume 36, pp. 461-471.

FPrimeC, 2017. *Half Cell Crrosion Mapping for Concrete.* [Online]
Available at: http://www.fprimec.com/half-cell-corrosion-mapping-for-concrete/
[Accessed 3 February 2018].

Gowers, K. & Millard, G., 1999. Measurement of Concrete Resistivity for Assessment of Corrosion. *ACI Materials Journal ,* 96(5), pp. 536-541.

Gromicko, N. & Shepard, K., 2006. *Visual Inspection of Concrete.* [Online]
Available at: https://www.nachi.org/visual-inspection-concrete.htm
[Accessed 1 January 2019].

Gu, P. & Beaudoin, J., 1998. *Obtaining Effective Half-Cell Potential Measurements in Reinforced Concrete Structures,* Ottawa: Institute for Research in Construction.

Guthrie, W., Pinkerton, T. & Eggett, D., 2008. *Sensititivity of Half-Cell Potential Measurements to Properties of Concrete Bridge Decks,* Utah: Utah Department of Transportation Research Division.

Hansson, C., Poursaee, A. & Jaffer, S., 2012. *Corrosion of Reinforcing Bars in Concrete,* Waterloo: The Masterbuilder.

HOŁA, J., BIEŃ, J., SADOWSKI, L. & SCHABOWICZ, K., 2015. Non-destructive and semi-destructive diagnostics of concrete structures in assessment of their durability. *BULLETIN OF THE POLISH ACADEMY OF SCIENCES TECHNICAL SCIENCES,* 63(1), pp. 87-96.

Jedidi, M. & Kaouther, M., 2014. Destructive and Non-destructive Testing of Concrete Structures. *Jordan Journal of Civil Engineering,* 8(4), pp. 432-441.

Keßler, S. & Gehlen, C., 2016. *Influence of Concrete Moisture Condition on Half-Cell Potential Measurement.* Shenzen, 5th International Conference on Durability of Concrete Structures, Shenzhen University.

Kevern, J., Halmen, C. & Hudson, D., 2015. *EVALUATION OF RESISTIVITY METERS FOR CONCRETE QUALITY ASSURANCE,* Missouri: Missouri Department of Transportation.

KURZ, J., STOPPEL, M., TAFFE, A. & BOLLER, C., 2012. *Condition assessment of reinforced concrete structures using automated multi-sensor systems.* Durban, 18th World Conference on Nondestructive Testing.

Lane, D., 2018. *Values of the Pearson Correlation.* [Online]
Available at: http://onlinestatbook.com/2/describing_bivariate_data/pearson.html
[Accessed 16 December 2018].

Larsen, C., Sellevold, E., Østvik, J. & Vennesland, O., 2006. *Electrical resistivity of concrete—Part II: influence ofmoisture content and temperature.* s.l., 2nd International RILEM Symposium on Advances in Concrete through Science and Engineering.

Layssi, H., Alizadeh, A., Ghods, P. & Salehi, M., 2015. Electrical Resistivity of Concrete: Concepts, applications, and measurement techniques. *Concrete International,* pp. 41-46.

Lee, H., Kim, D., Lee, J. & Cho, M., 2012. A Study for Carbonation Degree on Concrete using a Phenolphthalein Indicator and Fourier-Transform Infrared Spectroscopy. *World Academy of Science, Engineering and Technology International Journal of Civil and Environmental Engineering,* 6(2), pp. 95-101.

Leelalerkieta, V., Kyunga, J., Ohtsua, M. & Yokotab, M., 2004. Analysis of half-cell potential measurement for corrosion of reinforced concrete. *Construction and Building Materials,* Volume 18, pp. 155-162.

Liu, Y., Paredes, M. & Deuble, A., 2011. *Review and Evaluation of Techniques for Measurements of Concrete Resistivity,* Florida: Florida Department of Transportation.

Lo, T., 2005. *Carbonation & Chloride Penetration of Concrete Structures.* Hong Kong, Annua Concrete Seminar City University of Hong Kong.

Mackechnie, J., 2001. *Predictions of reinforced concrete durability in the marine environment,* Cape Town: Department of Civil Engineering University of Cape Town.

Mackechnie, J. & Alexander, M., 2001. *Repair principles for corrosion-damaged reinforced concrete structures,* Cape Town: Department of Civil Engineering University of Cape Town.

Maierhofer, C., Reinhardt, H. & Dobmann, G., 2010. *Non-destructive evaluation of reinforced concrete structures.* 2 ed. Cambridge: Woodhead Publishing Limited.

Malhotra, V. & Carino, M., 2004. *Handbook on Nondestructive Testing of Concrete.* 2nd ed. West Conshohocken: CRC Press.

Melchers, R. & Li, C., 2006. Phenomonological modelling of reinforcement corrosion in marine environments. *ACI materials journal,* 106(1).

Monteiro, A., Gonçalves, A., Gulikers, J. & Jacobs, F., 2015. Basis for the Statistical Evaluation of Measured Cover Depths in Reinforced Concrete Structures. In: Springer, ed. *Performance-Based Specifications and Control of Concrete Durability.* s.l.:RILEM TC 230, pp. 206-234.

Moreno, F. & Liu, Y., 2012. *Temperature Effect on Electrical Resistivity Measurements on Mature Saturated Concrete.* Florida, NACE - International Corrosion Conference Series.

Omar, T. & Nehdi, M., 2016. *CONDITION ASSESSMENT AND DETERIORATION PREDICTION TOOLS FOR CONCRETE BRIDGES: A NEW LOOK,* London: RESILIENT INFRASTRUCTURE.

Ortega, N. & Robles, S., 2014. Assessment of Residual Life of concrete structures affected by reinforcement corrosion. *HBRC Journal,* Volume 12, pp. 114-122.

Osterminski, K., Polder, R. & Schießl, P., 2012. Long term behaviour of the resistivity of concrete. *HERON,* 57(3), pp. 221-230.

Otieno, M., 2014. Durability of Concrete. In: *Construction Materials 1.* Johannesburg: The University of the Witwatersrand School of Civil & Environmental Engineering, pp. 24-34.

Otieno, M., Alexander, M. & Beushausen, H., 2010. *Transport Mechanisms in Concrete,* Cape Town: Concrete Materials and Structural Integrity Research group.

PCTE, 2014. *How to do a Concrete Cover Check.* [Online]
Available at: https://www.pcte.com.au/construction-ndt-october-2014
[Accessed 28 August 2018].

Phares, B., 2001. *Highlights of study of reliability inspectioj,* s.l.: FHWA.

Polder, R. et al., 2000. RILEM TC 154-EMC Test methods for onsite measurement of resistivity of concrete. *Materials & Structures,* Volume 33, pp. 603-611.

Portland Cement Association, 2002. Types and Causes of Concrete Deterioration. *Concrete information,* IS563(01).

Price, R., 1985. *DETERMINATION OF CHLORIDE ION CONTENT IN CONCRETE,* s.l.: State Department of Highways and Public Transportation.

Proceq, 2017. *Resipod Family: Operating Instructions Concrete Durability Testing,* Zurich: Proceq.

Ratner, B., 2009. The Correlation Coefficient: Definition. *Journal of Targeting Measurement and Analysis for Marketing,* 17(2), pp. 139-142.

Raupach, M., Elsener, B., Polder, R. & Mietz, J., 2007. *Corrosion of Reinforcement in Concrete: Mechanisms, monitoring, inhibitors and rehabilitation techniques.* Cambridge: Woodhead Publishing Limited.

Richardson, M., 2002. *Fundamentals of durable concrete, modern concrete technology,* London: Son Press.

RILEM, 2002. Analysis of total chloride content in concrete. *Materials and Structures,* Volume 35, pp. 583-585.

Roberge, P., 2008. *Corrosion Engineering Principles and Practice.* New York: McGraw-Hill Companies.

Rodriguez, J. et al., 1994. *On site corrsion rate measurements in concrete structures using a device developed under the Eureka project EU-401.* Odense, Concrete across borders.

Rumsey, D., 2016. *Statistics for Dummies.* 2nd ed. Ohio: Wiley.

Sagues, A., Moreno, E., Morris, W. & Andrade, C., 1997. *CARBONATION IN CONCRETE AND EFFECT ON STEEL CORROSION,* Tampa Florida: College of Engineering University of South Florida.

Sarkar, K. & Bhattacharjee, B., 2014. *MOISTURE PENETRATION IN CONCRETE SUBJECTED TO RAINFALL: EFFECT OF INTENSITY AND DURATION OF EXPOSURE.* New Delhi, Department of Civil Engineering, Indian Institute of Technology Delhi.

Schiessel, P. & Raupach, M., 1992. Monitoring system for the corrosion risk of steel in concrete structures. *Concrete International,* 14(7), pp. 52-55.

Silva, P., Ferreira, R. & Figueiras, H., 2011. *Electrical Resistivity as a Means of Quality Control of Concrete – Influence of Test Procedure.* Porto, International Conference on Durability of Building Materilas & Components.

Sivasubramanian, K., Jaya, K. & Neelemegam, M., 2013. Covermeter for identifying cover depth and rebar diameter in high strength concrete. *INTERNATIONAL JOURNAL OF CIVIL AND STRUCTURAL ENGINEERING ,* 3(3), pp. 557-563.

Smith, J. & Virmani, Y., 2000. *Materials & Methods for Corrosion Control of Reinforced & Prestressed Concrete Structures in New Construction,* Virginia: U.S Department of Transportation Federal Highway Administration.

Song, H.-W. & Saraswathy, V., 2007. Corrosion Monitoring of Reinforced Concrete Structures - A Review. *International Journal of Electrochemical Science,* pp. 1-28.

Spragg, R. et al., 2013. Factors that influence electrical resistivity measurements in cementious systems. *Journal of the Transportation Research,* Volume 2342, pp. 90-98.

Srinivasan, P., 2014. *Condition Assessment of Corrosion-Affected Concrete Structures with Case Studies,* Chennai: The Materbuilder.

Tuutti, K., 1982. *Corrosion of steel in concrete,* Stockholm: Swedish Cement and Concrete Research Institute.

TxDOTa, 2005. *Test Procedure for Determining Chloride in Concrete,* Texas: Texas Department of Transportation.

TxDOTb, 2005. Determining Chloride in Concrete. In: *Chemical Test Procedures.* Texas: Texas Departmet of Transportation.

Vassie, P., 1980. *A survey of site tests fr the assessment of corrosion in reinforced concrete,* Crowthorne: TRL.

Vavpetic, P., 2008. *Corrosion in concrete steel.* Kamnik, University of Ljubljana Faculty of mathematics and physics Department of physics.

Winter, N., 2012. *Understanding Cement.* [Online]
Available at: https://www.understanding-cement.com/carbonation.html
[Accessed 2018].

Yodsudjai, W. & Pattarakittam, T., 2017. Factors influencing half-cell potential measurement and its relationship with corrosion level. *Measurement,* Volume 104, pp. 159-168.

Zivica, 2003. Influence of w/c ratio on rate of chloride induced corrosion of steel reinforcement and its dependance on ambient temperature. *Materials Science,* 26(5), pp. 471-475.

APPENDIX

1. Zoomed out images of Locations 1-5

Figure 76: Location 1 (Rachel Bloch House) zoomed out

Figure 77: Location 2 (Hoerikwaggo building) zoomed out

Figure 78: Location 3 (Hoerikwaggo building) zoomed out

Figure 79: Location 4 (Hoerikwaggo building) zoomed out

Figure 80: Location 5 (Neville Alexander building) zoomed out

2. Zoomed out images of locations used for the cover depth assessment

Figure 81: Location for the cover depth assessment on the ground floor of the south side of the Neville Alexander building zoomed out

Figure 82: Location for the cover depth assessment on the ground floor of the east side of the Neville Alexander building zoomed out

Figure 83: Location for the cover depth assessment on the 1st floor of the east side of the Neville Alexander building zoomed out

Figure 84: Location for the cover depth assessment on the ground floor of the west side of the Neville Alexander building

Figure 85: Large location for the cover depth assessment on the ground floor of the west side of the Neville Alexander building

Figure 86: Location for the cover depth assessment on the 1st floor of the west side of the Neville Alexander building

Figure 87: Location for the cover depth assessment on the ground floor of the north side of the Neville Alexander building

Figure 88: Location for the cover depth assessment on the 3rd floor of the north side of the Neville Alexander building

3. Contour plots

Location 1: Rachel Bloch House Column

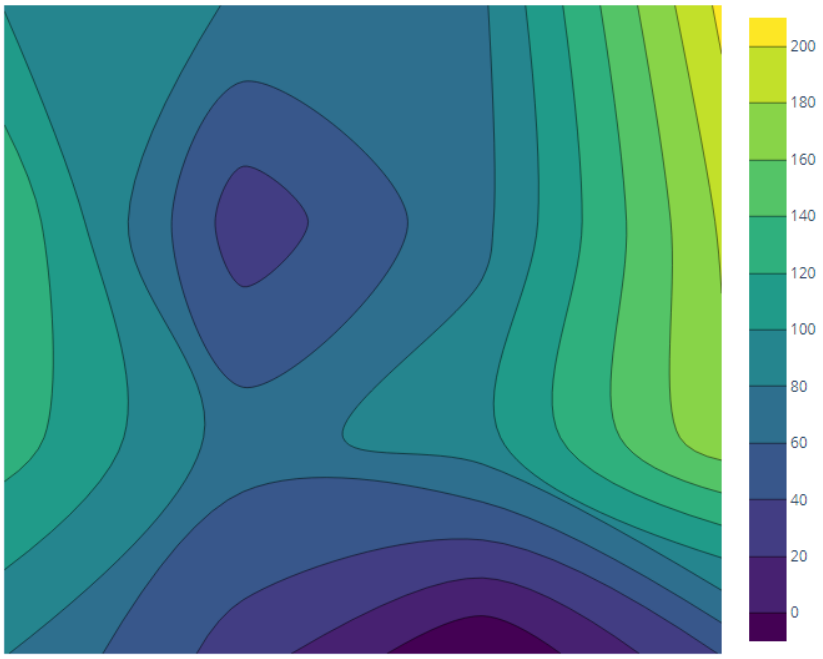

Figure 89: Location 1 contour plot on the 7th of August

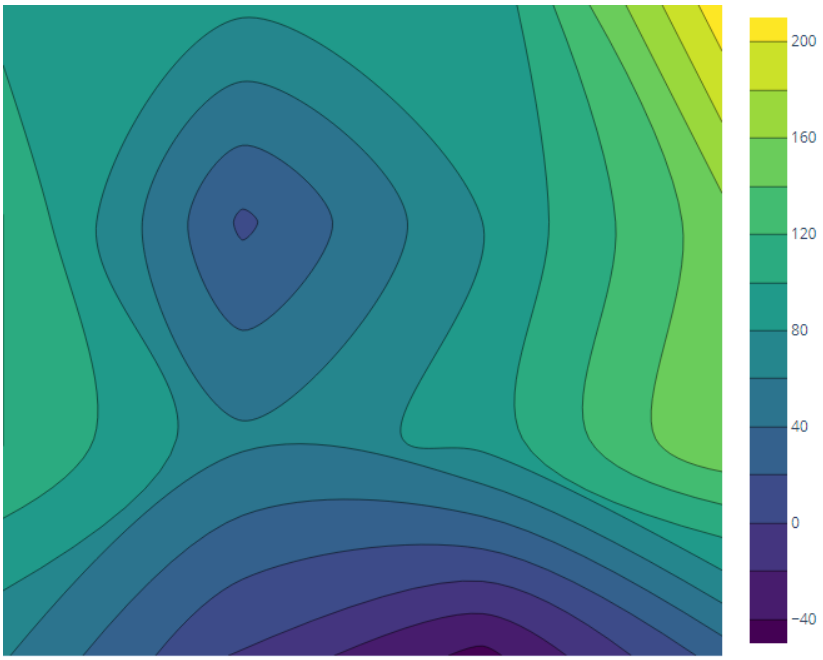

Figure 90: Location 1 contour plot on the 13th of August

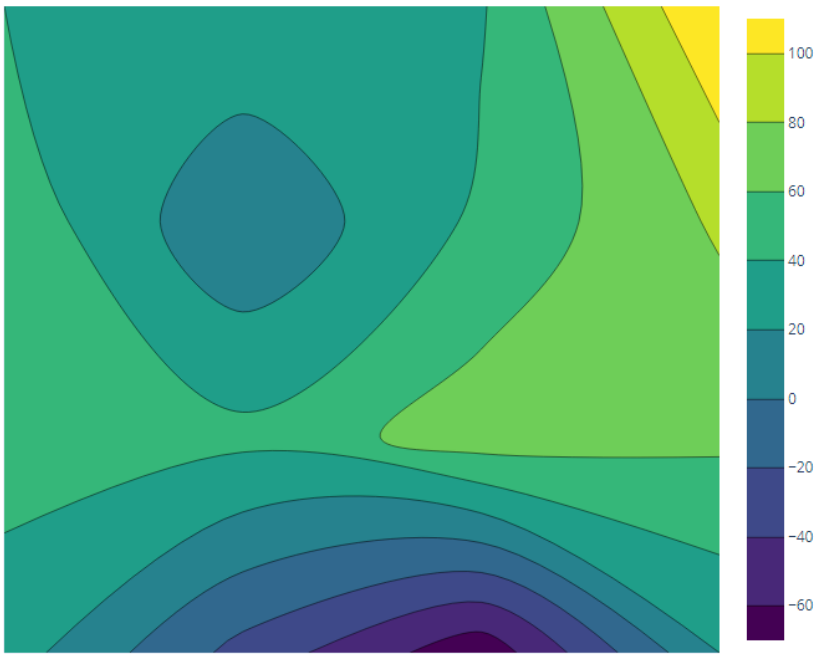

Figure 91: Location 1 contour plot on the 27th of August

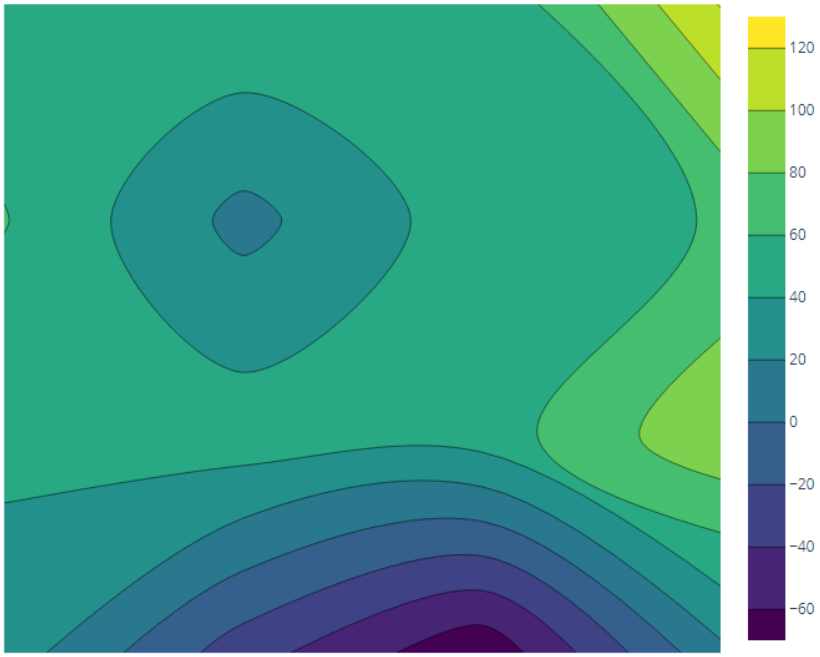

Figure 92: Location 1 contour plot on the 6th of September

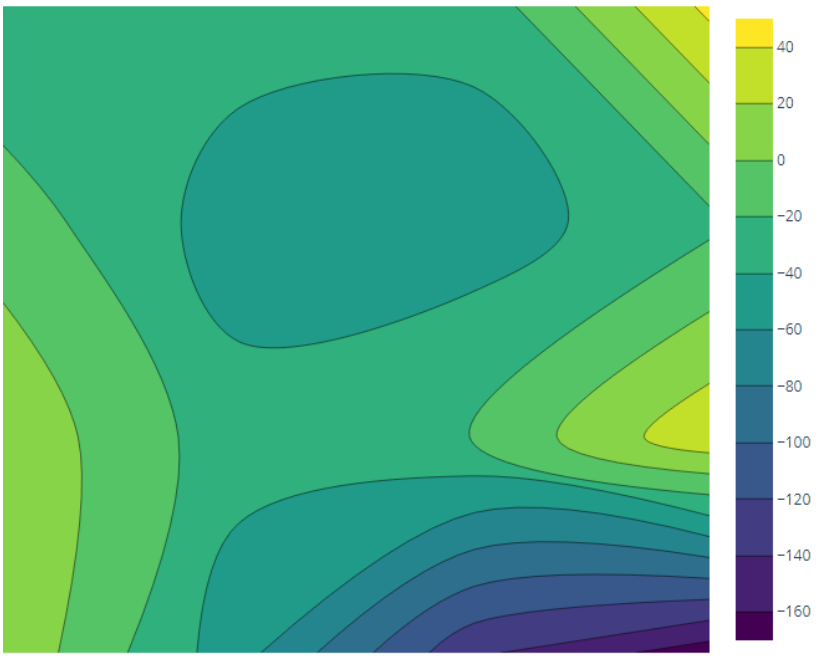

Figure 93: Location 1 contour plot on the 28th of September

Figure 94: Location 1 contour plot on the 27th of October

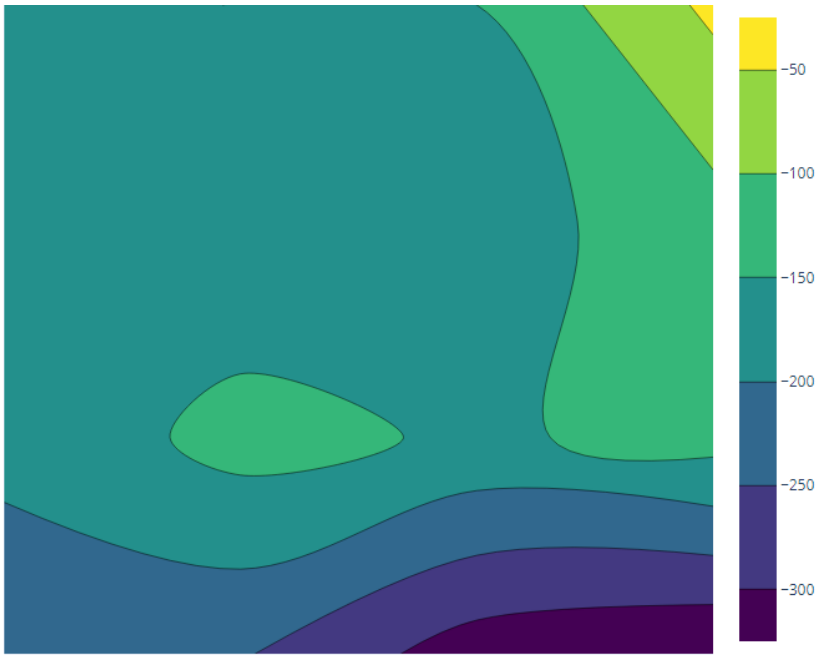

Figure 95: Location 1 contour plot on the 19th of November

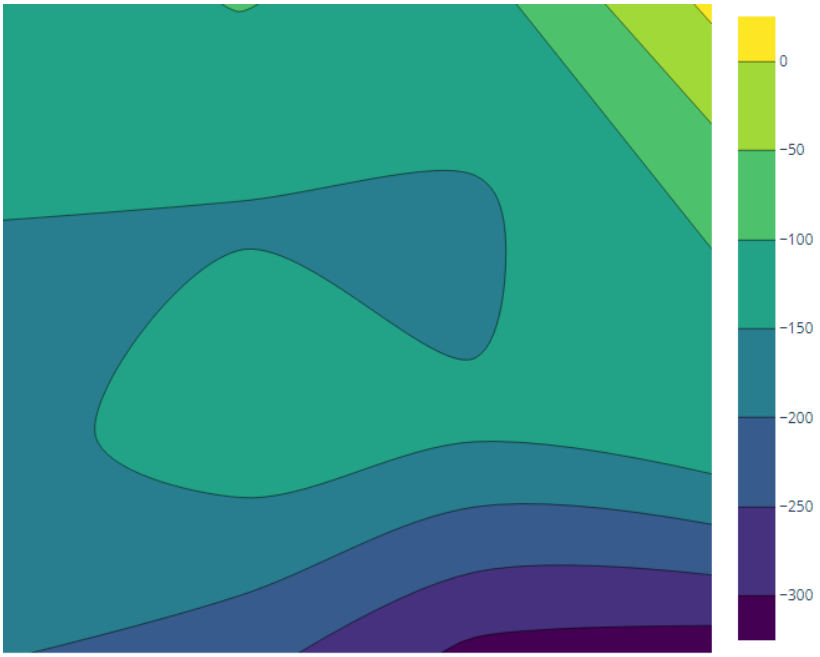

Figure 96: Location 1 contour plot on the 23rd of November

Location 2: Hoerikwaggo Building Chimney

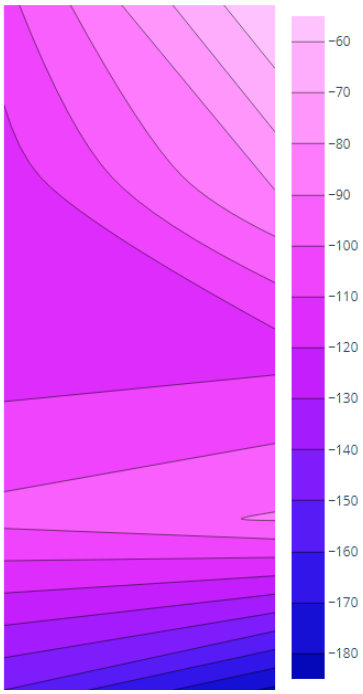

Figure 97: Location 2 contour plot on the 7th of August

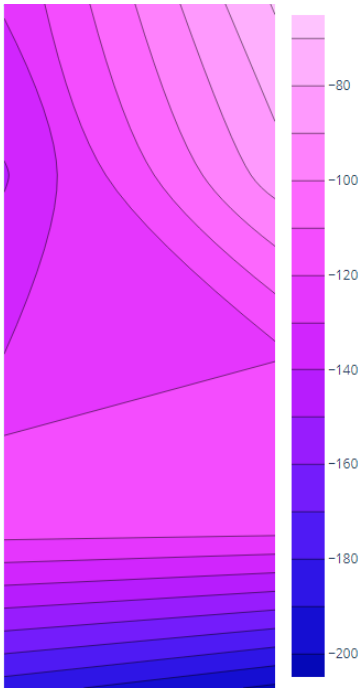

Figure 98: Location 2 contour plot on the 13th of August

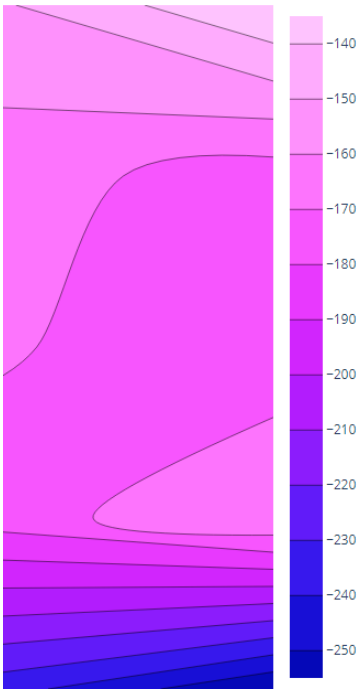

Figure 99: Location 2 contour plot on the 27th of August

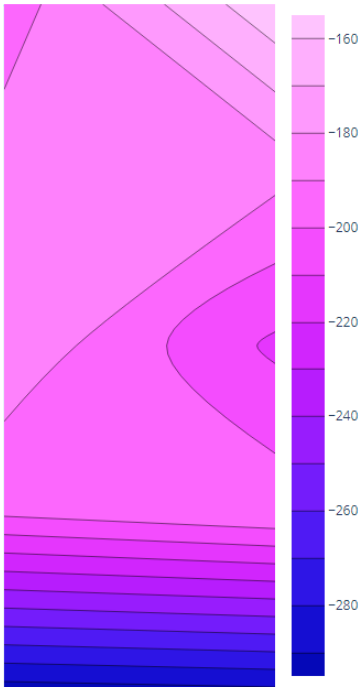

Figure 100: Location 2 contour plot on the 6th of September

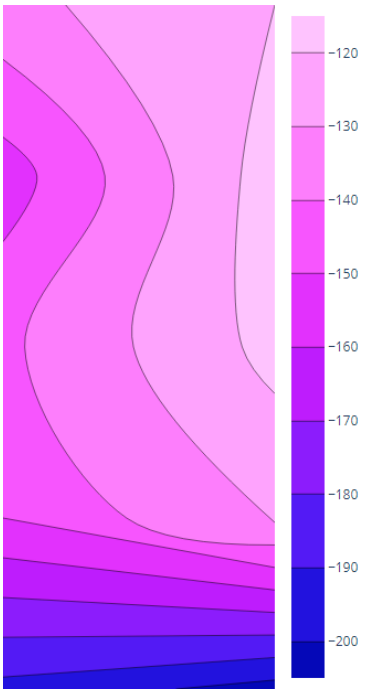

Figure 101: Location 2 contour plot on the 28th of September

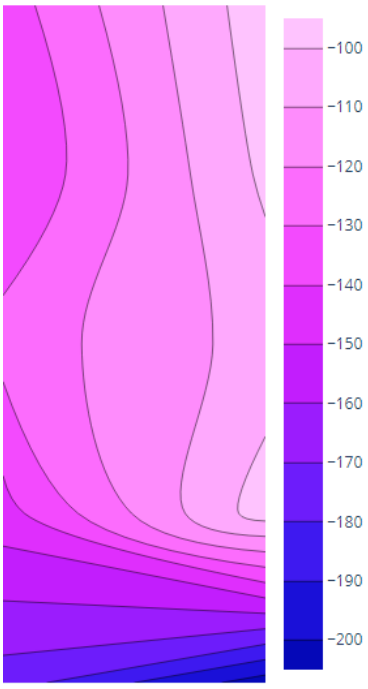

Figure 102: Location 2 contour plot on the 27th of October

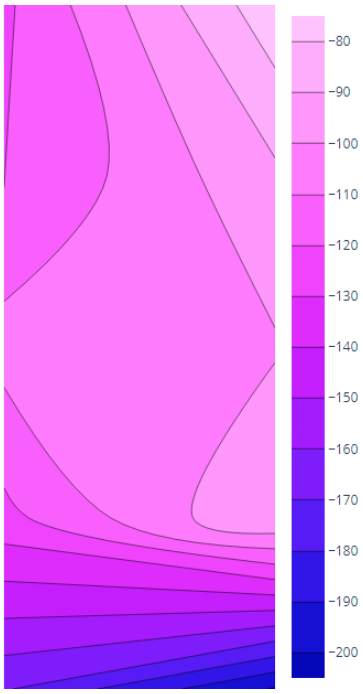

Figure 103: Location 2 contour plot on the 19th of November

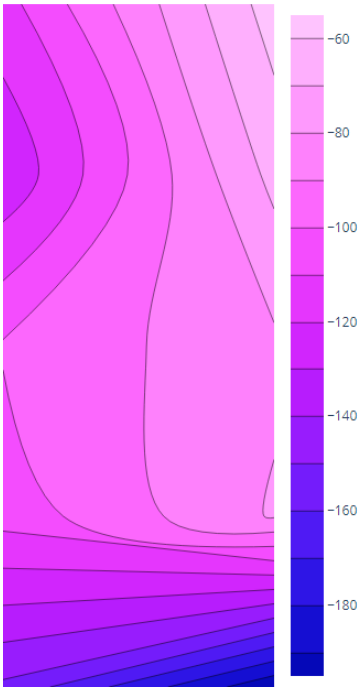

Figure 104: Location 2 contour plot on the 23rd of November

Location 4 Hoerikwaggo retaining wall

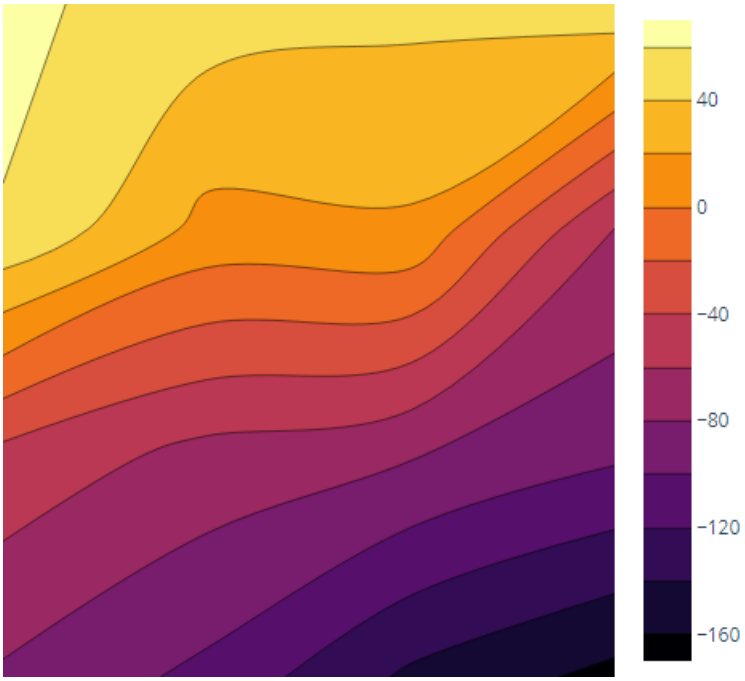

Figure 105: Location 4 contour plot on the 7th of August

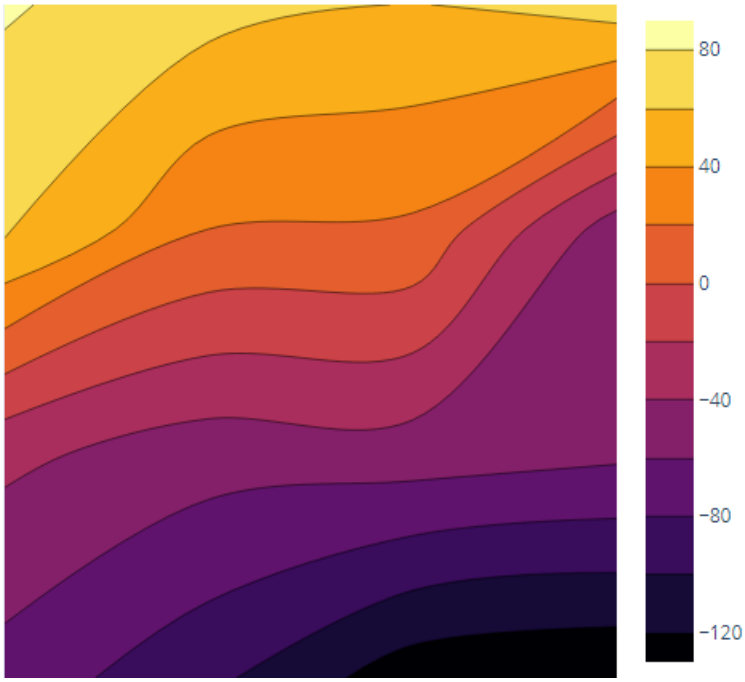

Figure 106: Location 4 contour plot on the 13th of August

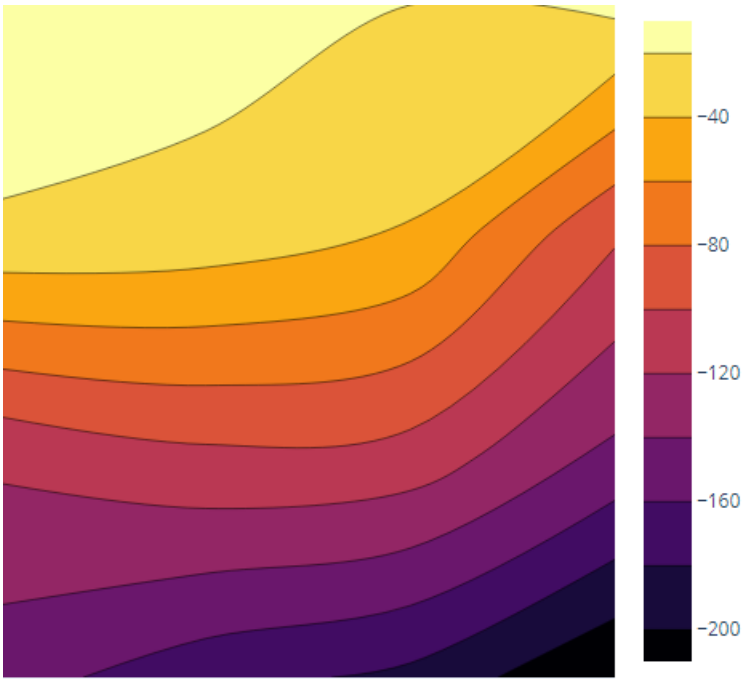

Figure 107: Location 4 contour plot on the 27th of August

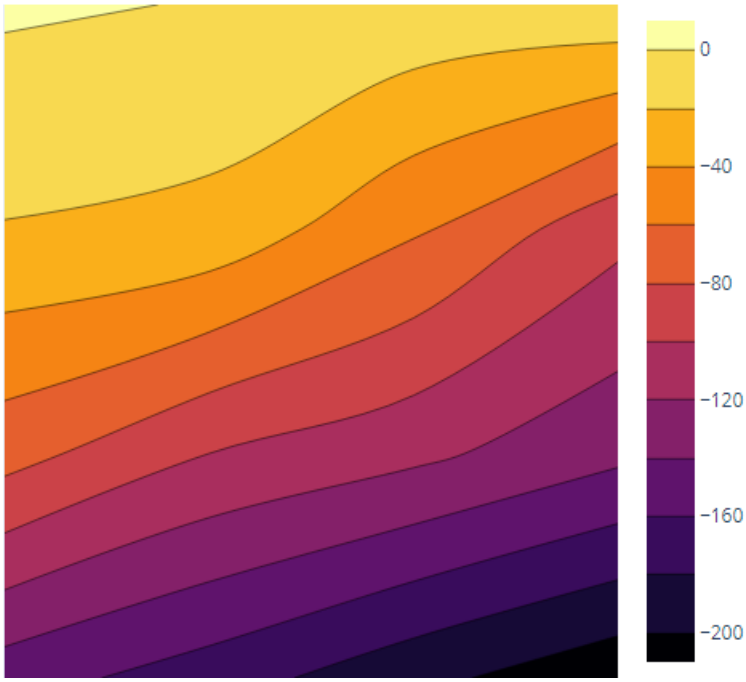

Figure 108: Location 4 contour plot on the 6th of September

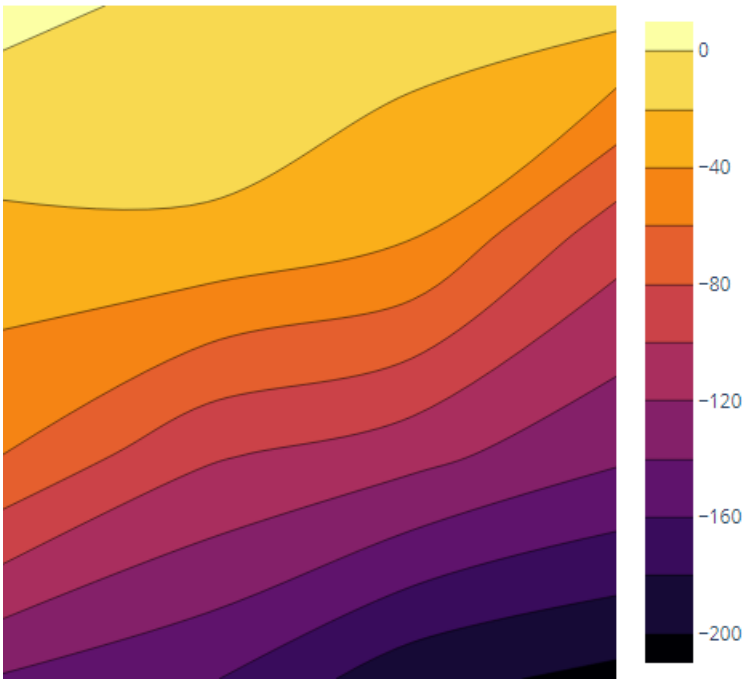

Figure 109: Location 4 contour plot on the 28th of September

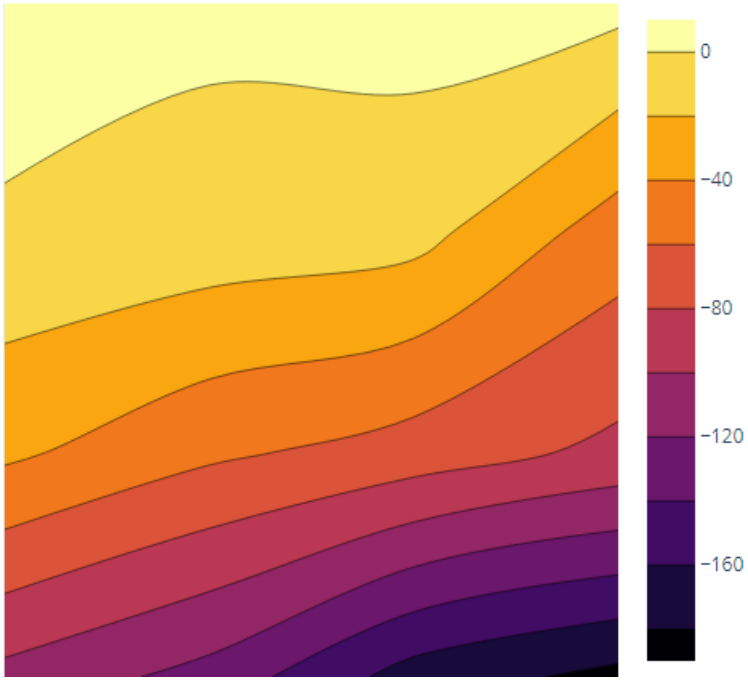

Figure 110: Location 4 contour plot on the 27th of October

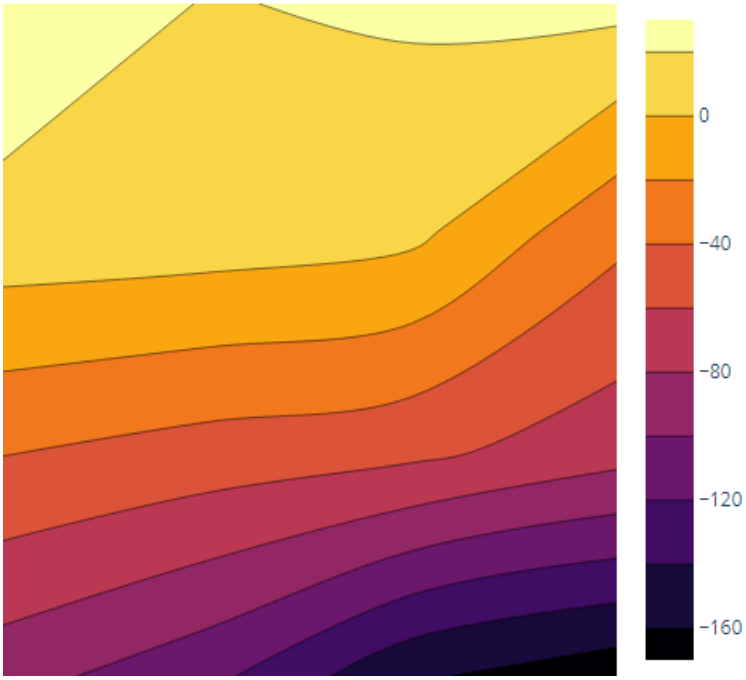

Figure 111: Location 4 contour plot on the 19th of November

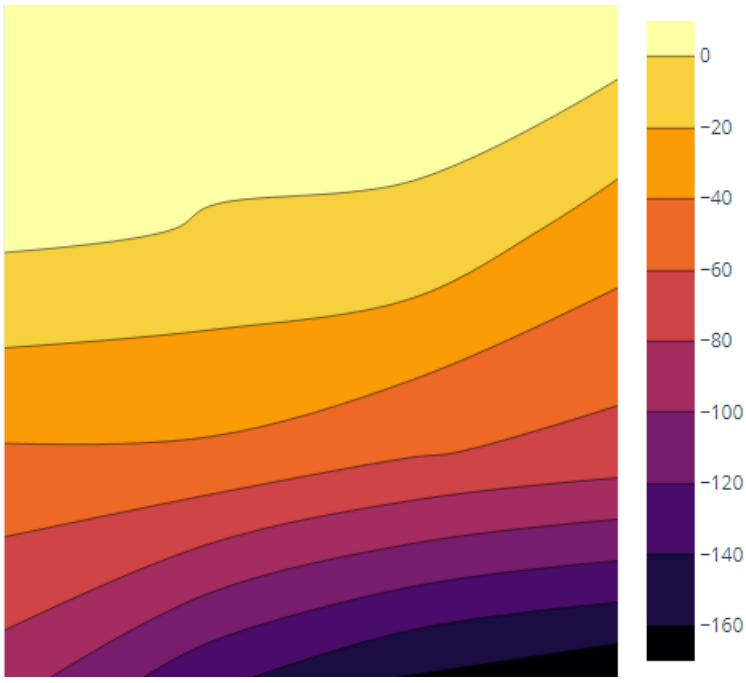

Figure 112: Location 4 contour plot on the 23rd of November

Location 5: Neville Alexander North Wall

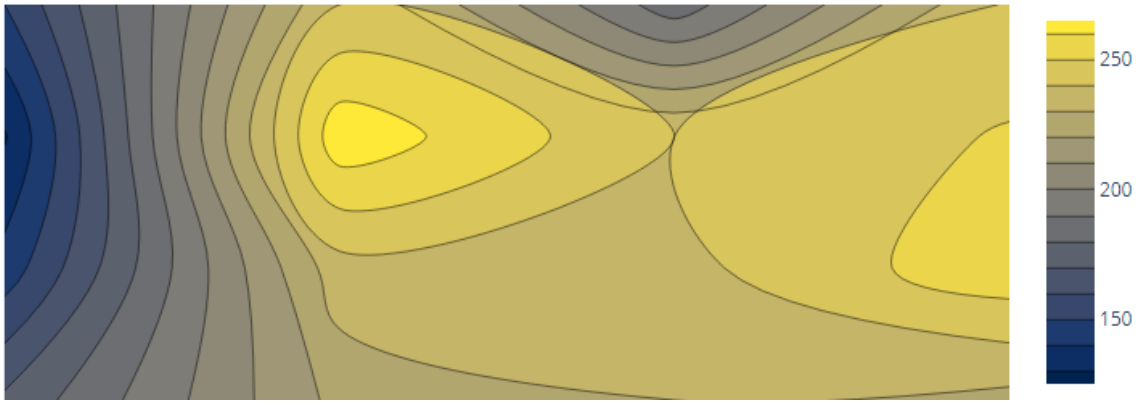

Figure 113: Location 5 contour plot on the 7th of August

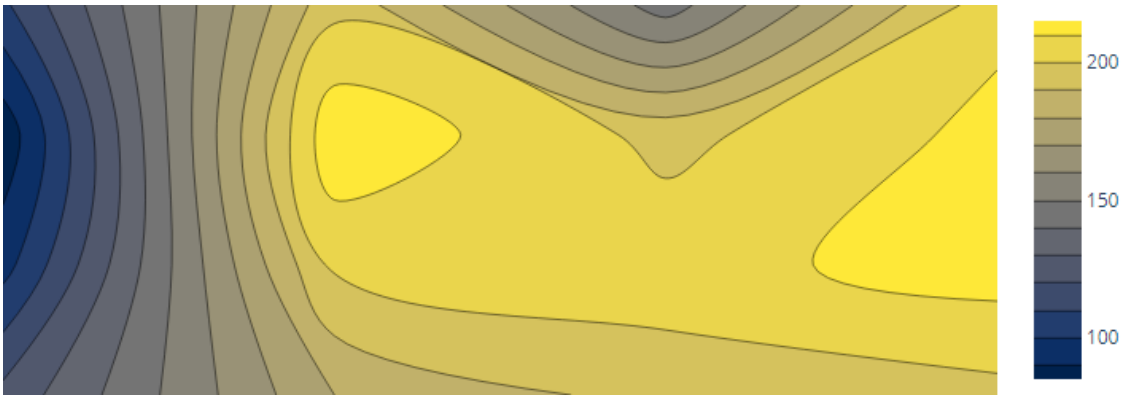

Figure 114: Location 5 contour plot on the 13th of August

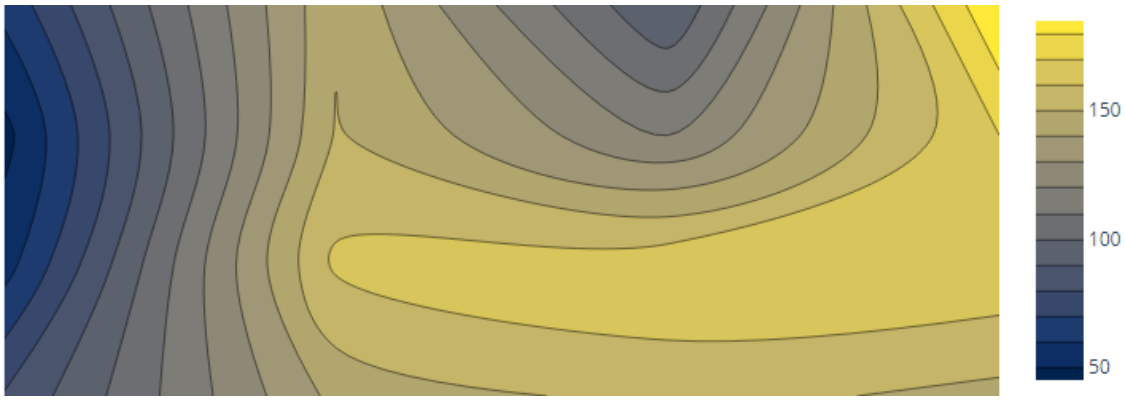

Figure 115: Location 5 contour plot on the 27th of August

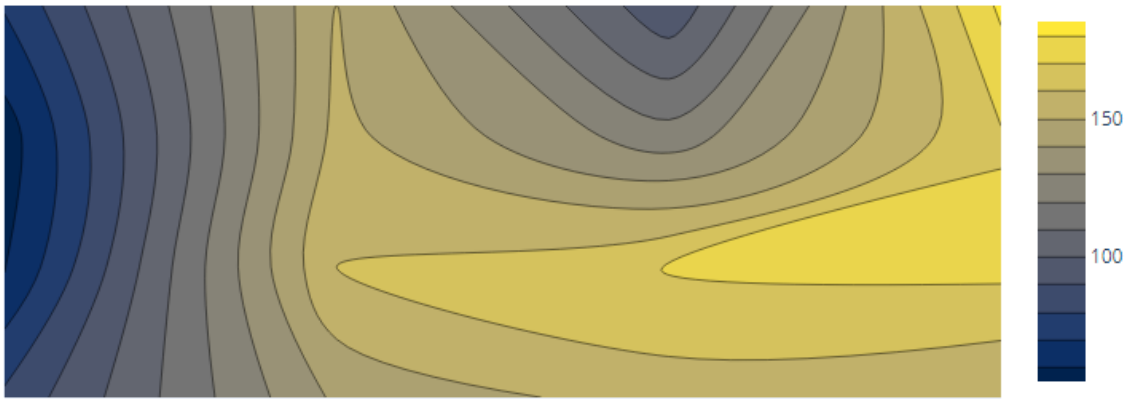

Figure 116: Location 5 contour plot on the 6th of September

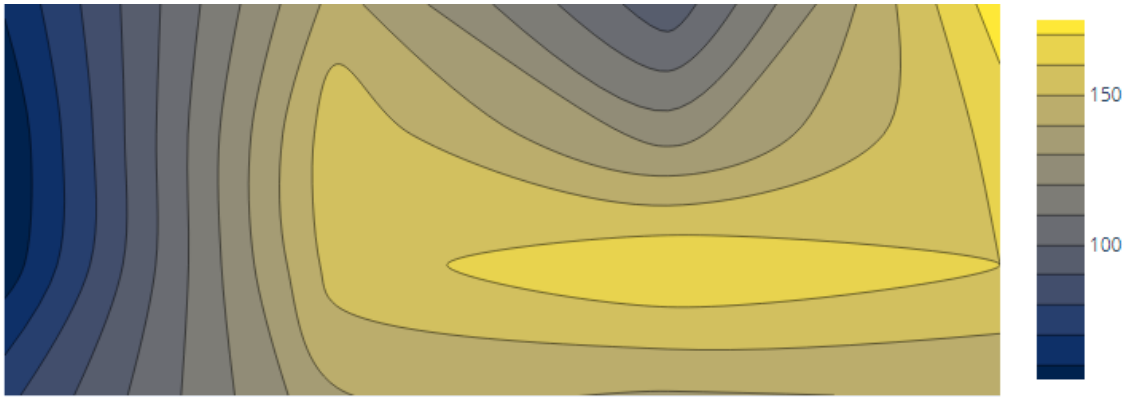

Figure 117: Location 5 contour plot on the 28th of September

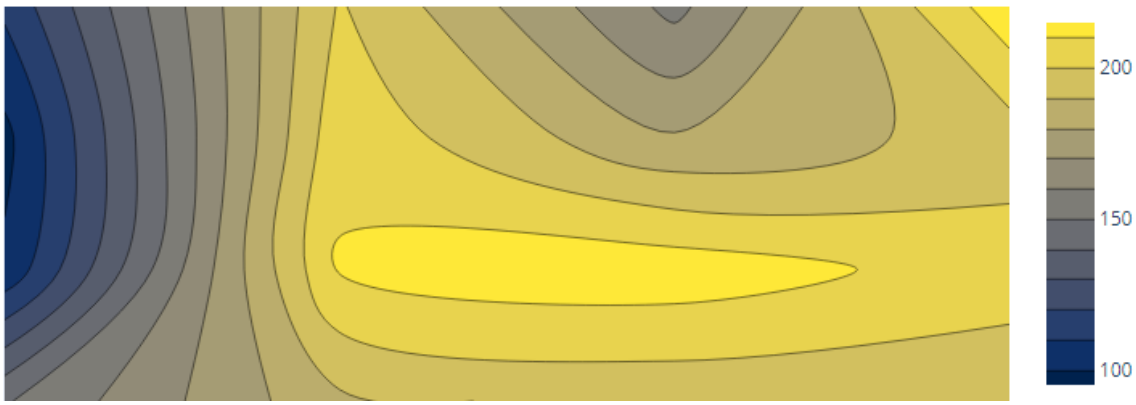

Figure 118: Location 5 contour plot on the 27th of October

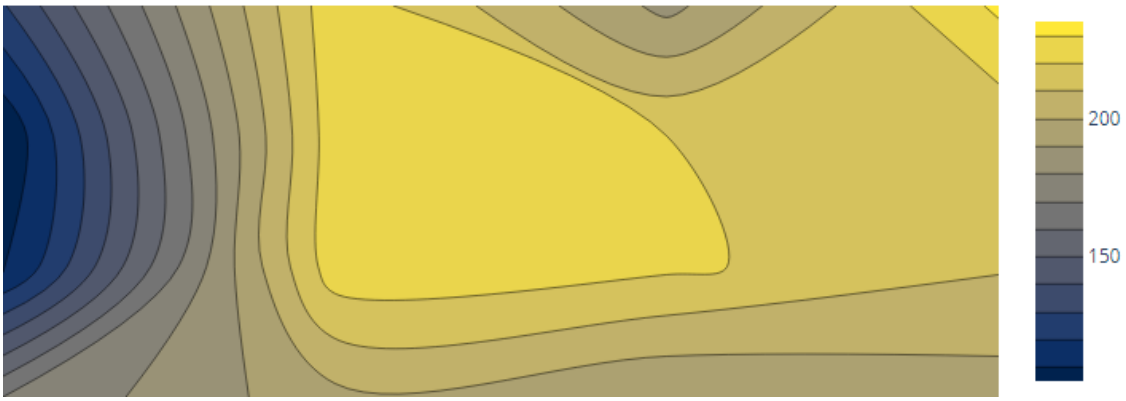

Figure 119: Location 5 contour plot on the 19th of November

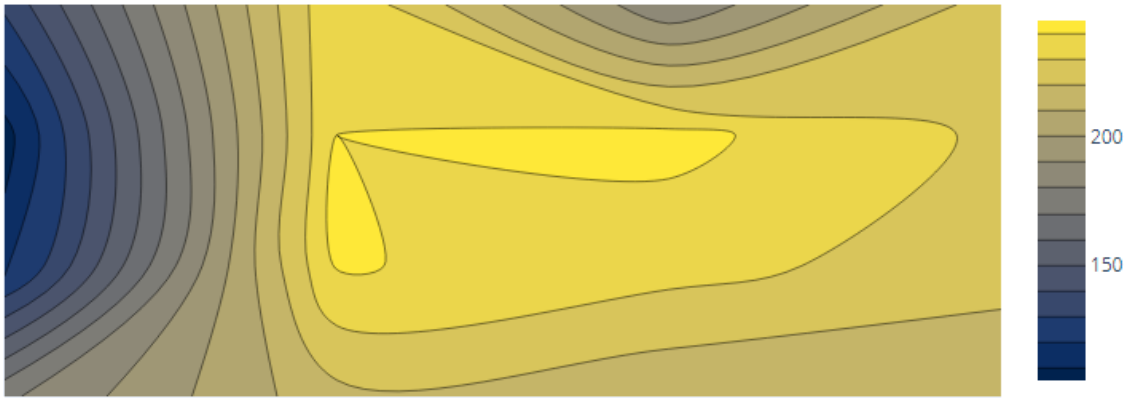

Figure 120: Location 5 contour plot on the 23rd of November

4. Additional cover depth statistics

Table 35: Detailed statistics for the vertical cover depth values from seven 1.5m^2 areas located all around the Neville Alexander Building.

General stats			Rilem									German		
Mean	49.02041			5th percentile				10th percentile						
Std dev	10.81513		Confidence level	50%	75%	90%	95%	50%	75%	90%	95%	r	48.51	5th percentile	10th percentile
Median	48		Tolerance factor	1.65	1.8	1.95	2.04	1.29	1.42	1.55	1.63	m	8.074		
Number of measuremnts	245	Min cover depth (mm)		31	30	28	27	35	34	32	31			34	37

Table 36: Detailed statistics for the horizontal cover depth values from seven 1.5m^2 areas located all around the Neville Alexander Building.

General stats			Rilem									German		
Mean	46.16393			5th percentile				10th percentile						
Std dev	11.20404		Confidence level	50%	75%	90%	95%	50%	75%	90%	95%	r	45.33	5th percentile	10th percentile
Median	44.5		Tolerance factor	1.65	1.8	1.95	2.04	1.29	1.42	1.55	1.63	m	7.283		
Number of measuremnts	245	Min cover depth (mm)		28	26	24	23	32	30	29	28			30	34

Table 37: Detailed statistics for the vertical cover depth values for 200 randomly selected cover depth measurements from the seven 1.5m^2 areas located all around the Neville Alexander Building.

General stats			Rilem									German		
Mean	48.77			5th percentile				10th percentile						
Std dev	10.9127		Confidence level	50%	75%	90%	95%	50%	75%	90%	95%	r	48.39	5th percentile	10th percentile
Median	48		Tolerance factor	1.65	1.8	1.95	2.04	1.29	1.42	1.55	1.63	m	7.981		
Number of measuremnts	200	Min cover depth (mm)		31	29	27	27	35	33	32	31			33	37

Table 38: Detailed statistics for the horizontal cover depth values for 200 randomly selected cover depth measurements from the seven 1.5m^2 areas located all around the Neville Alexander Building.

General stats			Rilem									German		
Mean	45.925			5th percentile				10th percentile						
Std dev	11.61419		Confidence level	50%	75%	90%	95%	50%	75%	90%	95%	r	45.46	5th percentile	10th percentile
Median	45		Tolerance factor	1.65	1.8	1.95	2.04	1.29	1.42	1.55	1.63	m	7.046		
Number of measuremnts	200	Min cover depth (mm)		27	25	23	22	31	29	28	27			30	33

Table 39: Detailed statistics for the vertical cover depth values for run 1 of 100 randomly selected cover depth measurements from the seven 1.5m^2 areas located all around the Neville Alexander Building.

General stats			Rilem									German		
Mean	47.01			5th percentile				10th percentile						
Std dev	10.59764		Confidence level	50%	75%	90%	95%	50%	75%	90%	95%	r	46.51	5th percentile	10th percentile
Median	46		Tolerance factor	1.65	1.8	1.95	2.04	1.29	1.42	1.55	1.63	m	7.899		
Number of measuremnts	100	Min cover depth (mm)		30	28	26	25	33	32	31	30			32	35

Table 40: Detailed statistics for the horizontal cover depth values for 100 randomly selected cover depth measurements from the seven 1.5m^2 areas located all around the Neville Alexander Building.

General stats			Rilem									German		
Mean	44.63			5th percentile				10th percentile						
Std dev	12.44882		Confidence level	50%	75%	90%	95%	50%	75%	90%	95%	r	43.32	5th percentile	10th percentile
Median	42		Tolerance factor	1.65	1.8	1.95	2.04	1.29	1.42	1.55	1.63	m	6.263		
Number of measuremnts	100	Min cover depth (mm)		24	22	20	19	29	27	25	24			27	30

Table 41: Detailed statistics for the vertical cover depth values for 50 randomly selected cover depth measurements from the seven 1.5m^2 areas located all around the Neville Alexander Building.

General stats			Rilem									German		
Mean	45.18			5th percentile				10th percentile						
Std dev	9.947241		Confidence level	50%	75%	90%	95%	50%	75%	90%	95%	r	44.84	5th percentile	10th percentile
Median	44.5		Tolerance factor	1.65	1.8	1.95	2.04	1.29	1.42	1.55	1.63	m	8.114		
Number of measuremnts	50	Min cover depth (mm)		29	27	26	25	32	31	30	29			31	34

Table 42: Detailed statistics for the horizontal cover depth values for 50 randomly selected cover depth measurements from the seven 1.5m^2 areas located all around the Neville Alexander Building.

General stats			Rilem									German		
Mean	46.78			5th percentile				10th percentile						
Std dev	9.996579		Confidence level	50%	75%	90%	95%	50%	75%	90%	95%	r	46.64	5th percentile	10th percentile
Median	46.5		Tolerance factor	1.65	1.8	1.95	2.04	1.29	1.42	1.55	1.63	m	8.398		
Number of measuremnts	50	Min cover depth (mm)		30	29	27	26	34	33	31	30			33	36

Table 43: Detailed statistics for the vertical cover depth values for 20 randomly selected cover depth measurements from the seven 1.5m^2 areas located all around the Neville Alexander Building.

General stats			Rilem									German		
Mean	46.4			5th percentile				10th percentile						
Std dev	9.728309		Confidence level	50%	75%	90%	95%	50%	75%	90%	95%	r	45.45	5th percentile	10th percentile
Median	44.5		Tolerance factor	1.65	1.8	1.95	2.04	1.29	1.42	1.55	1.63	m	8.409		
Number of measuremnts	20	Min cover depth (mm)		30	29	27	27	34	33	31	31			32	35

Table 44: Detailed statistics for the horizontal cover depth values for 20 randomly selected cover depth measurements from the seven 1.5m^2 areas located all around the Neville Alexander Building.

General stats			Rilem									German		
Mean	45.05			5th percentile				10th percentile						
Std dev	9.71841		Confidence level	50%	75%	90%	95%	50%	75%	90%	95%	r	45.03	5th percentile	10th percentile
Median	45		Tolerance factor	1.65	1.8	1.95	2.04	1.29	1.42	1.55	1.63	m	8.339		
Number of measuremnts	20	Min cover depth (mm)		29	28	26	25	33	31	30	29			32	35

Table 45: Detailed statistics for the vertical cover depth values for run 1 of 10 randomly selected cover depth measurements from the seven 1.5m^2 areas located all around the Neville Alexander Building.

General stats			Rilem									German		
Mean	42.9			5th percentile				10th percentile						
Std dev	11.87813		Confidence level	50%	75%	90%	95%	50%	75%	90%	95%	r	41.7	5th percentile	10th percentile
Median	40.5		Tolerance factor	1.65	1.8	1.95	2.04	1.29	1.42	1.55	1.63	m	6.319		
Number of measuremnts	10	Min cover depth (mm)		23	22	20	19	28	26	24	24			26	29

Table 46: Detailed statistics for the horizontal cover depth values for 10 randomly selected cover depth measurements from the seven 1.5m^2 areas located all around the Neville Alexander Building.

General stats			Rilem									German			
Mean	45.6			5th percentile				10th percentile							
Std dev	11.36838		Confidence level	50%	75%	90%	95%	50%	75%	90%	95%	r	46.55	5th percentile	10th percentile
Median	47.5		Tolerance factor	1.65	1.8	1.95	2.04	1.29	1.42	1.55	1.63	m	7.37		
Number of measuremnts	10	Min cover depth (mm)		27	25	23	22	31	29	28	27			31	35

Table 47: Detailed statistics for the vertical cover depth values for 5 randomly selected cover depth measurements from the seven 1.5m^2 areas located all around the Neville Alexander Building.

General stats			Rilem									German			
Mean	55.2			5th percentile				10th percentile							
Std dev	12.15566		Confidence level	50%	75%	90%	95%	50%	75%	90%	95%	r	55.1	5th percentile	10th percentile
Median	55		Tolerance factor	1.65	1.8	1.95	2.04	1.29	1.42	1.55	1.63	m	8.159		
Number of measuremnts	5	Min cover depth (mm)		35	33	31	30	40	38	36	35			38	42

Table 48: Detailed statistics for the horizontal cover depth values for 5 randomly selected cover depth measurements from the seven 1.5m^2 areas located all around the Neville Alexander Building.

General stats			Rilem									German			
Mean	45.6			5th percentile				10th percentile							
Std dev	2.416609		Confidence level	50%	75%	90%	95%	50%	75%	90%	95%	r	45.8	5th percentile	10th percentile
Median	46		Tolerance factor	1.65	1.8	1.95	2.04	1.29	1.42	1.55	1.63	m	34.11		
Number of measuremnts	5	Min cover depth (mm)		42	41	41	41	42	42	42	42			42	43

Table 49: Detailed statistics for the vertical cover depth values for run 2 of 10 randomly selected cover depth measurements from the seven 1.5m^2 areas located all around the Neville Alexander Building.

General stats			Rilem									German			
Mean	51.1			5th percentile				10th percentile							
Std dev	13.65613		Confidence level	50%	75%	90%	95%	50%	75%	90%	95%	r	49.05	5th percentile	10th percentile
Median	47		Tolerance factor	1.65	1.8	1.95	2.04	1.29	1.42	1.55	1.63	m	6.465		
Number of measuremnts	10	Min cover depth (mm)		29	27	24	23	33	32	30	29			31	35

Table 50: Detailed statistics for the vertical cover depth values for run 3 of 10 randomly selected cover depth measurements from the seven 1.5m^2 areas located all around the Neville Alexander Building.

General stats			Rilem									German		
Mean	49			5th percentile				10th percentile						
Std dev	11.36662		Confidence level	50%	75%	90%	95%	50%	75%	90%	95%	r	47.5	5th percentile	10th percentile
Median	46		Tolerance factor	1.65	1.8	1.95	2.04	1.29	1.42	1.55	1.63	m	7.522		
Number of measuremnts	10	Min cover depth (mm)		30	29	27	26	34	33	31	30			32	35

Table 51: Detailed statistics for the vertical cover depth values for run 4 of 10 randomly selected cover depth measurements from the seven 1.5m^2 areas located all around the Neville Alexander Building.

General stats			Rilem									German		
Mean	54.2			5th percentile				10th percentile						
Std dev	9.977976		Confidence level	50%	75%	90%	95%	50%	75%	90%	95%	r	54.35	5th percentile	10th percentile
Median	54.5		Tolerance factor	1.65	1.8	1.95	2.04	1.29	1.42	1.55	1.63	m	9.805		
Number of measuremnts	10	Min cover depth (mm)		38	36	35	34	41	40	39	38			40	43

Table 52: Detailed statistics for the vertical cover depth values for run 5 of 10 randomly selected cover depth measurements from the seven 1.5m^2 areas located all around the Neville Alexander Building.

General stats			Rilem									German		
Mean	46.7			5th percentile				10th percentile						
Std dev	10.79861		Confidence level	50%	75%	90%	95%	50%	75%	90%	95%	r	45.1	5th percentile	10th percentile
Median	43.5		Tolerance factor	1.65	1.8	1.95	2.04	1.29	1.42	1.55	1.63	m	7.518		
Number of measuremnts	10	Min cover depth (mm)		29	27	26	25	33	31	30	29			30	34

Table 53: Detailed statistics for the vertical cover depth values for run 6 of 10 randomly selected cover depth measurements from the seven 1.5m^2 areas located all around the Neville Alexander Building.

General stats			Rilem									German		
Mean	42.3			5th percentile				10th percentile						
Std dev	10.12966		Confidence level	50%	75%	90%	95%	50%	75%	90%	95%	r	42.65	5th percentile	10th percentile
Median	43		Tolerance factor	1.65	1.8	1.95	2.04	1.29	1.42	1.55	1.63	m	7.579		
Number of measuremnts	10	Min cover depth (mm)		26	24	23	22	29	28	27	26			29	32

Table 54: Detailed statistics for the vertical cover depth values for run 7 of 10 randomly selected cover depth measurements from the seven 1.5m^2 areas located all around the Neville Alexander Building.

General stats			Rilem									German			
Mean	45.2			5th percentile				10th percentile							
Std dev	6.705222		Confidence level	50%	75%	90%	95%	50%	75%	90%	95%	r	45.85	5th percentile	10th percentile
Median	46.5		Tolerance factor	1.65	1.8	1.95	2.04	1.29	1.42	1.55	1.63	m	12.31		
Number of measuremnts	10	Min cover depth (mm)		34	33	32	32	37	36	35	34			36	38

Table 55: Detailed statistics for the vertical cover depth values for run 2 of 100 randomly selected cover depth measurements from the seven 1.5m^2 areas located all around the Neville Alexander Building.

General stats			Rilem									German			
Mean	48.06			5th percentile				10th percentile							
Std dev	10.60643		Confidence level	50%	75%	90%	95%	50%	75%	90%	95%	r	47.03	5th percentile	10th percentile
Median	46		Tolerance factor	1.65	1.8	1.95	2.04	1.29	1.42	1.55	1.63	m	7.981		
Number of measuremnts	100	Min cover depth (mm)		31	29	27	26	34	33	32	31			33	36

Table 56: Detailed statistics for the vertical cover depth values for run 3 of 100 randomly selected cover depth measurements from the seven 1.5m^2 areas located all around the Neville Alexander Building.

General stats			Rilem									German			
Mean	48.55			5th percentile				10th percentile							
Std dev	10.17485		Confidence level	50%	75%	90%	95%	50%	75%	90%	95%	r	48.03	5th percentile	10th percentile
Median	47.5		Tolerance factor	1.65	1.8	1.95	2.04	1.29	1.42	1.55	1.63	m	8.496		
Number of measuremnts	100	Min cover depth (mm)		32	30	29	28	35	34	33	32			34	37

Table 57: Detailed statistics for the vertical cover depth values for run 4 of 100 randomly selected cover depth measurements from the seven 1.5m^2 areas located all around the Neville Alexander Building.

General stats			Rilem									German			
Mean	50.52			5th percentile				10th percentile							
Std dev	11.68373		Confidence level	50%	75%	90%	95%	50%	75%	90%	95%	r	49.26	5th percentile	10th percentile
Median	48		Tolerance factor	1.65	1.8	1.95	2.04	1.29	1.42	1.55	1.63	m	7.589		
Number of measuremnts	100	Min cover depth (mm)		31	29	28	27	35	34	32	31			33	37

Table 58: Detailed statistics for the vertical cover depth values for run 5 of 100 randomly selected cover depth measurements from the seven 1.5m^2 areas located all around the Neville Alexander Building.

General stats			Rilem									German		
Mean	48.92			5th percentile				10th percentile						
Std dev	10.29726		Confidence level	50%	75%	90%	95%	50%	75%	90%	95%	r	47.96	5th percentile	10th percentile
Median	47		Tolerance factor	1.65	1.8	1.95	2.04	1.29	1.42	1.55	1.63	m	8.384		
Number of measuremnts	100	Min cover depth (mm)		32	30	29	28	36	34	33	32			34	37

Table 59: Detailed statistics for the vertical cover depth values for run 6 of 100 randomly selected cover depth measurements from the seven 1.5m^2 areas located all around the Neville Alexander Building.

General stats			Rilem									German		
Mean	47.75			5th percentile				10th percentile						
Std dev	10.20723		Confidence level	50%	75%	90%	95%	50%	75%	90%	95%	r	47.63	5th percentile	10th percentile
Median	47.5		Tolerance factor	1.65	1.8	1.95	2.04	1.29	1.42	1.55	1.63	m	8.398		
Number of measuremnts	100	Min cover depth (mm)		31	29	28	27	35	33	32	31			34	37

Table 60: Detailed statistics for the vertical cover depth values for run 6 of 100 randomly selected cover depth measurements from the seven 1.5m^2 areas located all around the Neville Alexander Building.

General stats			Rilem									German		
Mean	50.98			5th percentile				10th percentile						
Std dev	11.7949		Confidence level	50%	75%	90%	95%	50%	75%	90%	95%	r	49.99	5th percentile	10th percentile
Median	49		Tolerance factor	1.65	1.8	1.95	2.04	1.29	1.42	1.55	1.63	m	7.629		
Number of measuremnts	100	Min cover depth (mm)		32	30	28	27	36	34	33	32			34	37

Table 61: Detailed statistics for the vertical cover depth values from a large 7.5m^2 area on the ground floor of the west side of the Neville Alexander Building.

General stats			Rilem									German		
Mean	49.67895			5th percentile				10th percentile						
Std dev	8.663115		Confidence level	50%	75%	90%	95%	50%	75%	90%	95%	r	49.84	5th percentile	10th percentile
Median	50		Tolerance factor	1.65	1.725	1.795	1.845	1.28	1.35	1.415	1.455	m	10.36		
Number of measuremnts	190	Min cover depth (mm)		35	35	34	34	39	38	37	37			38	40

Table 62: Detailed statistics for the horizontal cover depth values from a large 7.5m^2 area on the ground floor of the west side of the Neville Alexander Building.

General stats			Rilem									German		
Mean	54.27895			5th percentile				10th percentile						
Std dev	8.696102		Confidence level	50%	75%	90%	95%	50%	75%	90%	95%	r	54.64	5th percentile	10th percentile
Median	55		Tolerance factor	1.65	1.725	1.795	1.845	1.28	1.35	1.415	1.455	m	11.31		
Number of measuremnts	190	Min cover depth (mm)		40	39	39	38	43	43	42	42			42	45

Table 63: Detailed statistics for the vertical cover depth values for 100 randomly selected cover depth measurements from the large 7.5m^2 area on the ground floor of the west side of the Neville Alexander Building.

General stats			Rilem									German		
Mean	50.31			5th percentile				10th percentile						
Std dev	8.219118		Confidence level	50%	75%	90%	95%	50%	75%	90%	95%	r	50.66	5th percentile	10th percentile
Median	51		Tolerance factor	1.65	1.8	1.95	2.04	1.29	1.42	1.55	1.63	m	11.09		
Number of measuremnts	100	Min cover depth (mm)		37	36	34	34	40	39	38	37			39	42

Table 64: Detailed statistics for the horizontal cover depth values for 100 randomly selected cover depth measurements from the large 7.5m^2 area on the ground floor of the west side of the Neville Alexander Building.

General stats			Rilem									German		
Mean	49.44			5th percentile				10th percentile						
Std dev	8.525632		Confidence level	50%	75%	90%	95%	50%	75%	90%	95%	r	49.72	5th percentile	10th percentile
Median	50		Tolerance factor	1.65	1.81	1.97	2.06	1.29	1.43	1.56	1.65	m	10.5		
Number of measuremnts	50	Min cover depth (mm)		35	34	33	32	38	37	36	35			38	40

Table 65: Detailed statistics for the vertical cover depth values for 50 randomly selected cover depth measurements from the large 7.5m^2 area on the ground floor of the west side of the Neville Alexander Building.

General stats			Rilem									German		
Mean	54.71			5th percentile				10th percentile						
Std dev	8.968049		Confidence level	50%	75%	90%	95%	50%	75%	90%	95%	r	55.36	5th percentile	10th percentile
Median	56		Tolerance factor	1.65	1.8	1.95	2.04	1.29	1.42	1.55	1.63	m	11.11		
Number of measuremnts	100	Min cover depth (mm)		40	39	37	36	43	42	41	40			42	45

Table 66: Detailed statistics for the horizontal cover depth values for 50 randomly selected cover depth measurements from the large 7.5m^2 area on the ground floor of the west side of the Neville Alexander Building.

General stats			Rilem									German		
Mean	52.98			5th percentile				10th percentile						
Std dev	7.672001		Confidence level	50%	75%	90%	95%	50%	75%	90%	95%	r	51.74	5th percentile	10th percentile
Median	50.5		Tolerance factor	1.65	1.81	1.97	2.06	1.29	1.43	1.56	1.65	m	12.14		
Number of measuremnts	50	Min cover depth (mm)		40	39	38	37	43	42	41	40			41	43

Table 67: Detailed statistics for the vertical cover depth values for 20 randomly selected cover depth measurements from the large 7.5m^2 area on the ground floor of the west side of the Neville Alexander Building.

General stats			Rilem									German		
Mean	53.25			5th percentile				10th percentile						
Std dev	8.233316		Confidence level	50%	75%	90%	95%	50%	75%	90%	95%	r	54.63	5th percentile	10th percentile
Median	56		Tolerance factor	1.67	1.93	2.21	2.4	1.3	1.53	1.77	1.93	m	11.94		
Number of measuremnts	20	Min cover depth (mm)		40	37	35	33	43	41	39	37			43	45

Table 68: Detailed statistics for the horizontal cover depth values for 20 randomly selected cover depth measurements from the large 7.5m^2 area on the ground floor of the west side of the Neville Alexander Building.

General stats			Rilem									German		
Mean	51.4			5th percentile				10th percentile						
Std dev	7.838367		Confidence level	50%	75%	90%	95%	50%	75%	90%	95%	r	51.7	5th percentile	10th percentile
Median	52		Tolerance factor	1.67	1.93	2.21	2.4	1.3	1.53	1.77	1.93	m	11.87		
Number of measuremnts	20	Min cover depth (mm)		38	36	34	33	41	39	38	36			40	43

Table 69: Detailed statistics for the vertical cover depth values from a 1.5m^2 area located towards the top right corner of the 7.5m^2 area on the ground floor of the west side of the Neville Alexander Building.

General stats			Rilem									German		
Mean	41.81633			5th percentile				10th percentile						
Std dev	5.516852		Confidence level	50%	75%	90%	95%	50%	75%	90%	95%	r	41.41	5th percentile	10th percentile
Median	41		Tolerance factor	1.65	1.81	1.97	2.06	1.29	1.43	1.56	1.65	m	13.51		
Number of measuremnts	49	Min cover depth (mm)		33	32	31	30	35	34	33	33			33	35

Table 70: Detailed statistics for the horizontal cover depth values from a 1.5m^2 area located towards the top right corner of the 7.5m^2 area on the ground floor of the west side of the Neville Alexander Building.

General stats			Rilem									German			
Mean	46.26531			5th percentile				10th percentile							
Std dev	5.078066		Confidence level	50%	75%	90%	95%	50%	75%	90%	95%	r	46.13	5th percentile	10th percentile
Median	46		Tolerance factor	1.65	1.81	1.97	2.06	1.29	1.43	1.56	1.65	m	16.35		
Number of measuremnts	49	Min cover depth (mm)		38	37	36	36	40	39	38	38			39	40

Table 71: Detailed statistics for the vertical cover depth values from a 1.5m^2 area located towards the top left corner of the 7.5m^2 area on the ground floor of the west side of the Neville Alexander Building.

General stats			Rilem									German			
Mean	53.06122			5th percentile				10th percentile							
Std dev	3.633226		Confidence level	50%	75%	90%	95%	50%	75%	90%	95%	r	53.53	5th percentile	10th percentile
Median	54		Tolerance factor	1.65	1.81	1.97	2.06	1.29	1.43	1.56	1.65	m	26.52		
Number of measuremnts	49	Min cover depth (mm)		47	46	46	46	48	48	47	47			48	49

Table 72: Detailed statistics for the horizontal cover depth values from a 1.5m^2 area located towards the top left corner of the 7.5m^2 area on the ground floor of the west side of the Neville Alexander Building.

General stats			Rilem									German			
Mean	59			5th percentile				10th percentile							
Std dev	4.370588		Confidence level	50%	75%	90%	95%	50%	75%	90%	95%	r	59.5	5th percentile	10th percentile
Median	60		Tolerance factor	1.65	1.81	1.97	2.06	1.29	1.43	1.56	1.65	m	24.5		
Number of measuremnts	49	Min cover depth (mm)		52	51	50	50	53	53	52	52			53	54

Table 73: Detailed statistics for the vertical cover depth values from a 3m^2 area on the ground floor of the south side of the Neville Alexander Building.

General stats			Rilem									German			
Mean	46.7037			5th percentile				10th percentile							
Std dev	5.191266		Confidence level	50%	75%	90%	95%	50%	75%	90%	95%	r	47.6	5th percentile	10th percentile
Median	48.5		Tolerance factor	1.65	1.8	1.95	2.04	1.29	1.42	1.55	1.63	m	16.51		
Number of measuremnts	54	Min cover depth (mm)		38	37	37	36	40	39	39	38			40	42

Table 74: Detailed statistics for the horizontal cover depth values from a $3m^2$ area on the ground floor of the south side of the Neville Alexander Building.

General stats			Rilem									German		
Mean	45.7037			5th percentile				10th percentile						
Std dev	5.583141		Confidence level	50%	75%	90%	95%	50%	75%	90%	95%	r	46.85	5th percentile	10th percentile
Median	48		Tolerance factor	1.65	1.8	1.95	2.04	1.29	1.42	1.55	1.63	m	15.1		
Number of measuremnts	54	Min cover depth (mm)		36	36	35	34	39	38	37	37			39	41

Table 75: Detailed statistics for the vertical cover depth values from a $1.5m^2$ area located towards the top left corner of the $3m^2$ area on the ground floor of the south side of the Neville Alexander Building.

General stats			Rilem									German		
Mean	48.89286			5th percentile				10th percentile						
Std dev	3.039493		Confidence level	50%	75%	90%	95%	50%	75%	90%	95%	r	48.95	5th percentile	10th percentile
Median	49		Tolerance factor	1.66	1.88	2.1	2.25	1.29	1.48	1.67	1.8	m	28.99		
Number of measuremnts	28	Min cover depth (mm)		44	43	43	42	45	44	44	43			44	45

Table 76: Detailed statistics for the horizontal cover depth values from a $1.5m^2$ area located towards the top left corner of the $3m^2$ area on the ground floor of the south side of the Neville Alexander Building.

General stats			Rilem									German		
Mean	47.5			5th percentile				10th percentile						
Std dev	3.11104		Confidence level	50%	75%	90%	95%	50%	75%	90%	95%	r	47.75	5th percentile	10th percentile
Median	48		Tolerance factor	1.66	1.88	2.1	2.25	1.29	1.48	1.67	1.8	m	27.63		
Number of measuremnts	28	Min cover depth (mm)		42	42	41	41	43	43	42	42			43	44

Table 77: Detailed statistics for the vertical cover depth values from a $1.5m^2$ area located on the ground floor of the south side of the Neville Alexander Building/towards the top left corner of the $3m^2$ area on the ground floor of the south side of the Neville Alexander Building.

General stats			Rilem									German		
Mean	44.07143			5th percentile				10th percentile						
Std dev	5.793645		Confidence level	50%	75%	90%	95%	50%	75%	90%	95%	r	44.54	5th percentile	10th percentile
Median	45		Tolerance factor	1.66	1.88	2.1	2.25	1.29	1.48	1.67	1.8	m	13.84		
Number of measuremnts	28	Min cover depth (mm)		34	33	32	31	37	35	34	34			36	38

Table 78: Detailed statistics for the vertical cover depth values from a 1.5m^2 area at a location on the ground floor of the north side of the Neville Alexander Building.

General stats			Rilem										German	
Mean	42.75			5th percentile				10th percentile						
Std dev	6.045217		Confidence level	50%	75%	90%	95%	50%	75%	90%	95%	r	43.38	5th percentile	10th percentile
Median	44		Tolerance factor	1.66	1.88	2.1	2.25	1.29	1.48	1.67	1.8	m	12.92		
Number of measuremnts	28	Min cover depth (mm)		33	31	30	29	35	34	33	32			35	37

Table 79: Detailed statistics for the vertical cover depth values from a 1.5m^2 area located on the ground floor of the south side of the Neville Alexander Building/towards the top left corner of the 3m^2 area on the ground floor of the south side of the Neville Alexander Building.

General stats			Rilem										German	
Mean	50.66667			5th percentile				10th percentile						
Std dev	5.390321		Confidence level	50%	75%	90%	95%	50%	75%	90%	95%	r	51.33	5th percentile	10th percentile
Median	52		Tolerance factor	1.66	1.88	2.1	2.25	1.29	1.48	1.67	1.8	m	17.14		
Number of measuremnts	28	Min cover depth (mm)		42	41	39	39	44	43	42	41			43	45

Table 80: Detailed statistics for the horizontal cover depth values from a 1.5m^2 area at a location on the ground floor of the north side of the Neville Alexander Building.

General stats			Rilem										German	
Mean	56.53571			5th percentile				10th percentile						
Std dev	10.45221		Confidence level	50%	75%	90%	95%	50%	75%	90%	95%	r	56.77	5th percentile	10th percentile
Median	57		Tolerance factor	1.66	1.88	2.1	2.25	1.29	1.48	1.67	1.8	m	9.776		
Number of measuremnts	28	Min cover depth (mm)		39	37	35	33	43	41	39	38			42	45

Table 81: Detailed statistics for the vertical cover depth values from a 1.5m^2 area at a location on the ground floor of the east side of the Neville Alexander Building.

General stats			Rilem										German	
Mean	38.85714			5th percentile				10th percentile						
Std dev	5.954476		Confidence level	50%	75%	90%	95%	50%	75%	90%	95%	r	39.43	5th percentile	10th percentile
Median	40		Tolerance factor	1.66	1.83	2	2.11	1.29	1.44	1.59	1.69	m	11.92		
Number of measuremnts	42	Min cover depth (mm)		29	28	27	26	31	30	29	29			31	33

Table 82: Detailed statistics for the horizontal cover depth values from a 1.5m^2 area at a location on the ground floor of the east side of the Neville Alexander Building.

General stats			Rilem									German		
Mean	35.28571			5th percentile				10th percentile						
Std dev	5.081646		Confidence level	50%	75%	90%	95%	50%	75%	90%	95%	r	35.14	5th percentile	10th percentile
Median	35		Tolerance factor	1.66	1.83	2	2.11	1.29	1.44	1.59	1.69	m	12.45		
Number of measuremnts	42	Min cover depth (mm)		27	26	25	25	29	28	27	27			28	29

Table 83: Detailed statistics for the vertical cover depth values from a 1.5m^2 area at a location on the 1st floor of the east side of the Neville Alexander Building.

General stats			Rilem									German		
Mean	47			5th percentile				10th percentile						
Std dev	6.492303		Confidence level	50%	75%	90%	95%	50%	75%	90%	95%	r	46.75	5th percentile	10th percentile
Median	46.5		Tolerance factor	1.66	1.83	2.01	2.13	1.29	1.44	1.6	1.7	m	12.96		
Number of measuremnts	40	Min cover depth (mm)		36	35	34	33	39	38	37	36			37	39

Table 84: statistics for the horizontal cover depth values from a 1.5m^2 area at a location on the 1st floor of the east side of the Neville Alexander Building.

General stats			Rilem									German		
Mean	42.925			5th percentile				10th percentile						
Std dev	5.55152		Confidence level	50%	75%	90%	95%	50%	75%	90%	95%	r	42.21	5th percentile	10th percentile
Median	41.5		Tolerance factor	1.66	1.83	2.01	2.13	1.29	1.44	1.6	1.7	m	13.69		
Number of measuremnts	40	Min cover depth (mm)		34	33	32	31	36	35	34	33			34	36

Table 85: Detailed statistics for the vertical cover depth values from a 1.5m^2 area at a location on the 3rd floor of the north side of the Neville Alexander Building.

General stats			Rilem									German		
Mean	48.33333			5th percentile				10th percentile						
Std dev	5.312459		Confidence level	50%	75%	90%	95%	50%	75%	90%	95%	r	48.42	5th percentile	10th percentile
Median	48.5		Tolerance factor	1.66	1.87	2.08	2.22	1.29	1.47	1.66	1.78	m	16.4		
Number of measuremnts	30	Min cover depth (mm)		40	38	37	37	41	41	40	39			40	42

Table 86: Detailed statistics for the horizontal cover depth values from a 1.5m^2 area at a location on the 3rd floor of the north side of the Neville Alexander Building.

General stats			Rilem									German		
Mean	49.73333			5th percentile				10th percentile						
Std dev	6.662999		Confidence level	50%	75%	90%	95%	50%	75%	90%	95%	r	50.12	5th percentile	10th percentile
Median	50.5		Tolerance factor	1.66	1.87	2.08	2.22	1.29	1.47	1.66	1.78	m	13.54		
Number of measuremnts	30	Min cover depth (mm)		39	37	36	35	41	40	39	38			40	43

Table 87: Detailed statistics for the vertical cover depth values from a 1.5m^2 area at a location on the ground floor of the west side of the Neville Alexander Building.

General stats			Rilem									German		
Mean	41.6			5th percentile				10th percentile						
Std dev	5.607138		Confidence level	50%	75%	90%	95%	50%	75%	90%	95%	r	41.55	5th percentile	10th percentile
Median	41.5		Tolerance factor	1.66	1.87	2.08	2.22	1.29	1.47	1.66	1.78	m	13.34		
Number of measuremnts	30	Min cover depth (mm)		32	31	30	29	34	33	32	32			33	35

Table 88: Detailed statistics for the horizontal cover depth values from a 1.5m^2 area at a location on the ground floor of the west side of the Neville Alexander Building.

General stats			Rilem									German		
Mean	37.8			5th percentile				10th percentile						
Std dev	4.812484		Confidence level	50%	75%	90%	95%	50%	75%	90%	95%	r	37.15	5th percentile	10th percentile
Median	36.5		Tolerance factor	1.66	1.87	2.08	2.22	1.29	1.47	1.66	1.78	m	13.9		
Number of measuremnts	30	Min cover depth (mm)		30	29	28	27	32	31	30	29			30	32

Table 89: Detailed statistics for the vertical cover depth values from a 1.5m^2 area at a location on the 1st floor of the west side of the Neville Alexander Building.

General stats			Rilem									German		
Mean	61.73469			5th percentile				10th percentile						
Std dev	9.104328		Confidence level	50%	75%	90%	95%	50%	75%	90%	95%	r	61.37	5th percentile	10th percentile
Median	61		Tolerance factor	1.65	1.81	1.97	2.065	1.29	1.43	1.56	1.65	m	12.13		
Number of measuremnts	49	Min cover depth (mm)		47	45	44	43	50	49	48	47			48	51

Table 90: Detailed statistics for the horizontal cover depth values from a 1.5m^2 area at a location on the 1st floor of the west side of the Neville Alexander Building.

General stats			Rilem									German			
Mean	60.67347			5th percentile				10th percentile							
Std dev	10.61264		Confidence level	50%	75%	90%	95%	50%	75%	90%	95%	r	60.34	5th percentile	10th percentile
Median	60		Tolerance factor	1.65	1.81	1.97	2.065	1.29	1.43	1.56	1.65	m	10.23		
Number of measuremnts	49	Min cover depth (mm)		43	41	40	39	47	45	44	43			45	49